Optimization of Process Parameters in Plastic Injection Moulding for Virgin and Composite Materials

A THESIS SUBMITTED IN PARTIAL FULFILLMENT OF THE REQUIREMENT FOR THE AWARD OF THE DEGREE OF

Doctor of Philosophy

In

Mechanical Engineering

Submitted to

Malaviya National Institute of Technology, Jaipur, Rajasthan

By

Deepak Kumar

Student ID: – 2012RME9037

Department of Mechanical Engineering
Malaviya National Institute of Technology
Jaipur-302017, Rajasthan, INDIA

March 2017

Optimization of Process Parameters in Plastic Injection Moulding for Virgin and Composite Materials

A THESIS SUBMITTED IN PARTIAL FULFILLMENT OF THE REQUIREMENT FOR THE AWARD OF THE DEGREE OF

Doctor of Philosophy

In

Mechanical Engineering

Submitted to

Malaviya National Institute of Technology, Jaipur

By

Deepak Kumar

Student ID:–2012RME9037

Under the supervision of

Prof. G. S. Dangayach (MNIT, Jaipur)

and

Prof. P. N. Rao (Univ. Northern Iowa, USA)

Department of Mechanical Engineering

Malaviya National Institute of Technology

Jaipur-302017, Rajasthan, INDIA

March, 2017

CERTIFICATE

This is to certify that the thesis entitled "**Optimization of Process Parameters in Plastic Injection Moulding for Virgin and Composite Materials",** submitted by Deepak Kumar **(Reg. No: 2012RME9037)** in partial fulfilment of the requirements for the award of **Doctor of Philosophy** in Mechanical Engineering to the Malaviya National Institute of Technology, Jaipur is an authentic record of research work carried out by him under our supervision and guidance. To the best of our knowledge, the work incorporated in this thesis has not been submitted elsewhere for the award of any degree.

Prof. G. S. Dangayach

Supervisor
Professor,
Mechanical Engineering Department
MNIT, Jaipur

Prof. P. N. Rao

Supervisor
Professor,
Department of Technology
University of Northern Iowa,
USA

Acknowledgements

I would like to extend my sincere thanks to my supervisors **Prof. G. S. Dangayach** and **Prof. P. N. Rao** for their impetus, able and continual guidance throughout the research work, without their constant support and encouragements, completion of the thesis would not have been possible.

I am grateful to **Prof. Udaykumar R. Yaragatti**, Director, Malaviya National Institute of Technology, Jaipur (Rajasthan) who has been a constant source of inspiration for me. I am also grateful to Professor **Dr. Amar Patnaik**, Faculty, Mechanical Engineering Department, MNIT for his help and cooperation. I appreciate the encouragement from faculty members of the Mechanical Engineering Department, MNIT Jaipur.

I would also like to extend my appreciation to my PhD committee members **Dr. Harlal Mali and Dr. M. L. Meena.** I would like to thank all of them for kindly serving on my committee.

I am grateful to **Mr. Lalit Guglani**, Director, CIPET, Jaipur Centre for given me all required technical and laboratory support for completing the research work. Also I want to thank my fellow research scholars Mr. Sumit Gupta, Ms. Bhavana Mathur and Mr. Shiv Ranjan Kumar who offered a lot of help during my Ph.D. study.

I extend my deep sense of gratitude and respect towards honorable **Dr. S. M. Seth**, Chairperson, Poornima University and **Shri Shashikant Singhi**, Director General, Poornima Foundation for their continuous inspiration and motivation for the research.

I am grateful to my family members for the tremendous amount of inspiration and moral support during my research work.

I am also grateful to all those who have directly or indirectly contributed in providing me a stimulating environment for accomplishing my task.

Last but not least, I would like to thank God Almighty, my Lord for giving me the will power and strength to make it this far when I didn't see a light.

Date:

M.N.I.T. Jaipur **Deepak Kumar**

Abstract

The development of high-performance materials made from natural resources is increasing worldwide. The Polymer composites are mixtures of polymers with inorganic or organic additives having certain geometries like fibers, flakes, spheres, and particulates. Polymer composites have a great potential for advanced applications. Polypropylene (PP) is one of the most extensively produced polymers, especially widely used as automotive parts due to its good impact resistance as well as processability. In the present study two conventional ceramic powders (Al_2O_3 and TiO_2) and one industrial wastes (Marble powder) have been used as the filler materials. Polypropylene composites were fabricated by varying different weight percentages (0-20%) of Alumina (Al_2O_3), Titanium dioxide (TiO_2) and Marble powder by using Injection Moulding Technique. Then the fabricated composites were characterized by physical characterization using void content test, chemical characterization using Fourier-transform infrared spectroscopy, mechanical characterization using Shore D hardness test, flexural test, Izod impact test and compressive strength, thermo-mechanical characterizations using Dynamic Mechanical Analysis (DMA), Thermo-gravimetric analysis (TGA) and morphological characterizations using Scanning Electron Microscopy (SEM) and Atomic force Microscopy (AFM). ASTM standards for Shore D hardness, Izod impact strength, flexural strength and compressive strength were followed.

Dynamic mechanical analyzer (DMA) was used to measure the thermo-mechanical properties using storage modulus (E'), loss modulus (E'') and damping factor (Tan δ) of the fabricated PP composites over a temperature range of 0-160°C at 1Hz frequency to assess their properties. The inclusion of Alumina, Titanium dioxide and Marble powder into the Polypropylene led to an enhancement in hardness. The maximum value of Shore D hardness was found in PP- marble powder (20 wt.%) which was 30.35% higher than Shore D hardness of virgin PP.

Adding of Alumina and Titanium dioxide in PP composites, reduce the impact strength of the composites, however integration of Marble powder in PP, increases impact strength of the PP composites. Regarding flexural strength, in all the three series of composites, maximum flexural strength was obtained in PPM-5 which is 64.16 MPa.

The compressive strength of PP composites filled with different weight-percentage (5-20 wt. %) of alumina, titanium dioxide and Marble powder were found in the range of 98.63 - 121.34 MPa, 113.8 - 171.6 MPa and 103.4 – 159.4 MPa respectively. Thus maximum compressive strength was 87.8%, higher than virgin PP which is found in PP-TiO_2 composite having 20 wt.%.

It was also revealed that the storage modulus of the fabricated composites were found to be higher than that of the virgin PP because filler increases the stiffness of the composites. Thermo-gravimetric analysis (TGA) measurements indicate that both the initial degradation temperature and end degradation temperature increase with increasing filler content.

In this thesis, shrinkage and warpage behaviour of virgin Polypropylene (PP) and virgin Polycarbonate (PC) has been assessed and optimized with the help of Taguchi method. Initially steady state experimental shrinkage and warpage test was performed with respect to different parameters of injection moulding. With the help of modified linear graph and orthogonal array the parameters were optimized. Thus, shrinkage –warpage were minimized and impact strength were maximized for both virgin PP and virgin PC. Melt temperature, mould temperature and injection pressure with their interactions were found to perform the significant role.

*****

Table of Contents

*****

List of Figures

****

List of Tables

*****

Chapter 1

INTRODUCTION

In the modern era of sustainable materials, the usage of polymer composites has been increasing. The high demands of automotive industries and other associated applications have generated a novel field of polymer science that has rapidly developed and progressed to polymer composites for aerospace (structural mass of an aircraft) and other applications by modifying the commercial polymers to improve their mechanical and thermal properties and increase their shelf life.

Advanced materials such as ceramic-matrix nanocomposites, metal-matrix nanocomposites and polymer-matrix nanocomposites have drawn extensive interests from both researchers and manufacturers. Generally, the hybrid composites consist of two or more reinforcing phase in a single matrix. The reinforcing phase can be natural fibres or ceramic filler in grouping with fibres or filler particulates only etc. These kinds of phase grouping can create synergistic strengthening or ‘‘hybrid effect’’ and make enhancement in the mechanical properties of the composites [1].

A composite material is synthesized of two components or more, known as a matrix system or filler system. Polymers such as thermoplastics and thermosets can be used as a matrix material to form a composite, as well as metals, ceramics and carbon. At the same time, the matrix system works as a binder for the filler system; fiberglass, graphite, aramid, silica and aluminium can be used for this purpose. Both matrix and filler retain their individual identities when they join to form a composite and directly affect the properties of the final composite [2]. Polymer composites comprised of filler particles dispersed in an entangled matrix, have attracted substantial industrial and academic attention since the early 1990s.

Mechanical Properties, such as hardness, tensile strength, compressive strength, impact strength and flexural strength and other properties such as thermal conductivity, flame retardation, electrical conductivity, and visco-elasticity are improved with addition of fillers to a polymer matrix [3]. Polymer composites have been widely used in various industries and daily life, especially polypropylene (PP) and its copolymers due to the low density and cost, easy processing, and excellent mechanical properties [4].

Polymeric materials are widely used in automobile industry (door, panel design and body structure), construction industry, dentistry as denture material, adhesive materials, composite filling materials, cement, pits and fissure sealants etc.

1.1 History of polymer composites

On a macro-scale, composite materials are materials consisting of two or more chemically diverse constituents with an interface separating them. To form a composite material one or more discontinuous phases are embed in a continuous phase. Generally, the discontinuous phase is stronger and harder than the continuous phase and is expressed as the reinforcement while the continuous-phase is expressed as the matrix. Metallic, polymeric or even ceramic can be used as matrix material. Polymer Matrix Composite (PMC) is the material having polymer matrix combined with a fibrous reinforcing dispersed phase. Polymer Matrix Composites are incredibly admired due to their easy fabrication technique and low cost. The purpose of the matrix is to tie the fibres jointly and to transfer loads between them.

PMC can be divided into two groups: reinforced plastics, and advanced composites. The division is based on the level of mechanical and thermal properties; yet, there is no clear-cut line separating the two. Reinforced plastics, which are relatively low-cost, typically consist of polyester resins reinforced with low-stiffness natural and glass fibres. From last two decades, advanced composites have been in use, mainly in the segment of automotive and aerospace industry, have better strength and stiffness, and are less expensive. Simultaneously, the advancement of computer expertise has made it easier to characterize and anticipate mechanical and thermal properties at the micro and nanoscale with modelling and simulation.

In general, the exclusive arrangement of the micro and nanomaterials characteristics, such as particle size, thermo-mechanical properties, and low concentrations necessary to effect change in a polymer matrix, together with the advanced characterization and simulation techniques, have created interest in the field of micro and nanocomposites. Additionally, many polymer micro and nanocomposites can be fabricated and processed in different ways by making them particularly attractive and useful from a desired point of view.

1.2 Composition of Polypropylene composites

Many studies have been conducted based on filler technology i.e. increasing the filler content, decreasing the particle size of filler or treatment of filler etc. to get better mechanical performance; thus the filler particles play an important role in determining the mechanical properties of composite materials [5]. As a filler material, alumina is strategic additive to get better ductility and strength in the composite. Incorporating alumina as filler to the polymer based composite gives in an increase in mechanical properties such as hardness, compression strength, impact strength etc. [6]. Turnsek et al. [7] prepared macro-porous polymer composites with alumina particles and evaluated their mechanical and thermal properties. Alumina particles (Al_2O_3) are the most significant metal oxides with promising applications and the exceptional thermo –mechanical properties in fabrication of composite materials. Therefore, alumina is effective filler in the polymer composites having uniform dispersion and better interfacial interaction between reinforcement and the polymer matrix [8]. It is hard and wear-resistant, has excellent dielectric properties, resistance to strong acid and alkali attack at elevated temperatures, high strength and stiffness. TiO_2 is easy to use, inexpensive, very much stable and eco-friendly material. Excellent photo-catalytic and antimicrobial abilities have been important features of TiO_2 that lead to its exploitation in decomposition of organic - inorganic contamination of environment.

TiO_2 is possibly the most attractive filler due to combination of its exceptional properties such as chemical, corrosion, non-toxicity, non-flammability and photo stability, superior electrical properties, compatibility with a range of materials [9], good photo-catalytic property, better refractive index and capability to absorb ultraviolet (UV) light. It was also investigated that due to exceptional hydrophilicity, TiO_2 particles are involved in the modification of surface of polymer membranes for the antifouling application.

Scientists and researchers use TiO_2 in large quantities as the most influential photo catalyst under UV light in the industries such as desalination [10], in view of its good photo activity that is essential for most photo-catalysis reactions. It is also nontoxic and cheap to users, useful as environment friendly catalyst [11], and useful in medicine, foods, and inks and oily/water treatments.

Turkey, Italy, China, Spain, and India are the top five marble exporting countries that are dominating the marble production [12]. It was reported that India accounts for about 12% of marble produced globally. In the world, India is the third

largest producer of marble having 80% contribution of Rajasthan in this quantity [13]. After mining process, cutting and sawing operations are performed on marble. These operations generate marble powder as by-product. About 25% of the entire excavate marble ends up as marble slurry. In Rajasthan, in the year 2015, about 15.6 Million Metric Tons (Mt) marble was excavated, due to which 4- 6 Million Mt of marble slurry was generated [14]. Huge land area is occupied when this marble slurry is disposed of and let dried up. This marble slurry affected fertility and morphology of soil in the local area by reducing permeability and porosity. Therefore, discovering a suitable area of application for these types of waste marble material is currently of extreme important task for engineers. There has been an alarming rise in waste generation. Few research works have been carried out on utilization of marble powder by incorporating waste into polymer to get cheap final product.

Polymer composite has been widely used to produce useful products, having material consists of excellent mechanical and thermal properties. The effects of the fillers on mechanical and thermal characteristics of the composites depend on filler particle sizes and shapes, surface roughness along with degree of uniform dispersion. Polypropylene is one of the most widely used polymers because of its low down cost, steady and balanced mechanical and thermal properties, and easy processability. To enhance different properties and thus extending its application, combination of different type of fillers are added.

Most of the products we use in our daily life require some components, which are produced by injection moulding. Injection moulding has the highest efficiency, largest yield, and highest dimensional accuracy among all the processing methods [15]. Injection moulding is a suitable method to produce polymer composite with filler material [16]. Polymer composites can be produced with fillers and additives to improve the processability and performance of the final composite.

The main purpose of this thesis is to develop a new Polypropylene based composite with injection moulding having better physical, mechanical, chemical, thermal and morphological properties and to compare their performances. The use of micro-sized marble as filler material in Polypropylene composites is novel. Finally, the outcomes of the research work would comprehensively lead us to the understanding of practical optimization of performance parameters and its correlation to the compositional attributes, which would guide the research community for developing new generation composite material for the realistic

design of functionally advanced composite material for different engineering applications.

1.3 Thesis Outline

The reminder of the thesis is structured as follows:

Chapter 2 : Includes literature review considered to provide an outline of the basic knowledge existing involving the issues of present research interest. It describes the research works on physical, mechanical, thermo-mechanical behaviour of various types of Polymer composites by addition of different fillers. Research on injection moulding process is also discussed that was conducted by various researchers.

Chapter 3 : Includes an explanation of raw materials, fabrication by injection moulding and procedures of testing. It reveals details of fabrication and characterization of the polymer composites under examination and an explanation of the Taguchi experimental design.

Chapter 4 : Describes the physical and chemical characterizations of Polypropylene composites.

Chapter 5 : Presents the mechanical and thermo-mechanical analysis of Polypropylene composites.

Chapter 6 : It presents a detailed study on the effect of fillers on the morphological behaviour of Polypropylene composites.

Chapter 7 : Parameters of injection moulding are optimized by Taguchi method.

Chapter 8 : Presents summary of the findings of this research work, outlines explicit conclusions deduce from the investigations and optimization efforts and suggests thoughts and future directions.

The next chapter briefly discusses the literature review of various research papers on physical, mechanical, thermo-mechanical and morphological analysis of a series of experimental polymer composites. The specific objectives of this work are clearly outlined in the next chapter.

*****

Chapter 2

LITERATURE REVIEW

This review seek out to describe, summarize, evaluate, clarify and integrate the content of primary and previous reports on physical, mechanical, chemical and shrinkage behaviour of various polymer composite materials for the different applications. Intensive researches are still being carried out to develop an understanding for successful design and selection of polymer and new filler materials. Researchers have already shown interest for development of new polymer composites and study their different mechanical and thermal properties.

The Major goals designed for polymer composites are (i) material selection and (ii) to get aesthetic properties. Other important considerations are mechanical properties, thermal properties, shrinkage behaviour, reasonable cost, availability and biocompatibility.

The topics embraced in this literature review are:

2.1. Influence of filler constituents on the performance of polymers

Now a days, Polymer composites are considered as an imperative class of sustainable materials. They present exceptional mechanical and thermal properties, exceptional flexibility in design capability and simplicity of fabrication. Besides this, it has light specific weight, impact and corrosion resistance and high resistance to degradation.

The use of organic or inorganic fillers in most of the polymeric systems is prevalent in industry. For many diverse applications such as sporting goods (Skis, surfboards, windsurfing, table tennis boards, all kind of sports helmet), aerospace

structural components, panel and body structures of automobiles, etc. polymer composites are manufactured for the last 25 years. There has been a strong emphasis on the development of polymeric micro and Nano-scale composites, where at least one of the dimensions of the filler material is of the order 1-10 nanometers. In the early 1980s, the progress in the field of technology has been deeply facilitated by the advent of scanning electron microscopy and scanning probe microscopy. In general, the exclusive combination of the micro and Nano-material's characteristics, such as particle size and shape, mechanical properties and concentrations essential to effect change in a polymer matrix, coupled with the advanced characterization and simulation techniques, have generated much attention in the field of composites.

According to Li D. et al. [17] polymer composites are also useful for permeable membranes, which are the interior elements of the membrane water desalination i.e. reverse osmosis (RO) procedure and advanced osmosis process. The Chemical characteristics of the permeable thin membranes decide salt rejection, fouling resistance, water flux, and the chemical strength, which significantly affect power expenditure and operative costs in osmosis parting process. In present era, significant progress was made in the growth of high-efficient hybrid polymer composite thin membranes for the applications of desalination.

Polypropylene (PP) possesses balanced mechanical & thermal properties, better processability at reasonable cost and environmental friendliness. However, its use in the production of newly rising materials, such as blends and composites, where filler plays prospective role in controlling their properties, is progressively growing to meet engineering requirements [18]. Polymer composites have gained lot of consideration to engineering investigators in recent years, because the integration of fillers modify the structural, mechanical, thermal and electrical properties of the composite materials [19, 20]. Many investigations have been conducted based on filler technology that increasing the filler content, decreasing the size of filler treatment of filler, or filler treatment to get better mechanical performance; thus the filler particles participate an important role in determining the mechanical properties of composite materials [21, 22]. According to Ashby et al., as a filler material, alumina is strategic additive to get better ductility and strength in the composite [23]. Incorporating alumina as filler to the polymer produces new composite having enhancement in mechanical properties such as stiffness, impact and compressive strength, hardness and flexural modulus [24].

Alumina particles (Al_2O_3) are among the most important metal oxides with promising applications and the exceptional physiochemical properties in fabrication of composite materials. Therefore, alumina is effective filler in the polymer composites having suitable dispersion and proper interfacial interaction between reinforcement and polymer matrix. Mirjalili et al. [25] prepared polymer composites with alumina particles and evaluated their tensile and flexural properties. It is hard and wear-resistant, has excellent dielectric properties, resistance to strong acid and alkali attack at elevated temperatures, high strength and stiffness [26]. Alumina was incorporated in HDPE matrix and better elastic modulus and improved hardness were obtained [27]. Ammonium polyphosphate (APP)-based additives and Al_2O_3 were used in Polymethyl Methacrylate (PMMA) and thermal stability was improved [28].

Abenojar et al. [29] investigated epoxy-based composite materials reinforced with hard particles of SiC as anti-wear coatings. In their study, a commercial bicomponent resin was used, with 6 and 12% SiC particles in two different particle sizes. They evaluated hardness, bending strength and wear resistance of the composite. Similarly, by introducing Nano sized SiC fillers into an epoxy matrix, superior thermal and mechanical properties in the matrix was achieved [20].

In study of the erosion wear response, development of hybrid composites was performed with SiC ceramic, which improve the erosion resistance of glass–polyester composites significantly [30]. With discovery of carbon nanotubes (CNT) a new path has been paved in the direction of micro, nanostructures and electro mechanical systems (NEMS) [31]. Due to surprising physical, mechanical and electrical attributes, CNT's can be used as oscillators, reinforcements and sensors. In investigation conducted by Razlan et al. [32], using chemical vapour deposition, during hybridization of CNT and Al_2O_3 was synthesized; epoxy composites exhibit higher compressive strength and compressive modulus. Similarly, thermal stability was also improved in the composite system.

Effect of thermal treatment on mechanical properties and impact resistance of polypropylene-calcium carbonate composites ($CaCO_3$) was studied by Nascimento et al. [33]. In another work of Eiras and Pessan [34] with the use of optical microscopy, has showed that the integration of $CaCO_3$ particles decreases the sizes of polypropylene spherulites and rises the crystallinity of polypropylene and affects the crystallization behaviour of the developed composite.

As a waste of electric power plants, fly ash particulate having aluminium silicate ceramics, also used to fabricate polymer composites. Its usage has the added benefit of diminishing the pressure on the environment. In addition, fly ash has been used in industry because of such advantages as relatively low cost, low density, good flow-ability, round surface of particles and scattered internal stress in the composites and better processability of the composite. Improvements in damping property were also observed by use of fly ash [35].

Based on vermiculite–fly ash combination, the tribological performances of composite friction materials in terms of friction-recovery, friction-fade and wear behaviour was studied. Hardness drops with the integration of vermiculite while shear strength and compressibility remained unchanged [36].

Similarly, during study of mechanical and tribological behaviour of composite friction materials having combination of lapinus and flyash, better mechanical properties were exposed by the composites [37].

Reinforced thermoset composites holding inorganic fibres known as bulk moulding composites (BMC) are applied in bumper of automobile and structures of civil engineering industries. The fabrication of these materials is rising rapidly. BMC materials typically contain polyester resins with short glass fibres, colorants, inhibitors and high amount of fillers, e.g. calcium carbonate or fire retardant alumina trihydrate [38]. The filler integration to the matrix should provide the product with mechanical strength, psychical properties and quality. Fillers such as talc, carbon black, marble powder, glass, wood flour and metals are added to polymers at range from 10 to 50 wt%. The introduction of glass fibres into composites leads to good mechanical properties, while inorganic fillers reduce the product final price.

According to Zuniga et al. [39], TiO_2 (Titanium dioxide) is also useful and possibly the most attractive filler due to combination of its exceptional properties such as chemical, corrosion, non-toxicity, non-flammability and photo stability, superior electrical properties, compatibility with a range of materials, good photocatalytic property, better refractive index and capability to absorb ultraviolet (UV) light. It was also investigated by Pi et al. [40] that due to exceptional hydrophilicity, TiO_2 particles have involved in the modification of surface of polymer membranes for the antifouling application.

TiO_2 has many useful properties such as good photo activity that is essential for most photo-catalysis reactions, nontoxic and economical to users. As a result, it is

used in large numbers by scientists and researchers as the most influential photo catalyst under UV light in the industries [41] such as desalination of sea water [42], biomedical areas, useful as environment friendly catalyst and useful in medicine, foods etc. [43].

Huang et al. [44] investigated the kneading and moulding of PP (polypropylene) with nano-TiO_2 powder having sizes in the range of 50 nm. The wear abrasion of composites with 10wt. % and 40wt. %, filler loading was also tested. Zhao et al. [45] explored TiO_2 coated silicate micro-spheres particles to enhance the light diffusion property of polycarbonate (PC) composites. Kuo et al. [46] used Anatase TiO_2 films to grown at room temperature on PC substrates, with Radio frequency (RF) magnetron sputtering under different conditions and photocatalytic performance was enhanced.

For the last few years researchers struggling hard to determine the feasibility of a wide range of industrial by-products like fly ash, rubber and marble waste as a potential substitute for polymer ingredients [47]. For waste disposal, marble slurry is at high alarming distress, raising enormous environmental anxiety and threat for human health. It was reported that India accounts for about 12% of marble produced globally and thus, it is the third largest producer of marble having 80% contribution of Rajasthan in this quantity. Granite powder filled carbon epoxy composites were prepared and investigated by Pawar et al. [48] and impact strength of composites was observed in increasing trend for the reinforcement.

2.2 Study of Physical and Chemical behaviour of polymer composites

To evaluate the performance of polymer composites physical and chemical behaviour play important role. Density, porosity, Absorption coefficient, melt flow index (MFI) are generally determined by researchers for physical behaviour.

Density is a non-mechanical property of great significance. In many applications, the density criterion combined with stiffness and strength provides a sound basis for comparison of polymers with different materials, such as metals and alloys. In case of plastic materials particularly, the density is often a major significance as an indication of the end-use possibilities of the material. Density also depends upon the blend compositions and method of fabrication.

On a microscopic scale, mainly load bearing structural materials are heterogeneous. Under load, structural irregularities such as voids, discrepancy of local composition or orientation, inclusions, or random defects initiate stress and strain

concentrations, which affects the mechanical properties. Voids are pore that remains unoccupied in a composite material.

Medina et al. [49] enhanced physical properties of gypsum composites through a synergic work of polypropylene and recycled graphite filler. It was found that addition of graphite increases the density and ultrasonic modulus of the composites as it fills the microstructure of the composites. Moreover, the porosity and the water absorption were also reduced through the immediate filling effect of filler.

According to Michler et al. [50] the total number of coarse particles or voids in composites is huge, even small modifications of their local surroundings will add up to influencing mechanical performance. These effects, the resulting mechanical deformation mechanisms and the mechanical and thermal properties of typical Nano-structured polymers are subjected to discussion. Generally, void gap weakens the load bearing capability of a polymer composite; for this reason the phenomenon of density and voids has been widely studied [51, 52].

Fourier transform infrared spectroscopy (FTIR) is a method, which is used to obtain an infrared spectrum of the absorption or emission of the composites. FTIR spectrometer simultaneously collects high spectral resolution data over a wide spectral range. FTIR is considered as an easy, direct, and sensitive characterization technique, and it is widely used to clarify the structure and interactions in composites materials [53]. Thus, it shows the functional group of composite materials.

The FTIR spectra of the samples of PP and PP-lignocellulosics composites conducted by Darie et al. [54], the assignment of the bands were found for stretching vibrations of the methyl and methylene groups. In the 3850–2700 cm^{-1} four prominent bands at 2958, 2918, 2874, and 2848 cm^{-1} assigned to asymmetric and symmetric stretching vibrations of methyl and methylene groups, respectively.

In the ‘‘fingerprint’’ region, the composites spectra are more complex. The most prominent bands assigned to different stretching, bending, rocking and wagging vibrations in matrix are easily identified, but most of them are overlapped with the bands belonging to the filler /fibre component [55].

In the study of characterizations of dental composite toughened with silane-alumina filler conducted by Kumar [24], it was observed that the existence of the Si–O–Si peak at near about 1046 cm^{-1} showed that silane was effectively adsorbed on the surface of the filler. The effect of additive with silanol group produced bands due to Si–O–Si in the composite.

Xu et al. [56] observed during the FTIR spectra of oxidized Carbon Black, grafted Carbon nanotube and carbon filler, that after the oxidation, the carbon black showed a wide absorption band in the range of 3450-3100 cm^{-1}. It was found having the hydroxyl and carboxylate groups. The 1425 cm^{-1} peak was attributed to the in-plane deformation of C-OH. The peaks between 2945 and 2810 cm^{-1} were due to the stretching vibrations of C-H species belonging to coupling agent. The wide peak between the 1120 to 1050 cm^{-1} originates from Si-O-Si band.

Zapata et al. [57] synthesized composites of polypropylene (PP) by the melting process in the occurrence of titanium dioxide nanotubes. The FTIR spectra were obtained in the 1250-3750 cm^{-1} range. The increased absorbance at 1700 cm^{-1} was indicative of carbonyl group species being generated because of the photo-oxidation of the polymer. Similarly, the appearance of an absorption peak in the 3200-3600 cm^{-1} ranges was detected, indicating the formation of hydroperoxides as degradation of products.

2.3 Study of Mechanical behaviour of polymer composites

Significant research has been dedicated in fabrication of the polymer composites for functional and other useful applications. Different characterization of reinforced composites with metal oxides depends on degree of uniform dispersion of particles in the polymer structure and their interaction at interface within the polymer. On the other hand, in the last few years of research, the full potential of metal oxides and ceramics as reinforcement material was limited, due to problems related to inadequate dispersion of micro and Nano-metal oxide during the process and weak interaction at interface between the matrix and fillers. It was observed that with micro fillers, particles can regularly distributed into matrix, with the process of separation of micro particles [8].

In order to gain a more insight to model the thermo-mechanical properties of nanocomposites, Bernardo et al. [58] have modify the existing mechanics models and FEA (finite element analysis) for the microscale to nanoscale was adopted. It was observed that new formulations can be associated into advance software packages for to prediction of thermo-mechanical properties of the composites. Precisely modelling the interfacial region also recognized as the interphase, between the polymer matrix and fillers. Thus, it was investigated that it is possible to capture some more aspects of the actual behaviour of the composites.

In the insight of sustainable construction, a study was performed by Yap et al. [59] to compare the effect of Polypropylene and Nylon-fibres in enhancing the mechanical properties of oil palm shell fibre-reinforced composite. It was observed that the addition of Polypropylene and Nylon-fibres enhanced the mechanical properties of composite. The enhancement was primarily attributed to the fibre by bridging process that allowed additional stress for the cracks to propagate.

Polymer composites containing alumina micro and nanoparticles are a new group of the hybrid materials that show incredible improvement in properties with low Nano-fillers loading [60]. Chandra et al. [61] explored polymer surface coating technique to facilitate dispersion of Styrene-maleic anhydride (SMA) coated with alumina particles in polycarbonate (PC) and the improved optical properties of the resultant composites were obtained.

Mohseni et al. [62] presented the effects of incorporating two cementations materials: rice husk ash and alumina in polypropylene fibre reinforced cement mortars. Rice husk is an agricultural waste material and recycling of this material has considerable economic and ecological benefits. Flexural strength, compressive strength, water absorption and warpage of the hardened composites were improved.

Zhang et al. [63] investigated the effects of filler particle size and content on the different properties e.g. thermal conductivity, tensile strength and impact strength, of high density polyethylene (HDPE) - Al_2O_3 composites. It was observed that tensile strength and thermal conductivity of the composites increase with the decrease of particle size. It was also observed that particle size affects impact strength significantly. The SEM micrographs of the surface showed that Al_2O_3 with tiny particle size is more efficient for the improvement of the impact strength, while the bigger particles prone to aggregation due to their high surface energy decline the impact strength. Composite filled with Al_2O_3 having size of 0.5 μm showed the better synthetic properties. It was concluded that the integration of Al_2O_3 to HDPE would lead to better mechanical properties once properly dispersed.

Khumalo et al. [64] explored the effects of BA (boehmite alumina) on the thermal, morphology, thermooxidative and rheological behaviour of Polyethylenes (PEs). BA was integrated up to 8 wt. %, in both LDPE and HDPE through melt mixing method. It was observed that agglomerated BA was finely dispersed in the corresponding PEs. BA acted as a weak nucleating-agent because it reduced slightly

the under cooling (difference between the melting and crystallization temperatures) of both LDPE and HDPE.

Ngu et al. [65] studied the thermal properties of LDPE-Al_2O_3 composites produced by intercalation process. The addition of alumina particles increases the thermal stability of LDPE. Although, the onset temperature of the hybrid composites decreased with increasing filler contents.

Fu et al. [66] presented a review of the experimental outcomes based on particulate micro and Nano-composites. They investigated the effects of three factors, i.e. particle size, particle-matrix adhesion and particle loading on composite stiffness, strength and toughness of different particulate composites. It was observed that composite toughness and strength are strongly affected by all the three factors, especially particle-matrix adhesion. This was expected because strength depends on successful stress transfer between filler and matrix, and toughness-brittleness was controlled by adhesion between them.

According to Daneshpayeh et al., [67] addition of a small amount of TiO_2 particles (max. 4 wt. %) enhanced the mechanical properties of composites. However, deterioration takes place in the mechanical properties by further adding of TiO_2 particles in matrix due to the agglomeration of particles. According to Patel and Dhanola, [68] the good bonding strength between matrix, micro fillers, and fibre and flexibility of the interface molecular results in absorbing and dispersing more energy, and prevents the early initiation of cracks more effectively.

In the research of Threepopnatkul et al. [69], the effect of TiO_2 and ZnO on physical, thermal, mechanical and sterile properties of PET(Polyethylene terephthalate) and PBS-(Polybutylene succinate) blend film was investigated. Filler TiO_2 and ZnO were added at near 2% and 3 wt. % on PET-PBS (having ratio of 90:10) blend thin film. The addition of ZnO made film more transparency than TiO_2 because ZnO particles were actually bigger than TiO_2 particles. It was also established that TiO_2 increase thermal stability of PET-PBS blends. However, the decrease of flexural strength that low wt. % TiO_2 addition can be originate by the weak interfacial adhesion between the particles and matrix. The weak interfacial adhesion causes a greater extent of cavitation or voiding.

There is huge possibility to use marble wastes as a cement substitute in cement and concrete production. In the present scenario, various researchers conducted the characterization of marble wastes and various practical formulations of cement

composites and concrete mixtures. With regard to cement composites pastes, the marble wastes can be used to get better physical and mechanical properties of both cement composites and polymer composites. According to Mashaly et al. [13], the optimum percent of marble wastes that can attain the most suitable results of physical and mechanical properties having the control mix of 25%.

Ahmed et al. [70], prepared Polypropylene reinforced marble powder (PP-MP) and the effects of MP loading and compatibilizer polypropylene-g-maliec anhydride (PP-g-MAH) on mechanical properties were investigated. It was observed that tensile strength, tensile modulus and flexural strength increased with increasing the MP loading but tensile strength increased up to a limit. Further addition of MP in PP composites decreased the strength of composite. The percentage elongation at break and Izod impact strength reduced with increasing of MP loading. Studies exposed that PP-MP composites containing PP-g-MAH improve the properties compared to without compatibilizer.

The temperature is a key factor that influences the mechanical behaviour of marble and thus affects the stability of composites. Based on compression tests on undamaged and thermal-damaged specimens of a fine and coarse marble conducted by Peng Jun et al. [71], the mechanical properties of the specimens were investigated. Heating upto the temperature of 500°C, the color of the specimen changes from milk white to dark gray and the longitudinal wave velocity significantly reduces. With optical microscope observations on thin sections of the composites, it was found that microcracks and grain boundary exist in the thermal damaged specimen. Achaby et al. [72] investigated the Mechanical and thermal behaviour of graphene-based polypropylene composites and found the improvement in properties significantly.

2.4 Study of Thermo- Mechanical behaviour of polymer composites

This literature study describes various experimental results of thermo-mechanical behaviour of polymer composites. Conceptually, storage modulus (E') and loss modulus (E") represents the degree of elastically recoverable response and viscous-response caused by the dissipation by means of frictional and internal motions of the polymer-composites. In the material, storage modulus represents the energy stored elastically, whereas loss modulus represents the energy loss as heat. Storage modulus reveals the rigidity or relative stiffness of a composite.

TGA (Thermo-gravimetric analysis) is a technique to establish relationship between the loss of weight in a composite material with respect to temperature having a constrained surroundings and find out the thermal stability and composition of composites. Thus, TGA is used to observe the change in weight of a specimen as a function of temperature. In order to assess the physical, chemical and structural changes, the thermal investigation for the composite is conducted with an imposed change in temperature. TGA curves for different temperature of composite have generally three distinct stages viz, thermally-stable stage-I, decomposition stage-II, and thermal-degradation stage - III.

Pawar et al. [73] conducted study for wind turbine blade. They prepared two sets of jute epoxy composites varying first with fibre wt.% from 10-50 wt.% and second in the white marble-dust included in range of 0-24 wt.% having intermission of 8 wt.% in natural jute composites. Storage modulus was found approx. 86% and 12% enhancement for 28 wt.% fibre reinforced and 15 wt.% marble-dust filled composite in comparison to approx. 11 wt% jute fibre reinforced and without (0 wt%) marble-dust reinforcement, respectively. During TGA, there was no major variation in degradation curve of the natural jute-fibre composite and it was found that degradation begins somewhat earlier as the jute wt.% increased, it was probably due to decomposition of cellulose and hemicelluloses. More noteworthy difference was investigated in degradation of marble-dust filled composite and loss of weight for marble composites begins in advance but the degradation rate was observed to be decreased in comparison to virgin composite.

Ozdilek et al. [74] explored the effects of both untreated and surface grafted BA (boehmite alumina) on the mechanical-thermal behaviour and the morphology of polyamide 6 composites, showing that polymer crystalline phase is significantly changed and the storage modulus can be increased with integration of fine BA particles. Khumalo et al. [64] found that filling with BA strongly improved the stability to thermo-oxidative degradation of the corresponding PE matrix.

Mirjalili et al. [75] found that composites get improved properties with increasing of the Al_2O_3 loading. Storage modulus and loss modulus of composites are enhanced with increasing the loading percentages of Al_2O_3. These studies show development in the stiffness and energy-dissipation of the composites deformed under the stress. The effect of the dispersant (SDBS) on mechanical properties of PP-

nanoAl_2O_3 composites showed that SDBS is similar to a surfactant that crack the agglomerates and supports mapping of alumina with Polypropylene.

Xu R et al. [56] prepared carbon filler (Type S-filler) with treatment of passivation of the thin surfaces of CNT and the carbon black (CNT-CB) and resultant thermal conductive composites of the PP-Al_2O_3 with type S-filler were prepared. With mixing of 13 wt.% of type S-filler, composite showed high electrical resistivity as well as high thermal conductivity.

Flexible polyurethane (FPU) foams are generally used in transportation, construction, and electrical power industry. Xie H. et al. [76] explored a new method for the preparation of polyurethane-alumina aerogel (FPU-Alag) composites with better dispersion of alumina aerogel. Development in fire safety performance over pure FPU foams was investigated. These composites showed improved thermal degradation stability. A significant improvement in flame retardancy and smoke suppression properties of FPU foams were achieved with the addition of Alag. It is notable that the enhancement strongly depended on the combined effects of insulation, retention and adsorption of the ‘‘in-situ” formation of C-Alag in FPU matrix during combustion. It can be anticipated that alumina aerogel holds great potential for thermal insulation and fire retardancy purposes in polymeric composites.

Cui et al. [77] fabricated PCL/NaCl (Poly-ε-caprolactone-Sodium chloride), PCL-PEO-NaCl (Poly-Ethylene Oxide- PCL/PEO/NaCl-Hydroxyapatite (HA) composites with the process of injection moulding and characterized. To develop micro porous structures, water soluble and sacrificial polymer, PEO, and NaCl fillers in the composites were leached by treated water. Investigation was performed to know the effect of leaching time on residual contents and porosity of the composite, with the effect of addition of HA. It was found that leaching time depends on the spatial allocation of sacrificial PEO phase and the NaCl filler. The adding of hydroxyapatite (HA) has appreciably enhanced the storage modulus and loss modulus of PCL/HA composite. Elastic and loss modulus of PCL/HA composite was observed better than PCL composites (greater than 20% in elastic modulus and 36% in loss modulus). Thus, HA increases the mechanical and thermal properties of PCL composite.

Akil et al. [78] used different coupling-agents like silane Z-type (Aminoethylaminopropyl-trimethoxysilane), 3-GPS (Glycidyloxypropyl-trimethoxysilane), and TiO_2. The outcome of coupling-agents on the behaviour of PP-

Al_2O_3 has been studied. When both coupling-agents were added, it was observed that tensile strength of PP-Al_2O_3 composite has enhanced considerably. PP-Al_2O_3 composite along with titanium as coupling-agent exhibited better tensile strength and flexural strength in comparison to silane-treated and untreated PP-Al_2O_3 composite.

Polymer composites reinforced with customized inorganic particles combine the functionalities of the polymer matrices, which include lightweight and simple formability, with the exclusive features of the ceramic particles. The composites obtained by integration of these different materials can lead to improvements in several applications, such as electrical, mechanical, rheological, magnetic, fire retardancy and optical properties [79].

The dynamic factors such as storage-loss modulus and the damping factor (Tan delta) depends on the temperature and give an idea about chemical bonding between the fibre or filler and polymer-structure of composite material. Saba et al. [80] investigated that dynamic parameters influenced by changing the length of fibre and loading. Dynamic loading situations are rapidly uncertain in civil-infrastructure systems due to winds, sound waves, earthquakes and live-loads.

Duc et al. [81] explored the mechanical and damping properties of unidirectional (UD) and flax fibre reinforced thermoset (epoxy) and PP (polypropylene) and PLA (polylactic acid) composites having approx. 45 vol% of the fibres. It was evaluated with carbon fibre (CF) and glass fibre (GF) reinforced epoxy composites. It was observed that the composites reinforced with FF showed better damping as shown by DMA with respect to the composites reinforced with synthetic carbon and glass fibre. The adding of UD FF to epoxy shows 95% rise in loss factor with respect to both matrix and GF reinforced epoxy. It was found that flax fibre (FF)-PP showed the maximum damping value at 27 °C and 1 Hz of all the composites.

The rising attention in the suitable use of the natural fibre, paralleled to carbon and glass fibres are primarily due to its less cost, lightweight, elevated modulus, biodegradability, less power requirements, wide accessibility and the resistance to the deforestation with the other usual benefits. Integration of the natural fibres as the reinforcing agent in both the thermoplastic and thermoset composites has obtained better and wide applications in many areas of Engineering. Polymer composite materials based on different type of natural fibres was developed using synthetic approach to extend its application in many useful areas. Natural fibres such as fine jute, polished sisal, coconut, banana, pineapple leaf, fine bamboo fibre, palm, date,

fibre of sugarcane and fine cotton are usually reinforced in the polymer matrix for improvement in mechanical-thermal characteristics to match specific needs in the products [82-84].

Lu and Oza et al. [85] explored the effect of silane and diluted NaOH treatments of thin hemp fibre. Hemp-high density polyethylene composites were fabricated and their thermal and thermo-mechanical properties were observed. The results exhibited that thermal stability of composites decreased with increase in fibre loading and treated composites were found better thermal stability in comparison to untreated hemp composites. Increase in the storage modulus of the treated composites was observed, in comparison to untreated composites, during Dynamic mechanical analysis.

The thermal and viscoelastic behaviour of PP is stoutly influenced by variables that have an effect on the crystalline regions with crystallinity, lamellar thickness and the interface [86, 87]. During investigation of the storage modulus of TiO_2 filled Polypropylene composite, three region, i.e. glassy region, transition region and rubbery region was observed. Significant improvement in storage modulus with increasing TiO_2 was observed in glassy region which is possibly due to restriction of the molecular chain motion which generates a reinforcing effect [88, 89]. Glass Transition temperature (T_g) can be identified by the peak of Tan Delta. Wide area was observed below T_g. In all the PP-TiO_2 composites E' decreases with increase in temperature [90, 91]. It was also observed that glass transition temperature slightly shifts towards the higher value, indicating a decrease of the chain mobility imparted by the cross-linked and filled TiO_2 fraction in the composite [92, 93].

It was observed by researchers that TiO_2 filled composites confirm enhanced thermal stability. It can be observed that onset of degradation temperature of PP-TiO_2 composites was found higher than virgin PP. The increased Endset of degradation also reveals to the improved thermal stability of the composites [94].

Majid et al. [95] prepared PP-zinc oxide composites containing 5, 10 and 15 wt.% particles with melt-blending. The ZnO particles were uniformly dispersed, but with different level of coalescence. The different plots of experimental and theoretical storage modulus values at approx. 25^{o}C for various loadings of particles were observed. Dynamic rheometry illustrated that the rheological modulus of the composites increases with increase in filler concentration in the high frequency region.

In the middle of the most widely practical marble stone conservation products, we can certainly count the different organic consolidates based on epoxy resin, acrylic and micro fluorinated polymers. However, they are most widely used, the side effects related to low compatibility between polymeric composite and marble particles are still to be resolved. Due to the difference between the coefficient of thermal expansion of the organic micro layer and that of inorganic support. Meloni et al. [96] conducted thermal decomposition of different specimens of white marble powder in which TGA tests were performed up to 1150^{o}C and pyrolysis reactions was proposed based on the decomposition of whewellite (marble).

According to Barrera et al. [97], fibre reinforced concretes (FRC) show property improvement created by thin fibres. By using different gamma radiation, it was further better mechanical characteristics of hydraulic concretes elaborated with water-cement, fine silica sand, white marble and polypropylene fibres. It was found that improvement takes place in the strength and the elastic modulus dependent on PP fibre quantity and marble particle shape and sizes.

Kelestemur et al. [98] shown that the compression strength of the fine mortar specimens increased and simultaneously it leads to a reduction in porosity values. This was due to gray marble powder particles which act as perfect micro-filler in the interfaces between aggregate and the cement paste and deep pores in the bulk paste. It was observed that, when glass fibres were added to the mortar specimens, the compressive strength decreased and porosity value increased. This result can be attributed to the weak adhesion between the glass fibres and fine mortar.

2.5 Study of Morphological structure of polymer composites

Physically blending can established a proficient way to fulfil new thermo–mechanical property needs for the polymer materials. Though, polymer blends are generally immiscible and have biphasic morphology that establishes physical and mechanical characteristics. It was observed that the morphology of component polymer blends can be significantly affected by using micro-and Nano-fillers [99]. Most of them recommended that the localization of particles at interface of hybrid phases could minimize the apparent interfacial tension which can put off coalescence of dispersed phases.

An innovative method has been developed by Kalaitzidou et al. [100] for optimization of dispersion of particles in PP. It consists of coating polymer molecules

with micro-particles using a liquid phase non-solvent under the ultrasonication. Improved flexural strength and modulus were obtained by melt mixing and injection moulding. The improvement of the flexural properties was observed due to the regular dispersion of the particles in the solid state.

Fenouillot et al. [101] concluded that at the thermodynamic stability, filler dispersion in immiscible polymer blends was control by reducing the free energy produced by the existence of interfaces between the polymer and fillers. The particles can distribute unevenly among the phases and creates micro layer at the fluid interface that subsequently reduces shared area between hybrid phases. The segregation is connected to the wettability of the fine particles by polymers and it may be predicted. However, the lack of reliable method to determine precisely the filler–polymer interfacial bonding energy is a valid issue at high temperature. Thus, polymer–filler interfacial energy is most often predictable from surface tension of the fillers and this maybe one of the reasons why discrepancies can be exhibit between theory and the real situations.

Kudilil et al. [88] prepared TiO_2 nanoparticles with wet-synthesis technique and the micro particle size was determined by TEM (transmission electron microscopic) technique. Polypropylene-TiO_2 Nano- composites were prepared using different wt. % of TiO_2 by melt mixing. It was then processed by compression moulding into micro-films at 180^{o}C. Thermal- ageing was carried out in an air oven at 110°C for 20 hours. Mechanical and thermal properties of the specimens were investigated before and after thermal-ageing. Surface characterization of the tensile-fractured surfaces was analysed using SEM showed stability of PP-TiO_2 composites after thermal-ageing. Better dispersion of TiO_2 in the PP matrix was evident from SEM images. TGA of the samples showed that thermal stability of PP was improved by the integration of TiO_2.

Rajeshwari et al. [102] prepared HDPE-AlN (aluminium nitride) composites having wt. % loading of AlN particles by melt blending and technique of warm compression. The microstructure analysis by using both SEM and TEM exposes that nitride particles in HDPE show a tendency of the formation of the chain-like structure, having few agglomerations, particularly for composites with higher wt. % of the filler content.

To improve toughness of polypropylene (PP), a capable method was developed by Xu et al. [103] by integrating polypropylene copolymer and the beta-

nucleating agent all together into Polypropylene structure. Outcome showed that composite chains promote better crystal refinement and the rubbery phases with the propylene-ethylene segments gives better mechanical properties viz. impact strength and tensile strength. This establishes that the property of crystalline morphology, which correlate with the beta-nucleating agent content, is also significant factor that decides improved tensile strength along with toughness.

In the similar way, Kersch et al. [104] shown the effect of two chemical Benzenetrisamide beta-agents in contrast to a bisamide beta-agent and the effects on the mechanical and morphological properties of PP was explained. Thus, the PP and composite having Benzenetrisamide alpha-agent was explored. Investigations conducted by using wide-angle deep X-ray scattering which also confirmed that two Benzenetrisamides and the beta-agent make the refined beta crystal improvement of polymer, while only the alpha modifications was followed for the PP polymer and the Benzenetrisamide alpha-agent. SEM pictures of specimen visibly show a fine shish kebab structure occupied by PP with refined Benzenetrisamides. It was observed in two samples, Charpy impact investigations shows marked rise in toughness as compared to bisamide beta-agent. An amazing rise of 140% in the izod impact strength was observed for materials having benezenetrisamide beta-nucleating means. The behaviour can also be correlate with molecular structure of polymers. Because of rapid cooling in moulding process, only the benzenetrisamide additives can form structures similar to needle shape, that exhibits fine shish-kebab matrix in composite.

To prevent the agglomeration of the CNT due to Vander-Waals attractions, Razlan et al. [32] conducted study on the hybridisation of carbon nanotube (CNT) by using Al_2O_3 with the method of chemical vapour deposition. The Al_2O_3 particles act as “vehicles” for the CNTs which dispersed homogenously in the epoxy matrix and also improved the particle-matrix interface. In SEM images, it was observed that the CNT fully enveloped the Al_2O_3 particle. Furthermore, it can also be seen clearly that fully covered Al_2O_3 particle and CNT were attached to the Al_2O_3 particle. Thus, it proves that CNTs were directly grown on the Al_2O_3 particle. Wire-like structure and growth in unsystematic directions was found of CNT, which creates hollow and multi-layered wall structure.

Motsa et al. [55] prepared a composite of the polypropylene and the CLI (clinoptilolite) for the adsorption of lead by using the melt-mixing smooth compounding technique. During investigation with SEM, it was found that the surface

of 12% clinoptilolite–PP composite with the clinoptilolite fine particles surrounded in surface of PP matrix. The fine filler particles are properly dispersed in matrix with few agglomerates. Microvoids also generated due to rotor mixing during synthesis.

Pedrazzoli et al. [105] explored the effect of synthetic boehmite-alumina (BA) particles with a variety of surface cure processes on crystallization and morphology behaviour and mechanical characterization of PP-composites. With melt mixing and film-blowing, a series of PP-BA composites, were prepared containing up to 12 weight percentage of untreated and of octyl-silane- functionalized BA particles. SEM indicated that BA particles were finely dispersed, though agglomerated, in the PP composites. Surface-treated BA particles were dispersed in matrix in comparison to the untreated BA composites. The results showed that the tensile tests, particles could congeal PP even at small weight percentage filler content with treated BA, without a significant loss in ductility. Creep-tests revealed that creep compliance was really reduced by filler integration. Storage and loss modulus were increased in composites, representing the reinforce-effect of the fine BA particle [64,106,107].

Saffar et al. studied the various effect of grafting TiO_2 Nano particles on the PP in different wt. % [93]. The properties of composites depend on degree of crystallinity, internal structure and spinning conditions [108]. By the addition of TiO_2, tenacity of the PP is increasing which reveals reinforcing effect of TiO_2 in the composites. Dispersion of TiO_2 particles has a significant effect on the mechanical properties of the composites. A fine distribution and dispersion of TiO_2 particles in the matrix breaks aggregates and agglomerates to present a better interfacial area between TiO_2 particles and the immediate polymer phase [40, 109].

Tekin I. [110] produced a geopolymer composite paste by using marble wastes. Curing process was done in an oven. The compressive strengths of the specimens in the wet conditions were reduced depending on time, but in dry conditions were increased with curing time. Addition of marble can be useful for the durability performance of concrete when cement content is reduced by using marble sludge [111].

In building construction, the application of the composite materials has been increased during the last decade. Improvements on the different properties are based on light weight material and in corrosion resistant material and better fatigue loading. In these composites, polymeric materials are capable to contribute considerably to the development of comparatively better useful products. One of them are the polymeric

resins, which formed by integration of fine marble aggregates to develop the so-called polymer concrete [112].

Martínez-Barrera et al. [113] explored the effects of different intensity of gamma radiation and sizes of grey marble element on compression strength of polymer bricks. The results exhibits the compression strain and the elastic modulus depend on different combinations of marble particle sizes, shape and applicable intensity of radiation dose. By proper size of marble particle, improvement in elasticity modulus can be obtained. During SEM, scrap particles and few small fissures were observed on the surface of resin. While increasing the radiation dose, there are increase in the number of micro-particles and some voids and cracks passing through the marble surface. The micro cracks were resulted due to polyester constraints from the cross-linking of chains in the resin.

To decrease polarity by treating Calcium carbonate ($CaCO_3$) with stearic acid (SA), Cao et al. [114] proposed a method for studying the physical and thermal behaviour as well as mechanical properties of $CaCO_3$-HDPE composites. $CaCO_3$ is calcite derived from marble. Based on the obtained results, the $CaCO_3$ particles and HDPE matrix were more firmly packed in contrast to the conventional method. The proposed method was important for composite application where the role of the void contents is a significant factor. It considerably increases the density of the composite.

2.6. Plastic injection moulding and shrinkage-warpage behaviour of polymers

Plastic injection moulding (PIM) represents one of the most vital processes in the mass production of plastic parts with intricate geometries [115]. Injection moulding has the highest efficiency with enhanced dimensional accuracy, largest yield and among all the processing methods. The role of plastics in the new green concept of automotive and developments are going on the design process for replacing steel front side panels which is known as steel car fender, with the new plastic ones. Material selection, latest Conceptual design strategy in terms of strength, mouldability, and assemilability are very well predicted by researchers [116]. Some leading manufacturers of car such as Mercedes, BMW, Mitsubishi, GM, Nissan and Peugeot are trying for the development of plastic side fenders. More than 33% of all thermoplastic materials are prepared by injection moulding and more than 50% of all polymer processing equipment are for the injection moulding. Now -a- days, injection moulding bears the accountability of mass-producing plastic components to fulfil

speedily rising market as a large amount of the different types of customer products like automobile, therapeutic and electronics related products which are prepared by injection-moulding [117]. According to Wang et al. [118] injection moulding is an important manufacturing method to produce plastic parts due to the advantages of product quality, competitive cost, high production capacity and good thermo-mechanical properties. Injection moulding is a unique polymer processing technology when part with precision is to be made from a thermo plastic material. Injections moulding simulation softwares such as CAD Mold, Rem3D, Simuflow, Moldex3D and Autodesk Moldflow have become accepted in the industry for production and design optimization [119]. PIM is a cyclical process in which plastics feedstock is melted and injected under pressure into the mould cavity to produce three-dimensional parts [120].

Robust Quality is the prime need and concern of manufacturer, customers as elevated product quality consistency and rapid manufacturing rate is the main factor for the success of any industry. The quality of injection mouldings depends on different characteristics of raw material, mould design, sprue and gate location and the related process conditions [121].

Shrinkage and warpage of plastic parts is an important evaluation index for PIM (Plastic Injection Moulding). During PIM process, reducing shrinkages and warpage is a challenging task in the production of moulded thin and thick walled products. Azaman et al. [122] investigated the injection moulding of thin parts made by lignocellulosic polymer material like PP with fine wood. The defects shrinkage - warpage in thin and thick walled products were assessed under varying process conditions, with different moulding characteristics.

A Back Propagation neural-network (BPNN) model for prediction of warpage and optimization of injected plastic products has designed by Yin et al. [123] based on key process variables. The proposed methodology uses a Back Propagation Neural Network (BPNN) train by the input data and response data collected from FE (Finite Element) simulations, which are performed with the advance Moldflow software. Simultaneously, the quality of automobile glove box was also improved by the experiments. Trained by the outcome of the FE simulations performed with the help of Taguchi's orthogonal experimental design, the prediction model gives a mathematical modelling showing the correlation between the key process parameter

and the warpage of component. Thus, it has shown that prediction method has capability for prediction of warpage defect of plastic component.

Öktem et al. [124] presented a study on the modelling and analysis of effects of key process parameters on liner shrinkage by observing quality of the thin plastic parts. A mathematical relationship was developed between the process parameters (melt temperature, injection pressure, mould temperature, injection duration and cool duration) and the percentage shrinkage by utilizing statistical testing of the data. FE (Finite Element) analyses developed by Taguchi orthogonal arrays (OA) were conducted in Moldflow simulation software. ANOVA (Analysis of variance) was then determined to evaluate the competence of the developed regression model. It showed the significant effect of key process parameters on shrinkage. Experiments were performed to govern the correctness of the proposed regression model with FE analyses achieved from the advance Moldflow software.

According to Ozcelik et al. [125], due to either multi-gated moulds or barrier , the weld lines can occur in thin plastic parts. The weld line influence the surface and mechanical properties of plastic parts. It was observed that weld lines reduces the mechanical properties of injection moulded thin parts greatly. This weak point can be minimized with optimization of injection process parameters and the design conditions. By adjusting the location of sprue and gates, it is possible to alter the locations and intensity of weld lines. The presence of weld lines can be alleviated by regulating the processing conditions. Dang et al. [126] shown a general framework for optimization of plastic injection moulding parameters and two case studies were discussed to reduce warpage and residual stresses.

2.7. Study of fabrication of polymer composites with Injection Moulding

Injection moulding process is the most widely used processing technology of plastic products. The injection moulding of polymers but as well as composite materials are getting more attention in industry as well as research applications. With the application of composite materials, not only the mechanical characteristics, but also the thermal properties of polymeric matrices can be enhanced. Extensive and comprehensive research has been conducted on fabrication of composite materials with the help of injection moulding, out of which, few are discussing here in this literature review.

With the help of injection moulding Carbon-fibre-polypropylene composites have been prepared by Arao et al. [16]. Strength and flexural modulus of composites were improved by adding various the various Nano fillers. Niu et al. [127] prepared the Polypropylene and hemp fibre composites by melt compounding, followed by injection moulding.

With the help of injection moulding, different composites having ceramic powders were prepared by Suplicz et al. [128] such as - Boron-nitride, fine talc and titanium dioxide compounded with PP matrix. SEM showed that particles were properly dispersed in the polymer matrix. Few aggregates of filler were also found. With the numerical simulations and finite element (FE) analysis software, the cooling gradients were estimated.

The short glass fibre widely used to reinforce thermoplastic composites. In order to reduce fibre breakage problem, which affects thermal and mechanical properties of composite during the injection moulding, the reduction of fibre length reduce the reinforcing efficiency of the fibre [129]. The original manufacturing was modified by Mathurosemontri et al. [130] to a convenient technique, which has been called a direct fibre feeding (DFF) injection moulded process. The short fibre reinforced composite material can be fabricated easily with this concept. Similarly, Chang et al. [131] fabricated short glass fibre reinforced with Polycarbonate using injection moulding process.

New technologies, mainly in automobile and aerospace sectors (structural mass of an aircraft) that absorb design and production of complex-shaped ceramic parts have burgeoned in recent years. The development of superior hypersonic and the re-entry vehicles require sustainable materials that are resistant to oxidation and erosion along with the capability to withstand higher temperatures well above $1500^{o}C$, which are only possible by use of ceramics.

Altan et al. [132] prepared PP- TiO_2 composites by melt compounding with a twin screw extruder. Nanoparticles were modified with silane and then composites were injection moulded and mechanical tests were applied to obtain elastic modulus, impact strength and tensile strength. Wiesner et al. [133] prepared aqueous suspensions of ZrB_2 (zirconium diboride), B_4C (boron carbide) and WC (tungsten carbide) and processed in injection moulding and properties of composites were improved in environmentally friendly way.

Ou et al. [134] pretreated TiO_2 particles with Toluene-diisocyanate to synthesize TDI-functionalized and then PP-Polyamide blends containing 'TDI-functionalized TiO_2' were created with the twin-screw extruder followed by injection moulding. The Maleated-PP was used for further chemical treatment of the blends. Thus, mechanical properties of PP-Polyamide blends composites were investigated through flexural and tensile strength. Similarly, injection moulding of alumina parts was conducted with HDPE, paraffin wax and stearic acid and fabricated green parts were found with improved mechanical strength. [135,136].

2.8. Optimization of process parameters of injection moulding

During the injection moulding process, crystallinity and crystalline morphology are critical factors, because they are sturdily influenced by processing conditions, having melt temperature, moulding temperature, rate of cooling, packing duration and pressure [137, 138]. Thus, optimization of these parameters becomes essential to obtain good quality of products. In this part of literature review, injection moulding of parameters and their optimization are discussed.

According to López et al. [139], it is necessary to know the influence of injection moulding parameters on quality of parts. They focused a case study on application of Design of Experiments (DOE) on a complex part produced by injection moulding.

Kc et al. [140] investigated and evaluated the effect of injection moulding parameters on flow and x-flow shrinkage of sisal-glass hybrid bio composites. For two types of hybrid bio composites (10 and 20%), optimal injection moulding optimization was performed for minimization of shrinkage. This resulted in an Injection pressure of 90 bar, melt temperature of 210^{o}C, mould temperature of 40^{o}C, cooling time of 40 s and holding time of 6 seconds. After ANOVA analysis, injection pressure was found to be significant for shrinkage.

Oliaei et al. [141] selected combinations of PLA, PLA-TPU and PLA-TPS to produce disposable green plastic spoons with injection moulding. The warpage and shrinkage of the products were reduced by optimization of parameters with Taguchi method and numerical simulation. Packing times, coolant temperature, packing pressures, melt and mould temperatures were optimized. Using ANOVA technique, the percentage contribution of all single and binary interactions of factors were

determined. Meanwhile, ANN (artificial neural network) was also used for pattern recognition and optimization through modifying the processing conditions.

Berti and Monti [142] used a virtual prototyping environment, in which FEM and DOE technique – Response surface method (RSM) were integrated with Monte Carlo stochastic simulations. Taguchi parameter design can be used to identify significant processing conditions and to obtain different combinations of processing conditions for better quality of plastic products. Taguchi's efficient method of experimental design provides an easy and organized approach for optimization of the experimental designs for better quality in economical manner [143-145]. Similarly, by using Taguchi technique, Dangayach and Guglani [146] reduced the injection time from 3.98 seconds to 2.63 seconds of a plastic part.

Chiang and Chang et al. [147] presented an approach for optimization of parameters of an injection-moulded thin plastic part e.g. cell phone with PC-ABS, based on the orthogonal array (OA) with the Grey Relational Analysis (GRA) and the fuzzy logic analysis. Mould temperature, melt temperature, holding duration and holding time were optimized with considerations of several performance characteristics having strength of welding line, percentage shrinkage and temperature gradient.

Chiang et al. [148] also used L_{18} orthogonal array and presented a quick and effective approach for optimal process conditions of an injection-moulded plastic component with a light shell structure with GRA and fuzzy logic. They developed an optimal system in solving the optimal multi-objective problem, which uses the grey relational coefficient for every outcome and exchange a Grey fuzzy grade to estimate the production responses for cell phone shell.

According to D. Kumar et al. [149] warpage in injection moulding is generally a function of the part geometry, the mould, runners and gates design and the process parameters. In their research, Melt temperature, injection pressure and mould temperature with their interactions was used to carry out a significant role in minimization for shrinkage, and warpage and maximization of impact strength.

2.9. The Knowledge Gap in Previous Investigations

The literature review on polymer composites reveals a number of research gaps, which provide the basis for the objectives of the present research work.

Based on that the following research gaps have been identified from this literature review:

1. The research on micro filler ingredients, e.g. **comparative analysis of variation in different fillers** integrated with Polypropylene, on the performance of composites materials are lacking in literatures.
2. Research and Development to find an **alternative conventional fabrication** of composites have been considered as a challenge in the field of materials and any investigation in this regard would be beneficial in the development of composite materials.
3. Less study was found related to physical, chemical, mechanical, thermo-mechanical and morphological behviour of **injection moulded composites**.
4. Literatures based on **utilization of marble** as the composites are scarcely available.
5. The study of effect of the varying concentrations of micro filler on the properties of the polymer composites such as **hardness, glass transition temperature (T_g), shrinkage and warpage** is still untouched by the researchers.
6. The main challenge faced by the researchers are the fabrication of the composite materials with injection moulding using **ASTM standards.**
7. Studies carried out worldwide on mechanical and thermo-mechanical behaviour of polymer composites have been experimental and the development of **mathematical models** and **statistical methods** in analyzing different properties are rare.
8. Although, Taguchi technique is easy, systematic and efficient tool to **optimize** designs for quality and performance, it was applied in inadequate number of application of composites. Its execution in improvement of properties of composites has hardly been reported.

2.10. Proposed objectives of the research work

The objectives of this research work are outlined as follows:

- ➢ Fabrication of injection moulded composites filled and unfilled by micro fillers.
- ➢ Characterization of physical (such as void content) and chemical properties (such as Fourier Transform Infrared) of the proposed unfilled and particulate filled composite materials.
- ➢ Testing of specimens as per ASTM standards for characterization of mechanical properties such as Shore D hardness, impact strength, flexural strength and compressive strength.
- ➢ Study of thermo-mechanical, thermo-gravimetric analysis (TGA) and dynamic mechanical analysis (DMA) behaviour of micro composites.
- ➢ Study of shrinkage and warpage behaviour of polymers using L_{27} Taguchi orthogonal array design approach.
- ➢ Finally, Taguchi technique of optimization was implemented by taking into consideration the physical, chemical, mechanical and shrinkage –warpage characteristics of the unfilled polymer composites in order to get the optimal parameters of the injection moulding process.

Chapter Summary

This chapter has described:

- ➢ An exhaustive literature review of research works on various aspects of filler and particulate reinforced polymer composites investigated by various researchers.
- ➢ The knowledge gap in previous investigations.
- ➢ The objectives of the present thesis work.

The next chapter exhibits the materials for the fabrication of composites and methods used for the processing of the composites, the experimental planning, Taguchi method, the physical and mechanical characterization, thermal and thermo-mechanical properties.

*****

Chapter 3

MATERIALS AND METHODOLOGY

This chapter briefly illustrates the properties and specifications of the selected ingredients/materials, design of different sets of composite formulations for the research work, the standard fabrication procedure, the processing conditions adopted as per ASTM or Industrial standard and the different characterization performed in order to justify commercial viability of the product.

3.1. Materials selection, their properties and specifications

The research to explore the development of polymer composite material for better properties in terms of physical, mechanical, chemical, thermo-mechanical and morphological characterization than the virgin polymer materials is planned based on the research gaps presented and discussed in the chapter-2. For the same purpose, following materials were chosen as listed in Table 3.1.

Table 3.1: Materials used for fabricating Polymer composites

S.No.	Type of ingredient	Name of element	Supplier
1.	Resin	Polypropylene	Indian Oil Corp. Ltd., Haryana, India
2.	Filler	Alumina particle (mesh size 300)	Central Drug House Pvt. Ltd., New Delhi, India.
		TiO_2 particle (mesh size 300)	Central Drug House Pvt. Ltd., New Delhi, India.
		Marble particle (mesh size 300)	Kishangarh, Rajasthan
3.	Binding agent	Paraffin oil	Central Drug House Pvt. Ltd., New Delhi, India.

3.1.1. Polypropylene

Polypropylene (PP) is most widely used thermoplastic "addition polymer" created from the propylene monomers. It is widely used in various applications related to plastic parts for various industries including the automobile industry and packaging for consumer products.

Special devices like living hinges, and textiles. In Present era, it is recognized as one of the most commonly produced plastic all over world. Some of the most important properties of polypropylene are:

1. Elasticity and Impact strength: Polypropylene shows elasticity over a wide range of deflection in comparison to other plastics, but it will also give plastic deformation early in the deformation process, so it is normally consider as "tough" material.
2. Chemical Resistance: PP does not react easily with diluted acids and bases, which makes it an apparent choice for containers of cleaning agents, liquids, first-aid products and many more.
3. Fatigue Resistance: PP holds its physical shape after twisting and flexing. This property is very useful for creating living hinges.
4. Transmissivity: Although, PP can be prepared transparent, it is usually produced to be opaque in colour. PP can be used for application where limited transfer of light is required or where it is of aesthetic importance. In the applications where high value of transmissivity are required then plastics like Polycarbonate give better alternate.
5. Insulation: PP can work as good insulator, which make it very helpful for fabrication of electronic-components.

One of the important applications of PP is that it can be manufactured with injection moulding, CNC, thermoforming, or crimping, into a living hinge. Exceptionally thin pieces of plastic that bend without breaking are known as Living hinges. They are not particularly useful for heavy structural applications like holding up a door but are extremely useful for light-load-bearing applications as the cap on a bottle of medicine or ketchup. PP is exclusively proficient for living hinges because it does not crack when repeatedly twist. Chemical composition and General specification of the PP are shown in Figure 3.1and Table 3.2, respectively.

Table 3.2: General specifications of the Polypropylene (PP)

Properties	**Value**
Form	Solid Granules
Odour	Slight Waxy Odour
Colour	Translucent to White
Flash point	> 320^{o}C
Decomposition temperature	> 320°C
Ignition temperature	> 410°C
Max. Continued Use Temperature	85^{o}C
Impact Strength	2.5 - 35.0 kJ/m
Tensile Strength	0.96 - 1.35 N/mm^{2}
Glass Transition Temp. (atactic)	-10 ^{o}C
Glass Transition Temp. (isotactic)	90^{o}C
Thermal Coefficient of Expansion	100 - 155 × 10^{-6}
Density	0.89-0.95 g/cm^{3}
Melting Point	165^{o}C
Solubility in / Miscibility with Water	Insoluble
Danger of explosion	PP product is not explosive

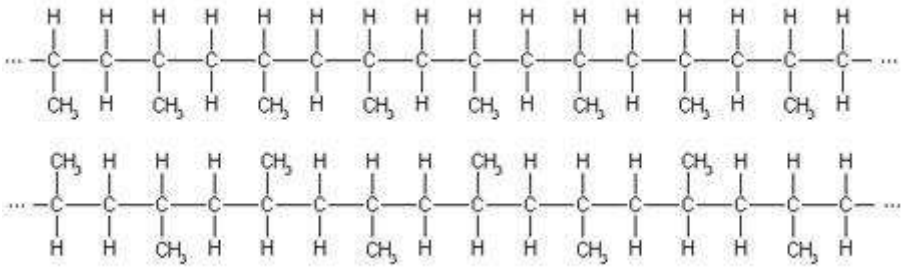

Figure 3.1 Chemical composition of Polypropylene

3.1.2. Paraffin oil

Paraffin oil is saturated hydrocarbon molecules with single bonds. Paraffins are commonly found in chains of hydrocarbon having different length and are defined by the formula C_nH_{2n+2}. Thus, paraffin oils are saturated hydrocarbons having a combination of different alkanes and are useful for phase change resource for application of thermal storage. They have desirable characteristics, viz., elevated latent heat of fusion, slight super-cooling,

chemical inertness, stability and low down vapour pressure in the melt. Due to self-nucleating property and availability in the market, they are used in many useful composites. In the chains of paraffin oil the number of carbon atoms having melting temperature between 30^{o}C and 90^{o}C ranges from C20–C50. Molecular weight increases due to increased length of chains of the carbon atoms, which results in elevated melting temperature of the material.

3.1.3. Filler Materials

3.1.3.1. Alumina filler (Al_2O_3) [[6] [52] [150]]

An aluminium oxide nanoparticle, also known as alumina particle or Nano alumina, exhibits the properties of improving electrical conductivity, ductility and toughness, and hardness and strength etc. compared to virgin material. The application of Nano alumina is increasing day by day. In periodic table, Aluminium is placed at Block P, Period 3, while oxygen is placed at Block P, Period 2. Alumina particles are spherical and appear as white powder.

Chemical Properties

The chemical properties of Al_2O_3 particles are shown in the following Table 3.3

Table 3.3 Chemical properties of Al_2O_3 particles

Chemical symbol	Al_2O_3		
Group	Aluminium 13 Oxygen 16	**Element**	**Content (%)**
		Aluminium	52.93
		Oxygen	47.05
Electronic configuration	Aluminium [Ne] $3s^2 3p^1$ Oxygen [He] $2s^2\ 2p^4$		

Physical Properties

The physical properties of aluminium oxide particles are given in the following Table 3.4.

Table 3.4 Physical properties of Al_2O_3 particles

Properties	**Metric**
Density	3.950 g/cc
Molar mass	102.87 g/mol

Thermal Properties

The thermal properties of aluminium oxide particles are shown in the following Table 3.5

Table 3.5 Thermal properties of Al_2O_3 particles

Properties	Metric
Melting point	2055°C
Boiling point	2988°C

Applications

The major applications of alumina includes formation of electrical circuit base-boards, transparent ceramics, moderate pressure sodium lamps, cosmetic fillers, Single crystal, sapphire, cutting tools, packaging materials, high-strength aluminium oxide ceramic, winding axle, crucible with high purity, furnace tubes, glass components, polishing materials, metal parts, semiconductor materials and grinding belts, wear-resistant polymer support, better water-proof materials, Catalyst and catalyst-carrier, analytical reagents, special glass, fluorescent materials, vapour deposition materials, composite materials etc. In the liquid form, alumina particles are used for the applications like Plastics/rubber, refractory parts, to improve ceramics density and softness, fracture-toughness, thermal fatigue-resistance, creep and wear resistance of plastic parts.

3.1.3.2. Titanium Dioxide (TiO_2) [[57] [108] [151]]

TiO_2 is available in the form of nano-crystals having a high surface area. Titanium belongs to Block-D, Period-4 while oxygen belongs to Block-P, Period-2 of the periodic table. Other common names of Titanium dioxide are flamenco, rutile, titanium dioxide and dioxotitanium.

Chemical Properties

The following Table 3.6 shows the chemical properties of TiO_2.

Table 3.6 Chemical properties of TiO_2 particles

Chemical symbol	TiO_2		
Group	Titanium 4 Oxygen 16	**Element**	**Content (%)**
		Titanium	59.93
		Oxygen	40.55
Electronic configuration	Titanium[Ar]$3d^2$ $4s^2$ Oxygen [He] $2s^2$ $2p^4$		

Physical Properties

Titanium dioxide nano-particles come into view in the form of black hexagonal-crystals. The following Table 3.7 presents the physical properties of TiO_2 particles.

Table 3.7 Physical properties of TiO_2 particles

Properties	Metric
Density	4.230 g/cc
Molar Mass	78.94 g/mol

Thermal Properties

The following Table 3.8 presents the thermal properties of TiO_2.

Table 3.8 Thermal properties of TiO_2 particles

Properties	Metric
Melting Point	1,845° C
Boiling Point	2,974° C

Applications

- TiO_2 shows good photo catalytic properties, so it can be used in antiseptic and antibacterial composition
- Degrading organic-germs and contaminants
- Useful for forming Ultra violet resistant material
- Formation of self-cleaning ceramics, glass, printing ink, coating, etc.

- Manufacturing of cosmetic products such as whitening-creams, sunscreen-creams etc.
- For improving the opacity of paper, it is used in the paper industry.

3.1.3.3. Marble Powder [152-155]

Marble is composed mainly of calcite, dolomite, serpentine, and other similar minerals. The exact chemical composition of marble will mainly depend on the location and the minerals or impurities present in the limestone during recrystallisation. Typically, the main constituents of marble are 36-43% Lime (CaO), 20-26% SiO_2, 2-4% Al_2O_3, 1.5-3.5% various oxides like MgO and NaO, and 28-34% various carbonates like $MgCO_3$ and others. Due to geological processes, marble is a type of metamorphic rock formed from limestone by heat and high pressure in the earth's crust. It is widely used in cement, construction and sculpture industries. In the last few decades, the marble production has gained industrial importance. Turkey, Italy, China, Spain, and India are the top five marble exporting countries that are dominating the marble production. During marble processing, 25-35% of the stone goes to marble slurry because of being smaller. Table 3.9 shows the Physical Analysis of Marble slurry.

Table 3.9: Physical Analysis of Marble slurry

S. No.	Properties	Value
1	Specific gravity	2.78
2	Water content	48.5%
3	Liquid limit	18.25%
4	Shrinkage limit	24%

Every year millions of tons of marble processed during extraction process around the world. As a result, significant environmental damage occurs due to the large quantities of marble powder produced in these industries. Marble powder may also lead to skin allergies. However, apart from these disadvantages, marble powder is also among the most useful substances in the planet and has found use in various applications, in a number of different forms. It is mainly used as a filler or additive in several industrial applications.

3.2. Fabrication of Polypropylene Composites by using plastic injection moulding technique

1. Four different ratios of 5 wt. %, 10 wt. %, 15 wt. % and 20 wt. % of filler were added into virgin Polypropylene.
2. For each composition, a mixture of Polypropylene and filler is prepared in an internal mixer with 10-20 ml of paraffin oil.
3. This mixture of Polypropylene and filler is fed into hopper of injection moulding (80 ton). Melt temperature is kept near 230°C.
4. The specimens for impact strength and flexural strength are prepared according to ASTM D-256 and ASTM D-790 respectively.
5. Injection moulding machine and moulds are shown in Figure 3.2 and Figure 3.3 respectively. Its specifications and process parameters are exhibited in Table 3.10 and Table 3.11, respectively.
6. As a releasing agent, the Silicon-spray is used to assist easy removal of the specimens of the PP-composites from the mould.

Figure 3.2 Injection Moulding Machine

Table 3.10 Specifications of Injection Moulding Machine

Specifications		Values
Clamping Force		220 MPa
Minimum mould Height		200 mm
Maximum mould Height		530 mm
Distance between Tie bars		420 x 420 mm
Total Mould carrying capacity		700 Kg
Max.mould.wt.in moving platen		450 Kg
Ejection Force		45 KN
Net Weight (Without oil)		4300 Kg
Injection Pressure		130 MPa
Machine Dimensions	Length	5000 mm
	Breadth	1400 mm
	Height	2000 mm

Table 3.11 Process parameters of Injection Moulding Technique

Parameters	Values
Melt Temperature	$230^{o}C \pm 10^{o}C$
Mould Temperature	$40^{o}C$
Injection Pressure	60 ± 10 MPa
Packing Pressure	50 MPa
Shot size	50 ± 5 gm

(a)Mould for Impact Test (b) Mould for Flexural Test

Figure 3.3 Mould for preparing specimens

Figure 3.4 Fabricated PP-Al_2O_3 composites by Injection Moulding

Figure 3.5 Fabricated PP-TiO_2 composites by Injection Moulding

Figure 3.6 Fabricated PP-Marble Powder composites by Injection Moulding

3.3. Designation and detailed composition of composites

Following Table 3.12, Table 3.13 and Table 3.14 shows the Designation and detailed composition of alumina filled, TiO_2 filled and Marble Powder Polypropylene composite respectively.

Table 3.12 Detail composition of Al_2O_3 filled Polypropylene composite

Sample Designation	Composition
PP	Virgin PP
PPA-5	PP + 5 wt% Al_2O_3
PPA-10	PP + 10 wt% Al_2O_3
PPA-15	PP + 15 wt% Al_2O_3
PPA-20	PP + 20 wt% Al_2O_3

Table 3.13 Detail composition of TiO_2 filled Polypropylene composite

Sample Designation	Composition
PP	Virgin PP
PPT-5	PP + 5 wt% TiO_2
PPT -10	PP + 10 wt% TiO_2
PPT -15	PP + 15 wt% TiO_2
PPT -20	PP + 20 wt% TiO_2

Table 3.14 Detail composition of Marble powder filled Polypropylene composite

Sample Designation	Composition
PP	Virgin PP
PPM-5	PP + 5 wt% Marble powder
PPM -10	PP + 10 wt% Marble powder
PPM -15	PP + 15 wt% Marble powder
PPM -20	PP + 20 wt% Marble powder

3.4. Physical and Chemical Characterization

3.4.1. Density & Void Content

According to Agarwal and Broutman [156], the theoretical density of composite materials in weight-fraction can be determined using the following Equations.1 and 2.

$$\rho_{ct} = \frac{1}{(W_p/\rho_p)+(W_m/\rho_m)} \quad (1)$$

where W and ρ represents the weight fraction and density respectively. The suffix p, m and ct indicate the filler powder, matrix and composite materials respectively. The actual density (ρ_{ce}) of the composite can be determined experimentally by Archimedes' Principle. The volume fraction of voids (V_v) in the composites is calculated using the following Equation 2. Figure 3.7 shows the Weighing Machine used for this purpose.

$$V_v = \frac{(\rho_{ct} - \rho_{ce})}{\rho_{ct}} \times 100 \quad (2)$$

Figure 3.7 Weighing Machine

3.4.2. Shrinkage Measurement

The shrinkage may be measured as the difference between the size of mould cavity and the size of finished part divided by the size of a mould cavity. The relative shrinkage of selected characteristics were calculated with following equation

$$S = (L_{cavity} - L_{Part})/ L_{Cavity} \times 100\% \quad (3)$$

where, S denotes the linear shrinkage in percentage, L_{cavity} denotes the length of cavity and L_{Part} denotes the length of specimen. The percentage of shrinkage being used in experiment is taken through the output of mean linear shrinkage.

3.4.3. Warpage Measurement

Warpage of specimen was measured on a Coordinate Measuring Machine (CMM). It was observed that warpage occurs at the ribs, where cross sectional area changes. For this reference points are marked on each rib and warpage was measured at these points. Maximum warpage value of all reference points has been taken as the warpage value of the whole model in this study.

3.4.4. Fourier Transformed Infra-Red Spectrometer (FTIR Analysis)

Fourier Transform Infra-Red spectroscopy (FTIR) has wide applicability in structure elucidation, which are either synthesized chemically or of natural origin. Perkin Elmer FTIR Spectrum-2 is a compact, easy to use, powerful instrument with fully integrated, universal sampling system for measurements in the range of 4000-500 cm^{-1} for samples (Figure 3.8).

Figure 3.8 Fourier Transform Infra-red Spectroscopy

Both virgin and composite polypropylene are also compressed into thin pellets and characterized using FTIR spectroscopy (Perkin–Elmer Spectrum) in the transmission mode over the frequency range of 400–4000 cm^{-1} with a resolution of 4 cm^{-1} performing 8 scans using ATR (Attenuated Total Reflection) Method.

3.5. Mechanical Characterization

3.5.1. Shore D (Durometer) Hardness Test

With a spring loaded needle-like indenter, the resistance of a material to penetration measured known as Shore D hardness. Hardness of plastics is normally measured by Shore scales. **Shore A** type scale is used for testing Elastomers (rubbers) and other soft polymers. **Shore D** scale is used for hard elastomers and other thermoplastic materials. Shore D hardness is tested with an instrument called Durometer which is shown in Figure 3.9. The depth of penetration by the indenter under the load

determines the hardness. Shore D hardness value may vary in the range from 0 to 100. Maximum penetration for each scale is 2.5-2.65 mm. This value corresponds to minimum Shore D hardness: 0. Similarly, maximum hardness value 100 corresponds to zero penetration.

Figure 3.9 Shore D (Durometer) hardness Instrument

Hardness of three specimens of each composition is taken. Hardness is determined with the application of 15 N load for 10 s. The mean-value of five indentations on each specimen is determined. It is calculated as per ASTM D 2240 [157].

3.5.2. Izod Impact Strength

Notched Izod Impact is a test that process a materials resistance to impact from a swinging pendulum. It can be defined as kinetic energy required to begin the fracture and continue the fracture until the specimen is broken. The Izod specimens are prepared with notch to prevent the deformation of specimen during impact. The specimen is mounted in a fixture with the notched side facing the striking edge of swinging pendulum. The pendulum is released with the help of lever and allowed to strike through the specimen. For notched izod impact strength measurement of specimen, the specimens are prepared with a milled notch. The size of specimen is $64.5\times10\times3$ mm^3. The notch angle is kept 45±1°. The impact strength is measured with a TMI Monitor Impact tester (model No. 44–02-01) according to ASTM D256 using a pendulum having effective length of 0.33m.

3.5.3. Flexural Strength

Flexural strength is a material property, which can be defined as stress in a material just before it yields in a flexure test. Using a three-point flexural test method, the transverse bending test is most frequently employed, in which a specimen having rectangular cross-section is bent until yielding. The flexural strength corresponds to the highest stress experienced within the material at its moment of failure.

In this study, three-point flexural test of specimen are performed with the help of flexural testing machine (Figure 3.10) for each composition of PP and filler material. The size of specimen is 60×10×3 mm^3. It was conducted according to ASTM D790 [158]. The flexural strength is measured on Instron Universal Testing Machine (UTM).

Figure 3.10 Photograph of Instron 1195 UTM machine

3.5.4. Compressive Strength

Compressive strength is the capacity of a material to bear up loads tending to reduce size, as opposed to tensile strength, which withstands loads tending to elongate. Thus, compressive strength resist compression, while tensile strength resists tension i.e. being pulled apart. Few polymer materials fracture at their limit of compressive strength; others deform irreversibly, so a certain quantity of deformation can be considered as the limit for compressive load. In this study, for compressive strength of

composite's specimen sizes 12.5×12.5×25.5 mm^3 were prepared for each composition according to ASTM D 695. The compressive strength was measured on Instron Universal Testing Machine (UTM).

3.6. Thermo-Mechanical Characterization

3.6.1. Dynamic Mechanical Analysis (DMA)

DMA is the technique of applying a stress on a specimen and analyzing the response to get phase angle and deformation data. These data allow the calculation of the damping or tan delta (δ) as well as complex modulus and viscosity data. DMA of fabricated composite specimen has been conducted by using Perkin Elmer DMA-8000 in the Nitrogen environment at a fixed frequency of 1Hz, heating rate of 3°C/min, at a temperature range of 0-160^oC in tensile mode (Figure 3.11). Rectangular specimens are prepared having dimensions 30×6×1.5 mm^3 for each composition of filler weight-percentage (0, 5, 10, 15, 20 wt.%). Specimen of PP – alumina and PP-Marble composites are shown in Figure 3.12. Elastic (Storage) modulus, Loss modulus and loss tangent are recorded for the composites.

Figure 3.11 Dynamic Mechanical Analyzer

Figure 3.12 Samples of PP –Alumina and PP-Marble composites

3.6.2. Thermo-Gravimetric Analysis (TGA)

TGA is a technique of thermal analysis of composites in which changes in physical and chemical properties are measured as a function of increasing temperature (having constant heating rate), or as a function of time (having constant temperature). TGA is commonly used to decide selected characteristics of polymer composites that show either mass loss or gain due to decomposition, oxidation, or loss of volatiles (e.g. moisture). It is particularly useful method for the study of polymeric materials, together with thermoplastics and thermosets, composites, fibre s, paints and coatings.

Perkin Elmer Pyris -7 instrument is used to analyze the thermal behaviour of fabricated composites (Figure 3.13). TGA has been carried out to analyze the high temperature stability and degradation behaviour. Under nitrogen atmosphere specimens are heated from 25^{o}C to 550^{o}C at a heating rate of 5°C /min.

Figure 3.13 Thermo-Gravimetric Analyzer

3.7. Morphological Characterization

3.7.1. Scanning Electron Microscopy (SEM)

As a great magnification tool, SEM is most widely used for morphological study of materials. It has focused beams of electrons to gain information. The high-resolution, 3-D images formed by SEM, make available morphological and topographical compositional information regarding the materials. It composes them invaluable in a field of knowledge and research applications. In addition to morphological and topographical -compositional information, a SEM can notice and analyze surface fractures, offer information in micro and nano structures, inspect the surface impurities and other contaminations, expose spatial variations in materials, present qualitative chemical analyses and recognize material structures. SEM is employed to characterize the composite morphology and reinforcement dispersion and analyze the failure mechanism in the fractured surface of polymer composites. Bruker Nova Nano SEM 450 model (Figure 3.14) was used for SEM images of samples. The samples used for microscopic analysis were cut from the failed section of fractured specimens and then fine polished using a fine grit abrasive wheel.

3.7.2. Atomic Force Microscopy (AFM)

AFM is a technique for analyzing the material surface to the level of the atom. AFM uses an automatic probe to enlarge surface features up to 100,000,000 times, and it produces 3-D images of the material surface. AFM analysis is carried out to investigate the surface functionalization or modification of alumina particles and the

dispersion quality of the alumina particles within the polymeric matrix. By using tapping mode fractured surface is imaging using a AFM - Bruker Nanoscope V, USA (Figure 3.15) on more than 5 samples for each composite.

This versatile instrument not only produces high resolution images of the composite surface in process relevant different environments but can also be used to quantify the forces acting at a surface which govern properties. Force is measured as a function of distance when a probe attached to the apex of the AFM cantilever, approaches the sample, makes contact and then retracts away from the sample. The displacement is varied using the extension and retraction of a piezoelectric crystal.

Figure 3.14 Scanning Electron Microscopy

Figure 3.15 Atomic Force Microscopy

3.8. Process Optimization and Taguchi Method

To improve the quality of a process or a product, statistical methods are commonly used. Such methods enable to define the effects of every single condition possible in an experiment (run), in which numerous parameters are generally involved. Polymer shrinkage and warpage phenomena in plastic industry are process defects in which a

number of control parameters together find out the product performance. Therefore, in the present research work a statistical method called Taguchi technique is used to optimize the process parameters of injection moulding leading to minimum percentage shrinkage and warpage of polymers under the investigation. This part of the chapter exhibits Taguchi design technique in detail.

3.8.1. Taguchi Experimental Design

Taguchi technique is a controlling tool for the design of quality systems based on Orthogonal Arrays (OA) experiments (runs) that make available minimum variance for the experiments with an optimum tuning of control parameters. In Orthogonal array, experiments are performed in such a way where the columns for the independent variables are "orthogonal" to one another. These experiments are sequence of tests either to verify a hypothesis or to appreciate a process for advance analysis. Experiments are designed with finding the optimum quality of process and product, which having high quality and cost efficient. The experimenter needs to recognize the parameters involved and its range, the levels assigned to each parameter as well as a method to compute and quantify the signal (outcome) of each parameter [30]. The single parameter at a time come within reach of the most favourable level for each parameter but not the optimum solution of all the interacting parameters involved. Thus, it is necessary to observe the combination of every parameter at each level and to establish the combination that gives the excellent response.

Selection of control parameters are the important step in the Taguchi method. Thus, initially a large number of parameters are included so that non-significant variables can be recognized at earliest. In this study, steady state experiments are performed to decide the range of parameters. The array chosen in this study is L_{27} orthogonal array design which consist 27 rows corresponding to number of variables selected.

To obtain the optimum response, this method accomplishes the integration of Design of Experiments (DOE) with the parametric optimization of the process. The orthogonal array involves a set of well-balanced experiments, which are the minimum experimental runs. For optimization, Taguchi technique uses a statistical measure of performance known as signal-to-noise ratio (S/N), which is logarithmic function of response to serve as objective functions [15] [98]. The S/N ratio judges both the variability and mean into consideration. It can be explained as the ratio of the signal (mean) to the noise (standard deviation). This ratio accommodates quality features of

the process, which is under study and to be optimized. The three categories of S/N ratios are used: lower is better (LB), Higher is better (HB) and nominal the best (NB). The experimental interpretation are changed into a S/N ratio. The S/N ratio for 'minimum shrinkage & warpage' and 'maximum impact strength' are coming under 'LB' and 'HB' characteristic, respectively, which can be calculated as logarithmic transformation of the loss function [30], as exposed in Eq. (4) and (5).

$$S/N_{LB} = -10\ Log_{10}\ \frac{1}{n}\quad (\sum y_i^2) \tag{4}$$

$$S/N_{HB} = -10\ Log_{10}\ \frac{1}{n}\quad (\sum 1/y_i^2) \tag{5}$$

Chapter summery

This chapter briefly presents/discusses following things:

- The properties and specifications of the filler materials selected along with the design of different sets of polymer composite formulations.
- The details of standard testing procedure adopted as per ASTM standards.
- The description of various physical, chemical and mechanical characterizations performed in order to justify commercial viability of the product.
- The description of thermo-mechanical characterizations performed with Dynamic Mechanical Analyzer (DMA) apparatus used to measure the temperature-dependent characteristics like stiffness and damping properties of the investigated composites.
- A brief discussion on performance attributes adopted for assessment of the performance of the fabricated composites.

The next chapter briefly discuss the various physical and chemical characterizations of the fabricated PP composites.

*****

Chapter 4

PHYSICAL AND CHEMICAL CHARACTERIZATIONS OF POLYPROPYLENE COMPOSITES

This chapter discusses the results based on the physical and chemical properties of Polypropylene composites according to the formulations discussed in previous chapter. The physical and chemical characterization include determination of void content test and Fourier-transform infrared spectroscopy respectively.

The interpretation of the comparison and the results of different Polypropylene composite specimens are also described. This chapter consists of three parts: part I consists of Polypropylene composite filled with alumina (Al_2O_3), part II consists of Polypropylene composite filled titanium dioxide (TiO_2) and part III consists of Polypropylene composite filled marble powder.

Part I

4.1. Physical and Chemical characterization of Alumina filled Polypropylene composites

4.1.1. Fourier Transform Infrared analysis of alumina filled Polypropylene composites

The FTIR spectra of PP-alumina composites are shown in Figure 4.1. In this work, formation of agglomerates is the result of the interaction occurring between the alumina particles themselves as they hold a lot of surface hydroxyl groups. Though, fine dispersion of Al_2O_3 particles in polymer matrices is evaluated studying the respective SEM micrographs. The transmittances of the samples as a function of wavelength exhibited that the absorbance of ultraviolet light of the PP–Al_2O_3 composite significantly increased with increasing alumina loading. The band of 1168 cm^{-1} is characteristic for bonding between paraffin oil and filler. The band of 1378 cm^{-1} and 1455 cm^{-1} are characteristic for a hydroxyl bond (O-H) a typical oxidation product, where a C-H bond is split up and oxidized to a C-O-H bond. The band of 1660 cm^{-1} is characterized for a carbon double bond (C=C). This bond can accrue by abstraction of hydrogen atoms of two abreast carbon atoms by oxygen to H_2O. Similarly, according to Pracella et al. [159] a small peak is attributed by the aromatic C=C bending. The strong peaks at 2920 cm^{-1} and 2895 cm^{-1} are attributed by the methylene groups (-CH_2-) of polymer matrix that were observed in PPA-15 and shift

towards lower peak values as decreasing filler wt. %. Band of 3200 - 3700 cm^{-1} is attributed by (OH stretching) suggested that there are hydroxyl groups in the composite. Eventually, physical cross-links confined inorganic particles with matrix to achieve hybridization. According to Lu et al.[85], the increase in intensity for NaOH treated fibre s at 1000 cm^{-1} and 3300–3500 cm^{-1} is due to the increase in -OH groups on the fibre , which provides active site for interaction between the fibre and thermoplastic matrix. Pandey et al. [160] suggested that the increase in the absorbance at 3200 - 3600 cm^{-1} and 1600 - 1800 cm^{-1} is rapid in composites in comparison to virgin PP.

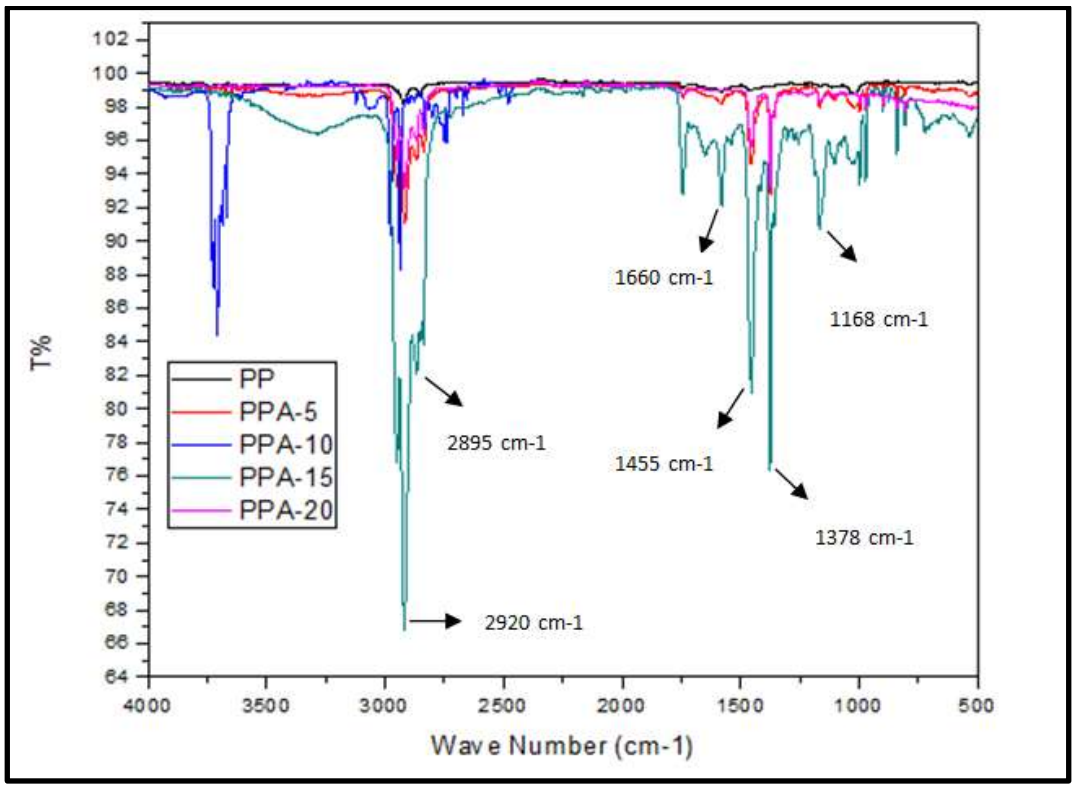

Figure 4.1 FTIR spectra of virgin PP and PP-Al_2O_3 composites

4.1.2. Effect of void content on Alumina Filled Polypropylene Composites

According to Agarwal and Broutman [156] the theoretical density of composite materials in terms of weight fraction can be obtained using the following Eqs.1 and 2

$$\rho_{ct} = \frac{1}{(W_p/\rho_p)+(W_m/\rho_m)} \quad (1)$$

where W and ρ represents the weight fraction and density respectively. The suffix p, m and ct indicate the filler powder, matrix and the composite materials respectively.

By Archimedes' Principle the actual density (ρ_{ce}) of composite can be determined experimentally. The volume fraction of voids (V_v) in the composites can be determined using the following equations:

$$V_v = \frac{(\rho_{ct} - \rho_{ce})}{\rho_{ct}} \times 100 \quad (2)$$

Table 4.1 Measured and theoretical density of the PP-Al_2O_3 composites

Composite	Measured Density (g/cc)	Theoretical Density (g/cc)	Volume fraction of Voids (%)
PP	0.905	0.906	0.11
PPA-5	0.940	0.942	0.30
PPA-10	0.959	0.982	2.43
PPA-15	0.972	1.025	5.46
PPA-20	0.990	1.071	8.25

In the present study of PP-Al_2O_3 composites, theoretical density was higher than the measured density as observed in Table 4.1 and the decrease in measured density can be due to the formation of air bubbles for the period of fabrication of the PP-Al_2O_3 composites. According to Bonderer et al. [161] this trapped air, known as voids, is undesirable because it decreases the mechanical and thermal properties of the fabricated composite. From Table 4.1, it can be observed that the void content for the PP-Al_2O_3 composite with a 20 wt. % is higher than virgin PP and filled composites.

Part II

4.2. Physical and Chemical characterization of TiO_2 (Titanium dioxide) filled Polypropylene composites

4.2.1. Fourier transform infrared analysis of PP- TiO_2 composites

The FTIR spectra of PP-TiO_2 composites are as shown in Figure 4.2. It can be seen that integration of TiO_2 in PP matrix resulted into shifting of peak at different wave number. The peak associated with groups of acrylic acid in the composites can be observed near band of 1460 cm^{-1}. In the spectrum of PP/TiO_2 composite, the sharp peak attributed to carbonyl group appears at 1715 cm^{-1} [162]. The peak at 1376 cm^{-1} was assigned to C-O stretching vibrations of the phenolic group. The peak at 2905 cm^{-1} was due to the stretching vibration of C-H bond from a methyl group. The

sharp peak of 2920 cm^{-1} corresponds to the stretching of CH_3 of paraffin oil which was stronger and sharper than that of CH_3 peak of PP [132]. There are sturdy characteristic absorptions in the region 2800–2865 and 540-690 cm^{-1}, confirming the dispersion of TiO_2 particles into the PP matrix. Small peaks observed between 900 and 1200 cm^{-1} were attributed to the various asymmetrical- symmetrical bending vibrations back and forth in plane of CH, CH_2 and CH_3.

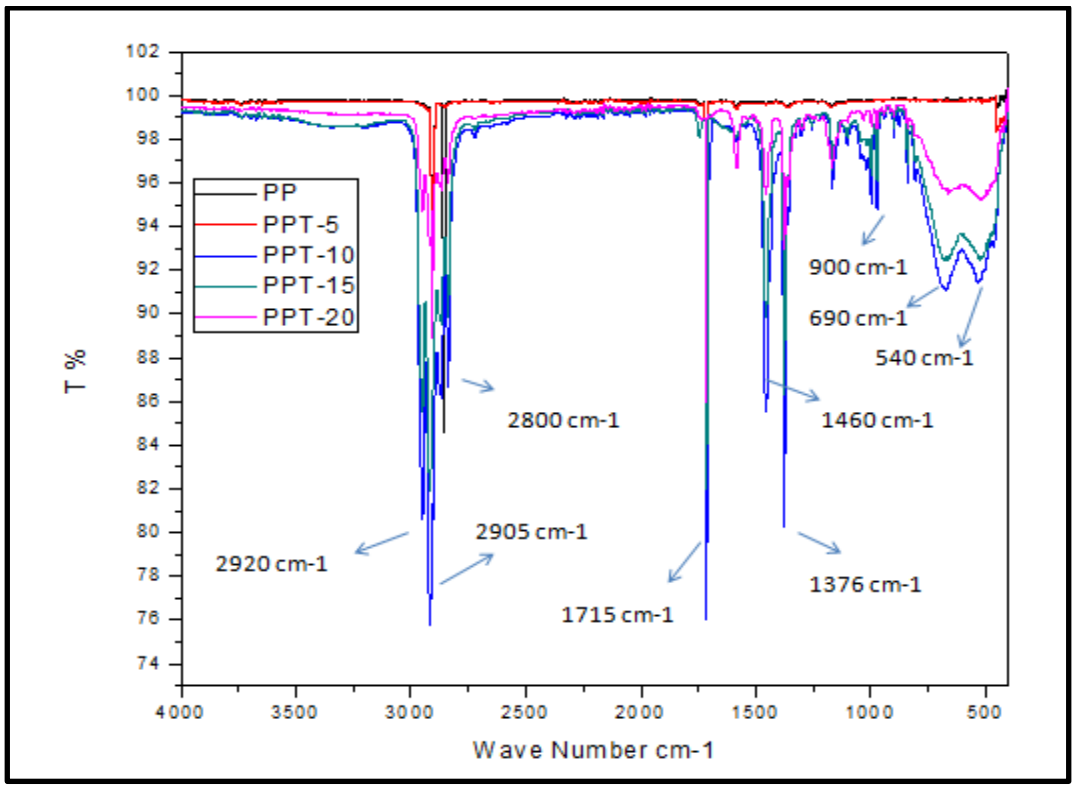

Figure 4.2 FTIR spectra of virgin PP and PP-TiO_2 composites

4.2.2. Effect of Void Content on TiO_2 filled Polypropylene Composites

In the present analysis, it was observed that theoretical density was somewhat more than the measured density as shown in Table 4.2. The drop in measured density was due to the formation of air bubbles during the fabrication of the PP-TiO_2 composites in injection moulding. This trapped air, referred to as voids, which are undesirable, unfavourably affects the mechanical and thermal properties of the polymer composite [163]. It was obviously seen that with the addition of TiO_2 filling from 5 and 10 wt.%, there was a increase in the void fraction from 0.28% to 2.38%, respectively. The main reason for rise in undesirable void content can be incomplete soaking out of the filler by PP matrix could show the way to the growth of undesirable voids in the PP

composites. On the other hand, with the increase in TiO_2 filler loading from 15 and 20 wt.%, the void content somewhat decreases from 1.75% to 1.38% respectively. This can be due to lower size of filler and improved filler matrix-interface chemical bonding of PP-TiO_2 composites.

Table 4.2 Measured and theoretical density of the PP-TiO_2 composites

Composite	Measured Density (g/cc)	Theoretical Density (g/cc)	Volume fraction of Voids (%)
PP	0.905	0.906	0.11
PPT-5	0.941	0.943	0.28
PPT-10	0.961	0.983	2.38
PPT-15	1.01	1.027	1.75
PPT-20	1.061	1.075	1.38

Part III

4.3. Physical and chemical characterization of Marble powder filled Polypropylene composites

4.3.1. Fourier transform infrared analysis of Marble powder filled Polypropylene composites

To observe the chemical bonding of the PP-Marble composites FTIR analysis was performed. The spectra of the composites are shown in Figure 4.3. In the beginning from high vibration band at 465 cm^{-1} followed by strong peak band at 841 cm^{-1} was observed in the composites due to presence of Mg - O bonds. Due to presence of carbonate in the marble, different peak obtained beyond in the range of 875-2867 cm^{-1}, (997 cm^{-1}, 1167 cm^{-1}, 1586 cm^{-1}, 1790 cm^{-1}, 1820 cm^{-1}, 2185 cm^{-1}, 2532 cm^{-1}, 2867 cm^{-1}) which exists in all the PP-marble composites. Due to stretching vibrations of the carbonate group bands at 1457 cm^{-1} and 1582 cm^{-1} were obtained. The characteristic bands for marble powder in the PP molecules were established by peaks at 1702 cm^{-1} from C=O stretching, 2917 cm^{-1} from =C-H stretching, 1510 cm^{-1} for aromatic C=C bond. With increase in calcinations temperature from 30 to 600^{o}C, a wide band spectra attributed to 1415 cm^{-1} due to changing of carbonate group. Furthermore, due to OH stretching and H-OH bending, few small peaks attributed at 3450 cm^{-1} and 3650 cm^{-1}.

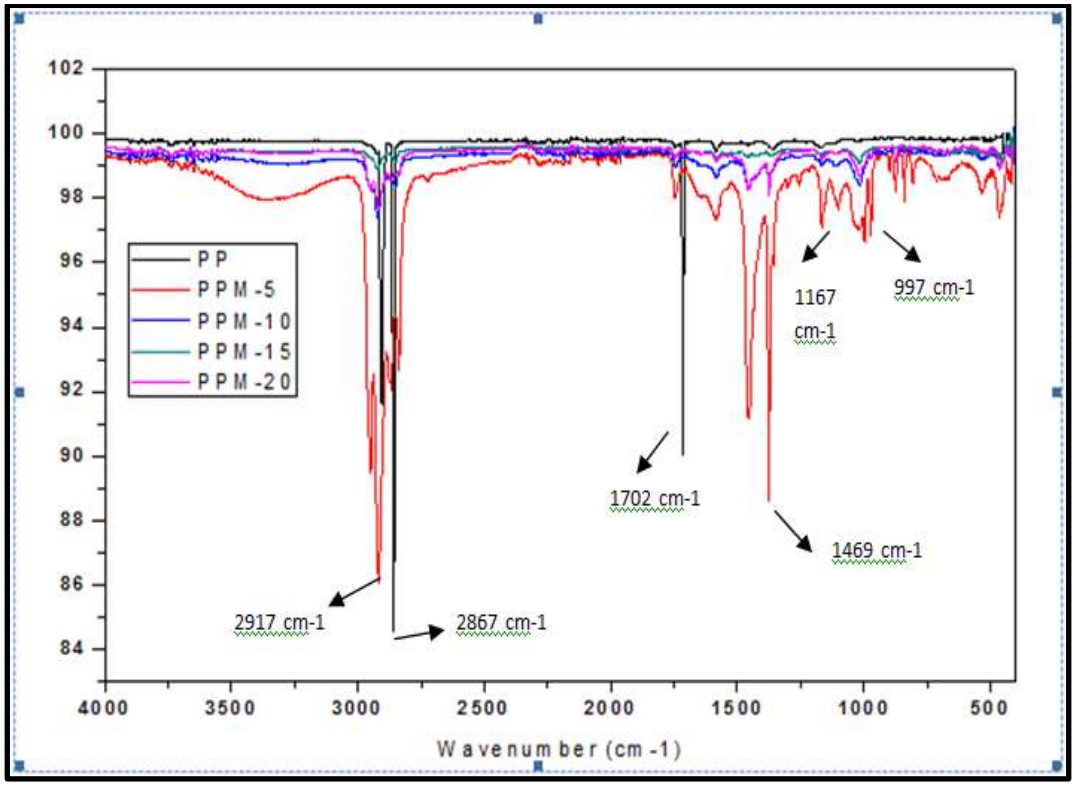

Figure 4.3 FTIR spectra of virgin PP and PP-Marble composites

4.3.2. Effect of Void Content on PP- Marble Powder composites

Physical and Mechanical properties are affected by void contents in the composites. In PP-Marble powder composites, it was observed that measured density was slightly less than the measured density as exhibited in Table 4.3.The reason for voids may be the air trapped during fabrication due to matrix is not able to expel all the air [114]. For good composites, void fraction should be less than 10%. For addition of 5, 10, 15 and 20 wt.% of marble powder in the composite increases the void content to 0.53%, 2.06%, 4.91% and 6.38%, respectively, compared to 0.11% for virgin PP. Using higher wt.% of marble powder increases the voids due to the high specific surface area of marble particles.

Table 4.3 Measured and theoretical density of the PP-Marble composites

Composite	Theoretical Density (g/cc)	Measured Density (g/cc)	Volume fraction of Voids (%)
PP	0.906	0.905	0.11
PPM-5	0.937	0.932	0.53
PPM-10	0.97	0.95	2.06
PPM-15	1.058	1.006	4.91
PPM-20	1.112	1.041	6.38

Chapter Summary

This chapter concluded that:

- This chapter presents the physical and chemical properties of the fabricated polypropylene composites. FTIR spectra of each composite are analysed.
- The filler particles alumina, titanium dioxide and marble powder are successfully dispersed with polypropylene.
- The void content of the PP-Al_2O_3 composite shows in increasing order (from 0.3% to 8.25%) with the increase in alumina content affects the properties of composites.
- The void content of PP composites filled with different weight-percentage of Titanium dioxide and marble powder are in the range of 0.28- 2.38% and 0.53- 6.38%, respectively.

The next chapter discusses the Mechanical and Thermo-Mechanical Properties of Polypropylene Composites under study.

*****

Chapter 5

MECHANICAL AND THERMO-MECHANICAL PROPERTIES OF POLYPROPYLENE COMPOSITES

This chapter presents the Mechanical and Thermo-mechanical properties of Polypropylene composites. The mechanical characterizations include determination of Shore D hardness, Izod Impact Strength, Flexural Strength and Compressive Strength of Polypropylene composites**.** The Thermo-mechanical characterizations include Dynamic mechanical analysis (DMA) and Thermo-Gravimetric Analysis (TGA).

The interpretation of the comparison and the results of various PP-composite samples are also presented. This chapter consists of three parts: part I consists of Polypropylene composite filled with alumina (Al_2O_3), part II consists of Polypropylene composite filled titanium dioxide (TiO_2) and part III consists of Polypropylene composite filled marble powder.

Part-I

5.1. Mechanical and Thermo-Mechanical characterization of Alumina filled Polypropylene composites

5.1.1. Mechanical characterization of Alumina filled Polypropylene composites

The variation in mechanical properties such as Shore D hardness, Izod Impact Strength, Flexural Strength and Compressive Strength of alumina filled Polypropylene composite are described below:

5.1.1.1. Effect of Shore D Hardness on Alumina filled Polypropylene composites

Figure 5.1 shows the hardness variation with filler content for alumina filled polypropylene composites. It reveals that hardness increases with increment in alumina filler content in polypropylene matrix. This increase in particulate may be attributed to stiffer and more brittle nature of Al_2O_3 than the PP matrix. According to investigation of Kumar et al. [164-165], the hardness test compacts the matrix and reinforcement arrangement, which results in improved stress transfer and resistance to indentation. The improvement in hardness of the composites reinforced with alumina filler from 0 wt. % to 20 wt. % in a step of 5 wt. % is 56, 58, 64, 68 and 70 respectively. The maximum hardness was observed 70 for 20 wt. % alumina filled polypropylene composites and minimum hardness was observed 56 for virgin PP matrix

material. Similar observation was found by Masouras et al. [166] and Mota et al. [167] for polypropylene composites.

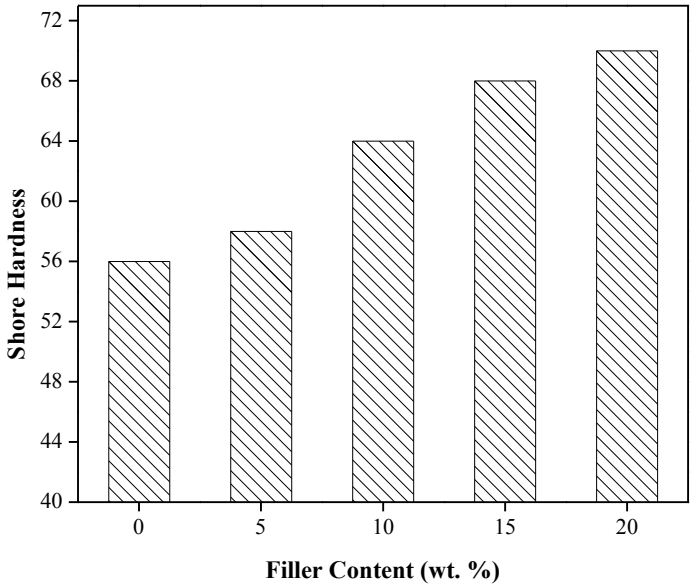

Figure 5.1 Effect on Shore D Hardness of virgin PP and PP-Al_2O_3 composites

5.1.1.2. Effect of Impact Strength on Alumina filled Polypropylene composites

The variation of impact strength with filler content for alumina filled polypropylene composite is shown in Figure 5.2. It depicts the impact strength decrease with increment in filler content in polypropylene matrix. The reason behind decrement in impact strength may be inherent ductility of the matrix, void content, weak inter-phase supporting the filler/matrix debonding and suitable inter- particle distance. The stress concentration first leads to debonding of the filler particles and voids formation. According to D. Kumar et al. [168] the particle content affects the inter particle distance and the stress state of the matrix polymer surrounding the voids. Impact strength decreases from 36 J/m to 21.32 J/m with increment of filler content from 0 wt. % to 20 wt. % in polypropylene matrix composites. The maximum impact strength was observed to be 36 J/m for virgin PP matrix and minimum impact strength was observed to be 21.32 J/m for 20 wt.% alumina filled PP composite. Similar observations were reported by Pedrazzoli et al. [105] and Akil et al. [78] for polypropylene composites.

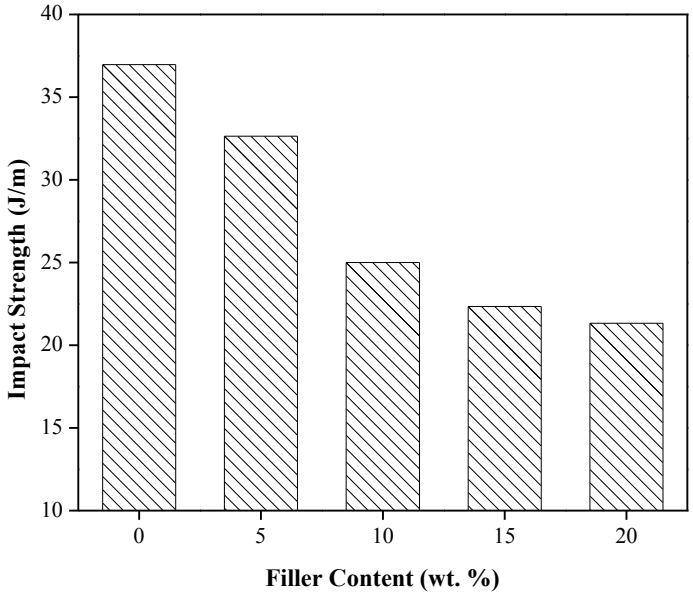

Figure 5.2 Effect on Impact Strength of virgin PP and PP-Al_2O_3 composites

5.1.1.3. Effect of Flexural Properties on Alumina filled Polypropylene composites

Flexural strength variation for unfilled and alumina filled polypropylene composites is indicated in Figure 5.3. It reveals that flexural strength increases with increase in alumina filler content in the polypropylene matrix. The reason behind the increase in flexural strength may be that addition of filler content enhance the interfacial adhesion between Al_2O_3 and the polymer matrix, which was not strong enough according to Mirjalili et al. [25]. Flexural strength for unfilled polypropylene was observed at 51.8 MPa with the increase of alumina filler from 0 wt. % to 5 wt. %, the flexural strength increases from 51.8 MPa to 53.04 MPa. Increase of filler 5 wt. % to 10 wt. % shows increase in flexural strength is 53.04 MPa to 56.11 MPa, further increase of filler from 10 wt. % to 15 wt. % shows increase in flexural strength from 56.11 MPa to 58.22 MPa. Again, increase of filler from 15 wt. % to 20 wt. % shows increase in flexural strength from 58.22 MPa to 59.26 MPa.

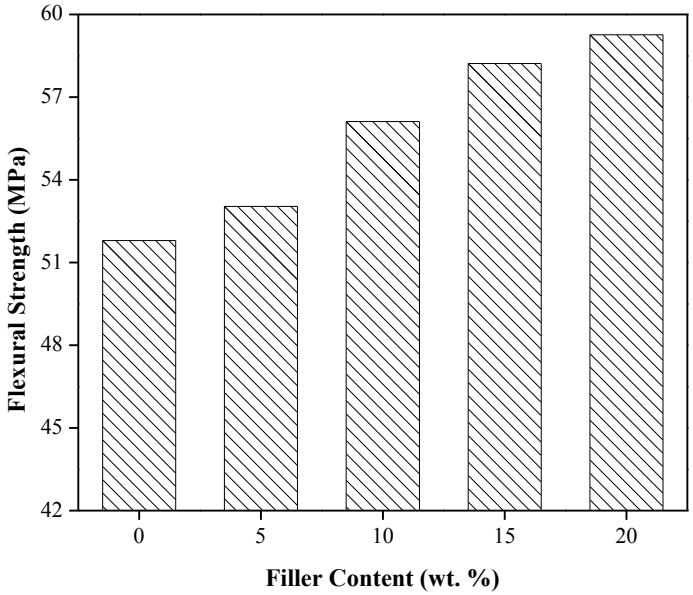

Figure 5.3 Effect on Flexural Strength of virgin PP and PP-Al_2O_3 composites

5.1.1.4. Effect of Compressive Strength on Alumina filled Polypropylene composites

Compressive strength variation with filler content for alumina filled polypropylene composites is presented in Figure 5.4. It shows that compressive strength increases with increase of alumina content up to 15 wt. % in polypropylene matrix while further increase of filler content shows slight decrease in compressive strength. The reason behind increase in compressive strength is stronger coupling between reinforcement and matrix that transmits the loads between them. Compressive strength for unfilled polypropylene was observed to be 91.36 MPa whereas with the increase of alumina filler from 0 wt.% to 5 wt.% the compressive strength increases from 91.36 MPa to 98.63 MPa respectively. Increase of filler 5 wt. % to 10 wt.% shows increase in compressive strength is 98.63 MPa to 108.82 MPa, further increase of filler from 10 wt.% to 15 wt.% shows increase in compressive strength is 108.82 MPa to 123.25 MPa. Further increase of filler from 15 wt. % to 20 wt. % shows decrease in compressive strength from 123.25 MPa to 121.34 MPa. It can be due to the existence of utmost void and air bubbles in the composite, which reduces the interfacial strength. Other possible reasons may be improper dispersion of filler particles in the matrix, which creates in-homogeneity in the composites. The other possible cause of reduction of compressive strength may be the clustering of particles as filler content

increases [163]. Similar results were observed for particulate filled polymer composites by Arao et al. [16] and Omar et al. [169]. The maximum compressive strength observed was 123.25 MPa for 15 wt. % alumina filled polypropylene composites which is 34.9% higher than virgin PP.

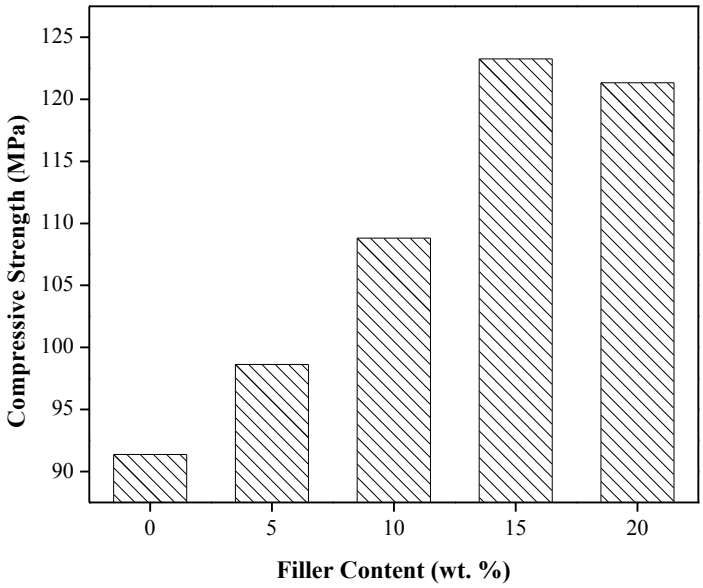

Figure 5.4 Effect on Compressive Strength of virgin PP and PP-Al_2O_3 composites

5.1.2. Thermo-Mechanical characterization of Alumina filled Polypropylene composites

The variation in Thermo-mechanical properties such as Dynamic mechanical analysis (DMA) and Thermo-Gravimetric Analysis (TGA) of alumina filled Polypropylene composite are described below:

5.1.2.1. Dynamic Mechanical Analysis (DMA) of PP-Al_2O_3 composites

Conceptually storage modulus (E') and loss modulus (E'') represent the extent of elastically recoverable-response and the non-recoverable viscous response due to energy dissipation by means of frictional and internal molecular motions of polymer composites. Storage modulus describes the energy stored elastically in composite material, while the loss modulus represents energy loss in terms of heat. Thus, the storage modulus depicts the relative-stiffness of a composite material.

Figure 5.5 indicates the storage modulus of alumina filled Polypropylene composite. It shows three distinct regions I, II and III viz, the glassy region (5-20°C), the glassy transition region (20-120°C) and the rubbery region (above 120°C), respectively.

During glassy region (5-20°C), Figure 5.5 shows the remarkable increment in storage modulus with increasing alumina content up to 10 wt.%, probably due to the restrictions of the molecular chain motion which developed a reinforcing effect according to Pedrazzoli et al. [106]. However, further addition of filler particles in composites produces the voids in composites, which probably weaken the storage modulus [63]. The formation of void in polymeric composites depends on number of reasons such as use of high viscosity resin in combination with closely packed fillers /fibers, which are not completely mixed with resin materials, improper arrangement of filler particles in the matrix, uniform mixing of resin and hardener so that bubble may be formed during preparation of structure [163].

From the peak of Tan delta, glass transition temperature (T_g) can be detected. Below T_g the storage modulus (E') values of the composites were found to be spacious to each other and showing greater contribution of the particulate towards the stiffness of the composites at low temperature. In all the composites, E' decreases with increase in temperature, however no variations was observed in (E') after 120° C.

Afterwards as the alumina content increases beyond 10 wt. %, due to agglomeration of alumina particles in matrix little improvement is observed in storage modulus in comparison to PP. It was observed that the E' improved for the composites by increasing the Al_2O_3 loading. This is because of the reinforcement passed by Al_2O_3, allowing higher stress transfer at interface from PP to Al_2O_3. Thus, it is concluded that incorporation of the ceramic filler has improved the stiffness property of the composites.

To determine the viscous response of composites, loss modulus was determined. It reflects the ability of a material to dissipate the energy. Figure 5.6, indicates the loss modulus of alumina filled Polypropylene composite. With increase in temperature value, E'' is increased and then decreased irrespective of percentage of alumina wt.%. Loss modulus peak shifted towards higher temperature with increase in filler loading. It was also observed that, T_g slightly increased in composite of higher filler content with respect to unfilled PP, reflecting the great restriction of motion of the polymer chains developed by the amalgamation of the composites. If the

molecular chain is greatly restricted, the motion of chain segment becomes difficult at the earlier glass transition temperature and more temperature will be required. Thus due to homogeneous dispersion of alumina element in polymer matrix, T_g values rise. Effect of alumina wt. % on value E" is found more influencing in region of T_g. The value of E" in transition state is significantly higher for the composites, which could be the result of increase in internal molecular friction that increases dissipation of the energy. Pedrazzoli et al. [106] investigated that amplitude of the loss modulus increased in existence of ceramic filler. This specifies that higher viscosity because of the existence of fillers creates a restriction in movement of molecules. Thus, higher the Al_2O_3 content, greater the viscosity, which ultimately needs additional energy for the dissipation. Thus, composites PPA-10 and PPA-15 shows higher loss modulus. On the other hand, in PPA-20 composite, further increasing filler content induces 'over-filled' composites attributed to agglomeration of filler particles. This damaging effect causes to decline the loss modulus.

The amount of damping factor (Tan delta) is indicator of the polymer system and it provides stability between the elastic and viscous phase in polymer material. Damping properties of composites are significantly affected by void content, reinforcement/matrix interaction, filler size and its distribution. Measurements of Tan delta give sensible information related to T_g and make available an indicator of strength of a composite's ability to store and dissipate energy. Tan delta values of injection moulded specimen of PP - alumina composites with temperature at a frequency of 1 Hz is shown in Figure 5.7. It was observed from Figure 5.7 that Tan delta increases with increase in temperature; it goes to maximum level in transition region and then reduces in the rubbery region. It was also observed that damping factor is low below T_g in all specimens due to spread chain segments in the frozen state at this stage. Therefore, higher the Tan delta peak values, greater is the degree of mobility of the molecules. As shown in Figure 5.7, Tan delta < 1, reflects fabricated composites behave analogous to solid. Additionally, interaction of alumina reduces the peak height of Tan delta, which is due to the integration of stiff ceramic filler that confines the movement of the molecules of polymer. Khalid et al. [170] investigated that the poorer interfacial adhesion of Polypropylene and filler lead to higher damping at the particle interface. Vishkaei et al. [171] explored that T_g of the polymer composites improved by rising the weight percentage of particles because micro particles limit thermally induced segmental random motions of the molecular chains

in the composite material resulting in a better T_g.

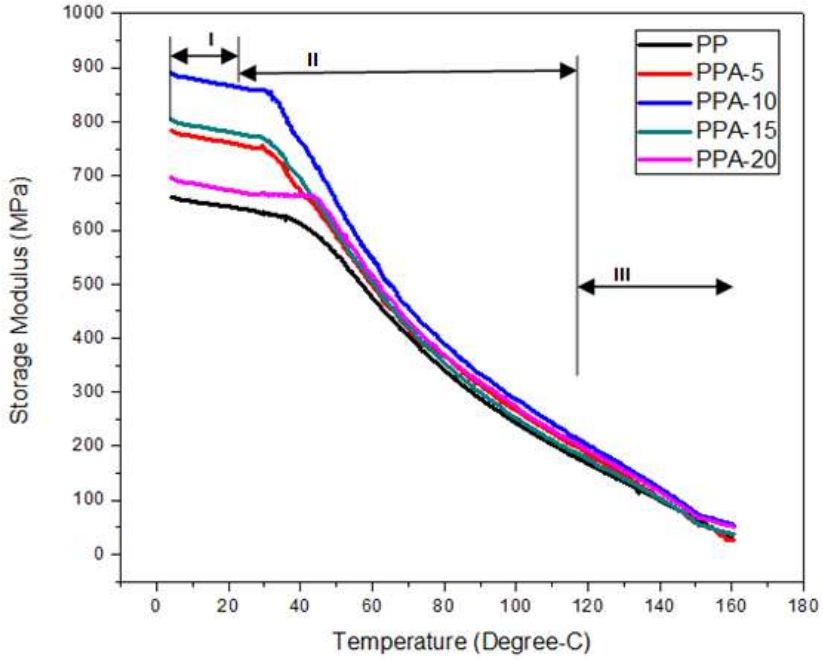

Figure 5.5 Variation of Storage Modulus (E') as a function of temperature for PP-Al_2O_3 composites

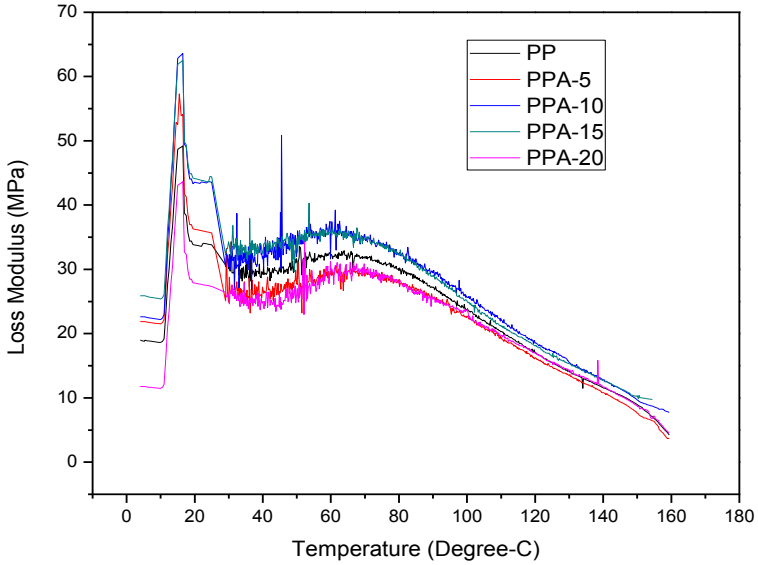

Figure 5.6 Variation of the Loss Modulus (E'') as a function of temperature for PP-Al_2O_3 composites

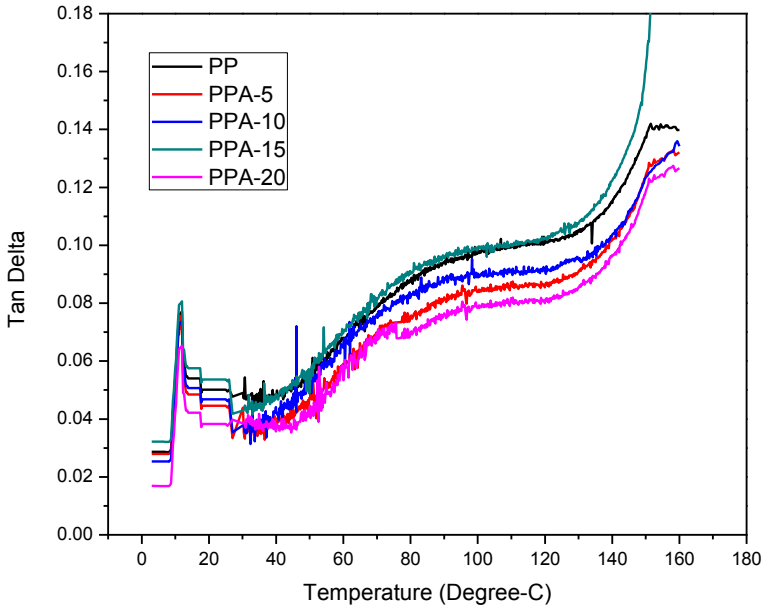

Figure 5.7 Variation of the Tan Delta (Tan δ) as a function of temperature for PP-Al_2O_3 composites

5.1.2.2. Thermo-Gravimetric Analysis (TGA) of PP-Al_2O_3 composites

TGA is applied to observe the change in the mass of a specimen as a function of temperature. The thermal stability curve of injection moulded specimen having different PP-Alumina wt.% compared to virgin PP is shown in Figure 5.8. The initial degradation temperatures (T_{ID}) of injection moulded specimen were determined at the point of inflection, by drawing two tangents to the thermo-gravimetric curve. It was observed that initial degradation temperature of virgin PP matrix was found to increase due to the reinforcement of particulate in matrix, due to the balanced bonding of the particulate to matrix. According to Siengchin and Kocsis [107], BA incorporation enhanced the resistance to thermal degradation of the PP matrix. It can be observed that the thermal stability of composites depends upon the matrix as well as the wt. % of Al_2O_3 particulate in the composite. Two steps degradation has shown in both virgin PP and Al_2O_3 composites. Probably, due to the higher thermal stability of alumina particulate, injection moulded composites show considerable raise in thermal stability. It was also observed that the initial degradation occurs at near 340–430^oC and final degradation occurs near 460−485^oC. The initial degradation temperature (T_{ID}) of injection moulded specimen for PP is about 345^oC. Adding Al_2O_3 to PP (20 wt. %) shifted T_{ID} to just about 425^oC. It means that T_{ID} increased by

about 80°C with the addition of Al_2O_3. It occurs as the increased absorbed thermal energy that results higher temperature degradation of polymer composite.

Consequently, as Al_2O_3 particulate increases there is an increase in degradation temperature. Similar behaviour was reported by Pedrazzoli et al. [106] for TGA analysis. The effect could be linked with the dehydration process of filler which delays the polymer degradation. The addition of Al_2O_3 particulate can increase in the end degradation temperature (T_{ED}). Zanetti et al. [172] investigated the thermo-oxidative degradation of PP/MMT (montmorillonite) composites by using TGA. They found that the composites were more stable in comparison to virgin polymer and with the anticipated mechanism that oxygen attacks at the carbon radical within the chain by H abstraction. Approximately 210-250°C hydrogen abstraction becomes more likely thus resulting in oxidative dehydrogenation. As the temperature rises, the concentration of chain end radicals increases due to beta scission of radicals turn into competitive with either oxygen addition or the abstraction of hydrogen. Thus, direct thermal scission of carbon-carbon bonds (C-C) becomes possible near 300° C.

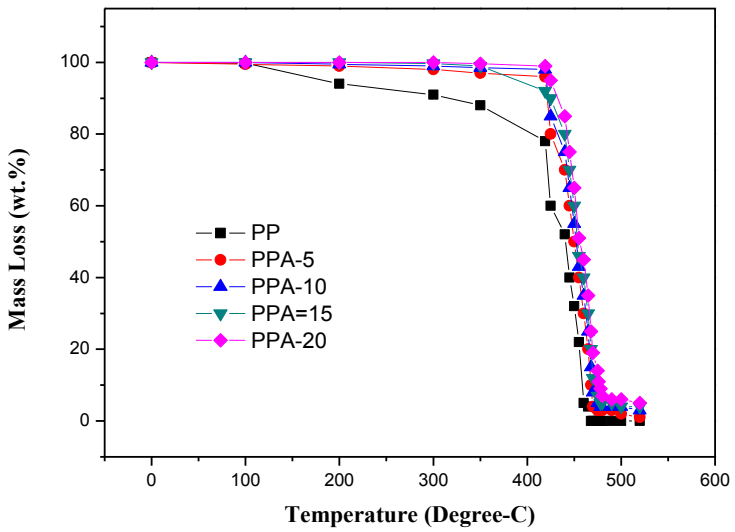

Figure 5.8 TGA for PP-Al_2O_3 composites

Part-II

5.2. Mechanical and Thermo-Mechanical characterization of Titanium Dioxide filled Polypropylene composites

5.2.1. Mechanical characterization of TiO_2 filled Polypropylene composites

The variation in mechanical properties such as Shore D hardness, Izod Impact Strength, Flexural Strength and Compressive Strength of titanium dioxide filled Polypropylene composite are described below:

5.2.1.1. Effect on Shore D Hardness with TiO_2 filled Polypropylene composites

The variation in Shore D hardness with different filler content in PP- TiO_2 composites is shown in Figure 5.9. It reveals that hardness increases with increase in TiO_2 filler content in polypropylene matrix. An increased hardness may be because of a more compact/rigid structure at the material's surface, which creates greater resistance to indentation that resulting in the hardness of the composites showing higher values. This behaviour may be due to an increased crystallinity. According to Siddhartha et al. [173] the force experienced by the injection moulding makes possible the formation of a graded molecules arrangement due to conglomeration of high density TiO_2 particles towards the external edge of the matrix material and the resultant higher viscosity can limit the configuration of a functionally graded composition during injection moulding process.

The improvement in hardness of unfilled composites and TiO_2 filled composite from 5 wt.% to 20 wt.% in steps of 5 wt.% was 56, 67, 68, 69 and 70 respectively. The maximum Shore D hardness of 70 was observed for 20 wt.% PP-TiO_2 composites due to conglomeration of high density TiO_2 particles . Minimum hardness of 56 was observed in Polypropylene.

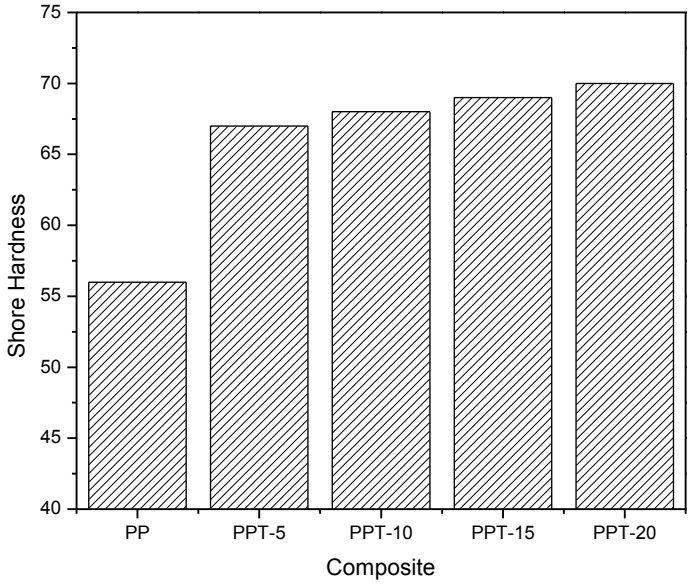

Figure 5.9 Effect on Shore D Hardness of virgin PP and PP-TiO_2 composites

5.2.1.2. Effect on Impact Strength with TiO_2 filled Polypropylene composites

Impact strength variation for virgin PP and TiO_2 filled polypropylene composites are shown in Figure 5.10. Virgin PP, PPT-5, PPT-10, PPT-15 and PPT-20 have impact strength to be 36, 35, 32, 29 and 24 J/m respectively. It reveals that impact strength going to decrease with increment in TiO_2 filler content in polypropylene matrix; it was due to the hardness of the inorganic particles. Generally elastic modulus, tensile strength, stress at break increase while elongation and impact strength decrease. Thus no improvement was found in impact strength of the composites by the addition of filler TiO_2. It was clear that all composites having impact strength less than impact strength of virgin PP. According to Daneshpayeh et al. [4], addition of a small amount of TiO_2 particles (max. 4 wt.%) enhanced the mechanical properties of composites. However, deterioration takes place in the mechanical properties by further adding of TiO_2 particles in matrix due to the agglomeration of particles.

According to Zohrevand et al., [174] presence of anhydride-modified polypropylene AM-PP provides uniform dispersion of the particles, primarily with the TiO_2 volume having less than 5 wt.%. By increasing TiO_2 volume, the amount of aggregates raises and the surface morphologies of the compatibilized and uncompatibilized specimens became analogous. According to Patel and Dhanola, [68] the good bonding strength between matrix, microfillers, and fiber and flexibility of the

interface molecular results in absorbing and dispersing more energy, and prevents the early initiation of cracks more effectively.

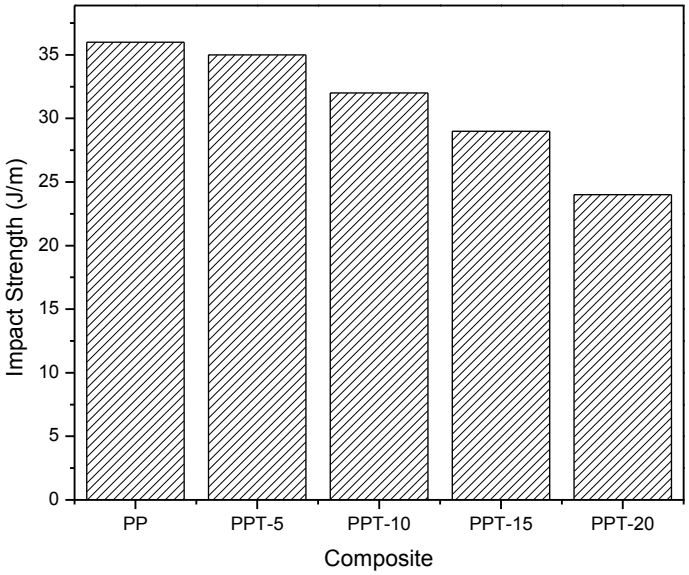

Figure 5.10 Impact Strength of virgin PP and PP-TiO_2 composites

5.2.1.3. Effect on Flexural Properties with TiO_2 filled Polypropylene composites

Flexural strength variation for unfilled and TiO_2 filled polypropylene composites is indicated in Figure 5.11. In composite PPT-5, flexural strength to be 58.9 MPa which was 13.7 % higher than flexural strength of virgin PP. Similarly, composites PPT-10, PPT-15 and PPT-20 have flexural strength 57.4, 56.3 and 50.8 MPa respectively. Thus, further increment of TiO_2 filler content in PP matrix reduce the flexural strength, as there are some parameters that influence the flexural properties of the composites. It consists of the degree of uniform dispersion of filler in the matrix; interfacial tension, filler's aspect ratio and need of stabilize the morphology against elevated stresses during forming of the filler-matrix interface. The treatment layer has been established on the surface of the TiO_2 particles so that it become hydrophobic which is same as PP. However, the decrease of flexural strength that low wt.% TiO_2 addition can bring by the weak interfacial adhesion between the particles and the matrix [7]. The weak interfacial adhesion causes a greater extent of cavitation or voiding. The high degree of TiO_2 particles in the matrix can initiate the crack in the PP matrix and cause the early failure of specimen. With further adding

of the TiO_2 filler, the composite specimens became more brittle and added filler particles acts as terminator of trend.

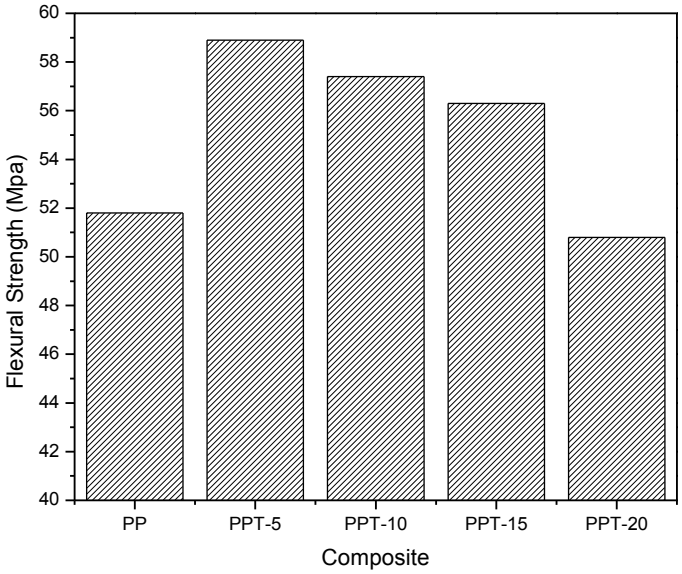

Figure 5.11 Effect on Flexural Strength of virgin PP and PP-TiO_2 composites

5.2.1.4. Effect on Compressive Strength with TiO_2 filled Polypropylene composites

The variation of compressive strength with filler content for TiO_2 filled polypropylene composites was presented in Figure 5.12. It was observed that as the filler content increases, the compressive strength of the composite also increases. The fabricated composites PPT-5, PPT-10, PPT-15 and PPT-20 have compressive strengths of 113.8, 132.5, 163.2 and 171.6 MPa respectively. Thus, composite PPT-20 has highest compressive strength which was 87.8% higher than virgin PP. This was due to excellent dispersion and better interfacial interaction between filler and matrix.

Duan et al., [175] investigated that adding of TiO_2 improves compressive strength of polymer that is proportional to the content of TiO_2. According to Zu-hua et al., [176] the strength improvement effect of TiO_2 on polymer was more obvious when 5 wt.% TiO_2 was introduced. The results illustrate that compressive strength of the PP having fly ash by steam curing containing 32% (mass fraction) at 80℃ was improved by 35.5%. Particle size of filler play an important role to increase the compressive strength of the composites.

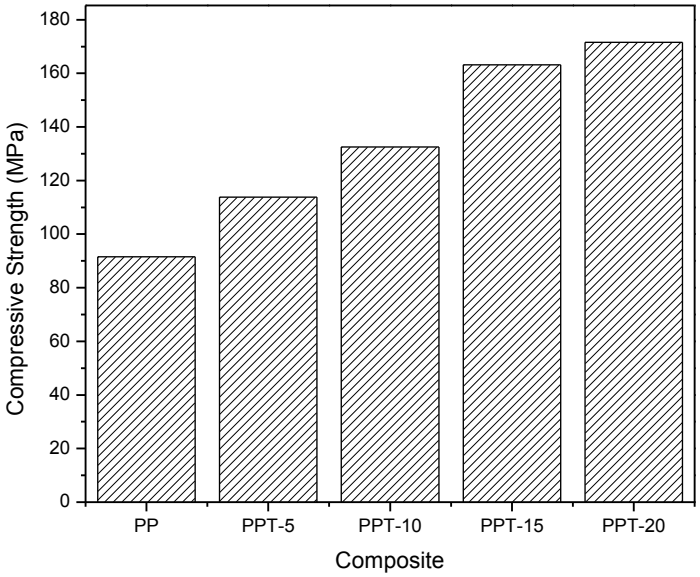

Figure 5.12 Effect on Compressive Strength of virgin PP and PP-TiO_2 composites

5.2.2. Thermo-Mechanical characterization of PP-TiO_2 composites

The variation in Thermo-mechanical properties such as Dynamic mechanical analysis (DMA) and Thermo-Gravimetric Analysis (TGA) of titanium dioxide filled Polypropylene composite are described below:

5.2.2.1. Dynamic Mechanical Analysis (DMA) of PP-TiO_2 composites

DMA is an essential and efficient technique for investigating the morphology and viscoelastic property of the composite materials which are integrated to principal relaxations and further important factors, such as the dynamic fragility, cross-linking density and dynamic viscosity [177]. The viscoelastic behaviour of PP was stoutly influenced by variables that have an effect on the crystalline regions with crystallinity, lamellar thickness and the interface [86]. Figure 5.13 indicates the storage modulus of TiO_2 filled Polypropylene composite. Three distinct regions were identified as stage - I, stage - II and stage -III as glassy region (5-25^oC), transition region (25-120^oC) and rubbery region (above 120^oC), respectively. Significant improvement in storage modulus with increasing TiO_2 was observed in glassy region which is possibly due to restriction of the molecular chain motion which generates a reinforcing effect. PPT-10 has maximum value of storage modulus. Glass Transition temperature (T_g) can be

identified by the peak of Tan δ. Wide area to be found below T_g. In all the PP-TiO_2 composites (E') decreases with increase in temperature.

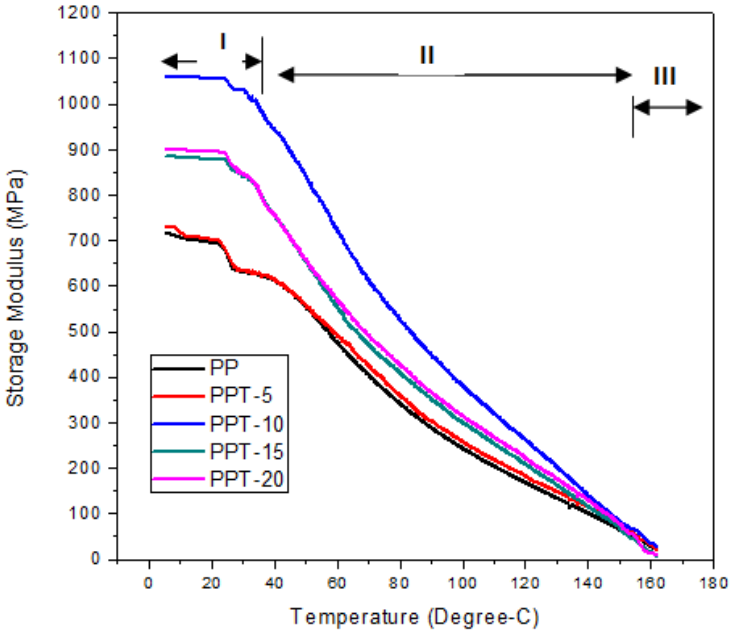

Figure 5.13 Variation of Storage Modulus (E') as a function of temperature for PP-TiO_2 composites

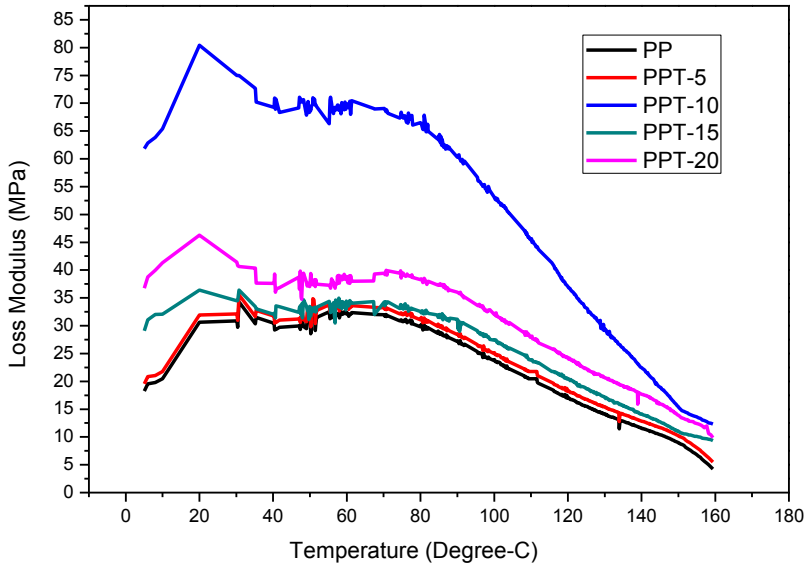

Figure 5.14 Variation of Loss Modulus (E'') as a function of temperature for PP-TiO_2 composites

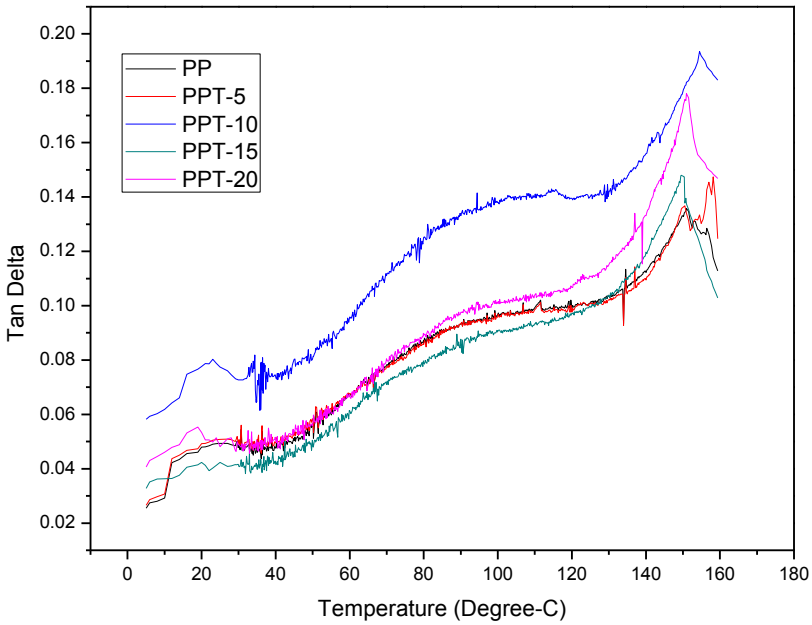

Figure 5.15 Variation of Tan Delta (Tan δ) as a function of temperature for PP-TiO_2 composites

Loss modulus used to identify viscous response of composite material. It reveals the capacity of a material to dissipate energy. Figure 5.14 indicates the loss modulus of TiO_2 filled PP composite. With increase in temperature value, E' also increased and then decreased irrespective of wt.% of TiO_2. It was obtained in most cases that the enhancement of stiffness significantly decreases the ductility. But PP/TiO_2 composites show increased stiffness without reducing ductility.

It can be observed in Figure 5.14 that loss modulus increases with the increase of TiO_2 content during the entire temperature range. The rise in loss modulus with rise in filler element is recognized as the increase in energy absorption with increasing filler element. The existence of short hemp fillers in matrix created a great amount of filler–matrix interfacial area in composites where energy can be easily dissipated. By lower energy dissipation a stronger interface can be characterized.

Between the elastic and the viscous phase of a composite material, the magnitude of Tan δ is indicative of a polymer. Tan δ values of PP-TiO_2 composites with temperature at a frequency of 1 Hz is exhibited in Figure 5.15. There is an increase in Tan δ value with addition of TiO_2 due to the agglomeration of TiO_2 in the composite. This reflects an increase in damping property. It can be observed from

Figure 5.15 that Tan δ rises with rise in temperature; and approaches utmost level in the transition-region and then reduces in the rubbery region.

It was also exhibited that glass transition temperature slightly shifts towards the higher value, representing decrease of the particles chain mobility imparted by the cross- linked and filled TiO_2 fraction in the composite [92]. However for higher TiO_2 wt.% the T_g of the corresponding PP-TiO_2 composite decreased due to larger inter particle spacing in composite leads to increase the mobility of PP molecules chains and thus decrease the T_g of PP phase in the composite. T_g was found in the range of 9-14^oC for the PP-TiO2 composites. It can be added that cluster size and homogeneous dispersion of TiO_2 particles in the matrix leads towards support in the dissipating energy under viscoelastic deformation [178].

For evaluation of damping property of composite materials Tan $\delta > 0.1$ is considered as a standard. The temperature duration and range with Tan $\delta > 0.1$ for neat PP was set up to be 115^oC – 158^oC and corresponding Tan δ peak was 0.11 and for composite PPT-5, PPT-10, PPT-15 and PPT-20 wt.% the range was 116 ^oC-159 ^oC, 121 ^oC-163 ^oC, 117 ^oC-160 ^oC and 116 ^oC-161 ^oC with corresponding peaks 0.11, 0.15, 0.13 and 0.12 respectively.

5.2.2.2. Thermo-Gravimetric Analysis (TGA) of PP-TiO_2 composites

TGA is used to examine the change in weight of a specimen as a function of temperature. The thermal stability curve of injection moulded composites having different TiO_2 wt.% compared to virgin PP are shown in Figure 5.16. TiO_2 filled composites confirm enhanced thermal stability in comparison to virgin PP. It can be observed that Onset of degradation temperature (T_{Od}) of all the composites are higher than virgin PP. It was also observed that Onset of degradation temperature increased by 80^oC of PPT-10 composite in comparison to virgin PP. The increased Endset of degradation temperature (T_{Ed}) also reveals the better thermal stability of all the composites [94]. Rise in degradation temperatures can be recognized due to the increased adhesion force at PP/TiO_2 interface.

As a general rule, to reflect on the degradation temperature at 50% weight (T_{dd}) is a sign for composite structural destabilization. Thus, it can be observed, that the virgin PP was seen to be stable up to 420.4^oC, while composites PPT-5, PPT-10, PPT-15 and PPT-20 wt.% show the thermal stability at higher temperatures of 450.5^oC, 462.7^oC, 454.6^oC and 457.2^oC, respectively. Thus, in case of very well

interfacial interaction, particles are able to confine the movement of a polymer chain, creating the scission of molecular chains which are harder at the lower temperature. As a result, the degradation temperature of the composite shifts to higher temperature according to Torres et al., [179]. According to Mirigul Altan, [180] the mechanism can be explained by H abstraction molecules of oxygen attacks at the carbon radical inside the chain. In the region of 220-250^{o}C, hydrogen abstraction turn into further stable phase, resulting in oxidative dehydrogenation. Further, as the temperature rises, the absorption of chain end radicals also rises due to beta scission of radicals.

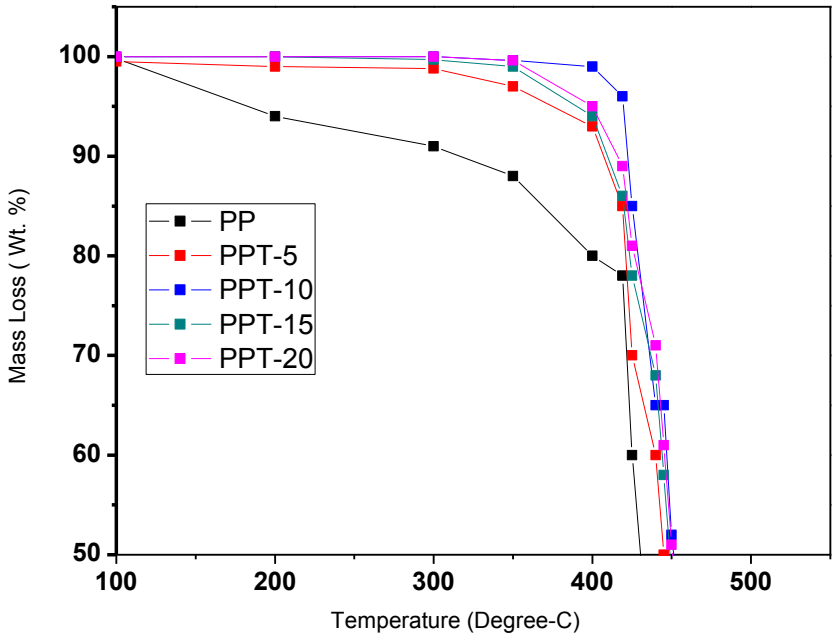

Figure 5.16 TGA of PP-TiO_2 composites

Part-III

5.3. Mechanical and Thermo-Mechanical characterization of Marble Powder filled Polypropylene composites

5.3.1 Mechanical characterization of Marble Powder filled Polypropylene composites

The variation in mechanical properties such as Shore D hardness, Izod Impact Strength, Flexural Strength and Compressive Strength of marble filled Polypropylene composite are described below:

5.3.1.1. Effect on Shore D Hardness with Marble Powder filled Polypropylene composites

The variation in Shore D hardness with different filler content in PP- Marble composites are shown in Figure 5.17. It reveals that hardness increases with increment in Marble powder filler content in polypropylene matrix. This is the indication of the reinforcement of the Marble powder in the PP matrix. Agglomeration of marble particles can be observed in SEM analysis. The improvement in hardness of unfilled composites reinforced with marble powder filler from 0 wt. % to 20 wt. % in a step of 5 wt. % is 56, 67, 70, 72 and 73 respectively. The maximum Shore D hardness was observed 73 in PPM-20.

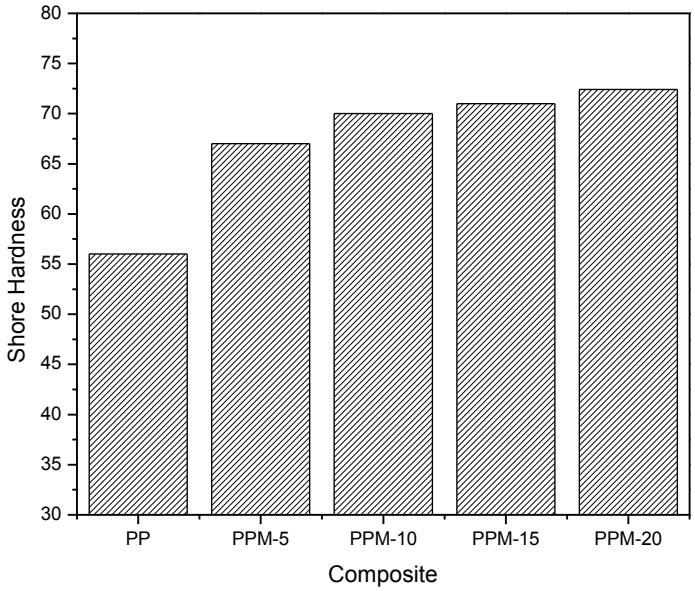

Figure 5.17 Effect on Shore D Hardness of virgin PP and PP-Marble composites

5.3.1.2. Effect on Impact Strength with Marble powder filled Polypropylene composites

The variation of impact strength with filler content for Marble powder filled polypropylene composite is shown in Figure 5.18. It shows the impact strength improvement with increment in filler content into polypropylene matrix. The reason behind increment in impact strength is inherent ductility of the matrix and strong inter-phase supporting the filler/matrix bonding. Marble powder having 5 and 10 wt.% consist impact strength to be 37 J/m and 38.5 J/m. Similarly, marble powder having 15 and 20 wt.% consists impact strength 39.7 and 40.6 J/m respectively**.**

Similar results were obtained by Ahmed et al. [181] during the study of behaviour of the effects of silica on the properties of marble filled natural rubber composites. In another study by Ahmed et al. [182] curing characteristics and mechanical properties of natural rubber hybrid composites reinforced with marble powder-Silica and marble powder-rice husk derived silica, were studied. The results from this study showed that the performance of rubber hybrid composites with Marble-Silica and rice husk as fillers has better mechanical properties compared with the case where only marble was used as single filler. The addition of silica and rice husk in marble composites improves significantly the tensile strength; tear strength hardness, modulus and crosslink density of the composites.

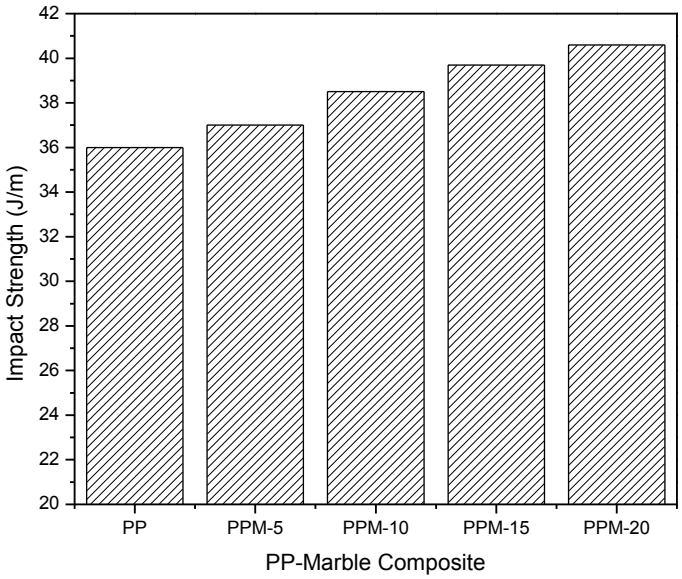

Figure 5.18 Effect on Impact Strength of virgin PP and PP-Marble composites

5.3.1.3. Effect on Flexural properties with Marble Powder filled Polypropylene composites

Flexural strength variation for unfilled and the Marble powder filled polypropylene composites is exhibited in Figure 5.19. In composite PPM-5, flexural strength to be 64.16 MPa which was 23.86% higher than flexural strength of virgin PP. Similarly, composites PPM-10, PPM-15 and PPM-20 have flexural strength 57.5, 56.4 and 52.56 MPa respectively. Thus, further increment of Marble powder filler content in PP matrix reduces the flexural strength, as there are some factors that influence the flexural properties of the composites. Some of these factors are interfacial tension,

degree of uniform dispersion of filler in the matrix, filler's aspect ratio and need of stabilize the morphology against elevated stresses during forming of the filler-matrix interface.

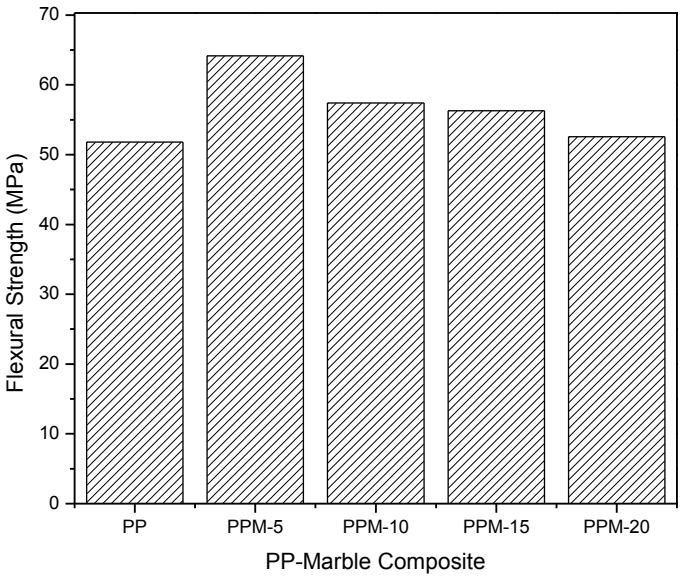

Figure 5.19 Effect on Flexural Strength of virgin PP and PP-Marble composites

5.3.1.4. Effect on Compressive Strength with Marble Powder filled Polypropylene composites

The variation of compressive strength with filler content for marble powder filled polypropylene composites is presented in Figure 5.20. It is observed that as the filler content increases, the compressive strength of the composites also increase. The fabricated composites PPM-5, PPM-10, PPM-15 and PPM-20 has compressive strength of 103.4, 115.8, 134.7 and 159.4 MPa respectively. Thus, in all the composites of PP-Marble powder, PPM-20 has highest compressive strength which is 74.4% higher than virgin PP. This is due to the excellent dispersion and better interfacial interaction between filler and matrix.

Yen et al. [183] investigated the engineering properties and the hydration characteristics of eco-cement pastes. The tests also concluded the feasibility of replacing up to 50% of the limestone which was used in the production of cement with marble powder. Because of the mass amount of $Ca(OH)_2$, the hydration of the cement pastes increased in number, which obviously enhanced the rate of the

compressive strength. This supported the fact that the eco-cement confirmed engineering practicability.

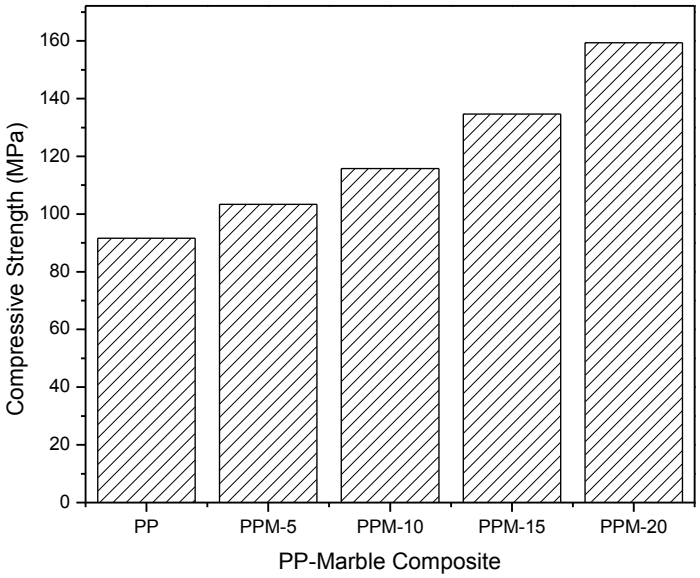

Figure 5.20 Effect on Compressive Strength of virgin PP and PP-Marble composites

5.3.2. Thermo-Mechanical characterization of Marble Powder filled Polypropylene composites

The variation in Thermo-mechanical properties such as Dynamic mechanical analysis (DMA) and Thermo-Gravimetric Analysis (TGA) of marble powder filled Polypropylene composite are described below:

5.3.2.1. Dynamic Mechanical Analysis (DMA) of PP-Marble Powder composite

Dynamic mechanical analysis is an efficient tool for investigating the morphology and viscoelastic properties of composite materials which are related to principal-relaxations and further important factors, such as dynamic fragility, cross-linking density and dynamic viscosity.

Figure 5.21 attribute the curve for variation of the storage modulus (E') with respect to the temperature for PP-marble powder composites. It shows three separate areas I, II and III viz, glassy region (5-30^{o}C), glassy transition region (30-140^{o}C) and the rubbery region (over 140^{o}C), respectively.

It was observed that with increase in temperature, there was decrease in the storage modulus, which is the general trend. It was attributed because the increase in the temperature led to raise the mobility of molecules inside the PP, which in turn, results into soften the composite material. It was observed from 5-30°C, the atoms were strongly arranged and the storage modulus was elevated. In the zone of glassy stage to rubbery stage, this decreased drastically. It was observed that in rubbery zone, storage modulus became almost constant.

It was observed in composite PPM-5, when Marble powder filler was integrated in PP, the measured storage modulus was found enhanced. Further increment of marble powder filler resulted into large enhancement in storage modulus. Due to high modulus, ceramic and brittle inorganic oxide-filler, rise in storage modulus with the rise in marble filler was recognized. Due to better interfacial bond and better dispersion, additional storage modulus was obtained between PP matrix and marble powder filler.

To determine the viscous response of composites loss modulus was determined. It reflects the ability of a material to dissipate energy. Figure 5.22 shows the loss modulus of marble filled composite. The figure shows that in the glassy region up to 5-30°C, loss modulus rises with the rise in temperature, but after reaching maximum value at the glass transition temperature, it taking place to decrease considerably in the region of glass transition. The rise in loss modulus with rise in marble powder was characterized the phenomenon that rise in filler content gives rise in inner molecular friction that boost up the energy dissipation. While in adding up of the marble powder up to 10 wt.% in the PP rises the loss modulus and it achieves optimum value. It was found that, 20 wt.% of addition of the marble powder resulted in decrease in the loss modulus. Drop in loss modulus could be due to the clustering of marble filler tiny particles, fragile interfacial chemical bond between resin and filler or non-uniform dispersion of the marble filler in PP-structure.

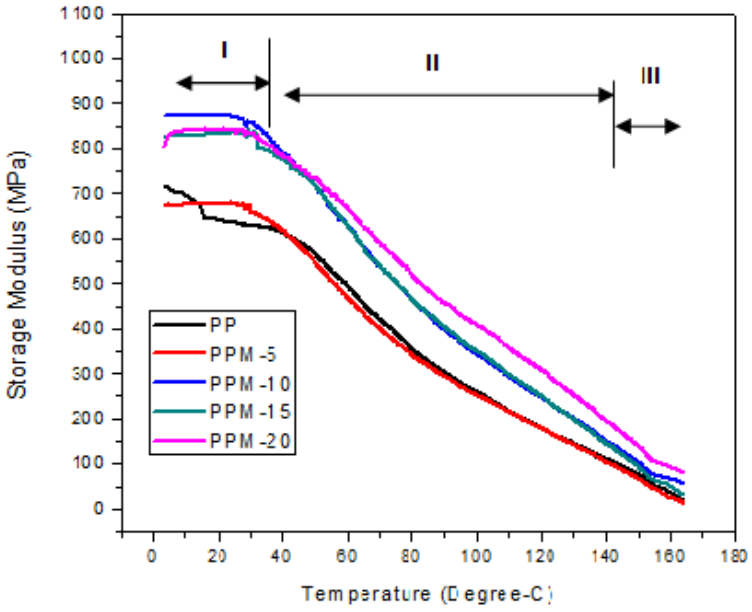

Figure 5.21 Variation of Storage Modulus (E') as a function of temperature for PP-Marble composites

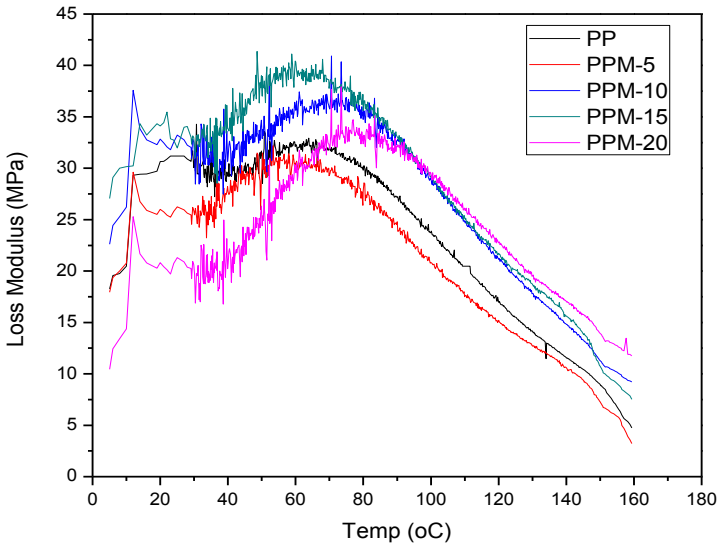

Figure 5.22 Variation of Loss Modulus (E'') as a function of temperature for PP-Marble Composites

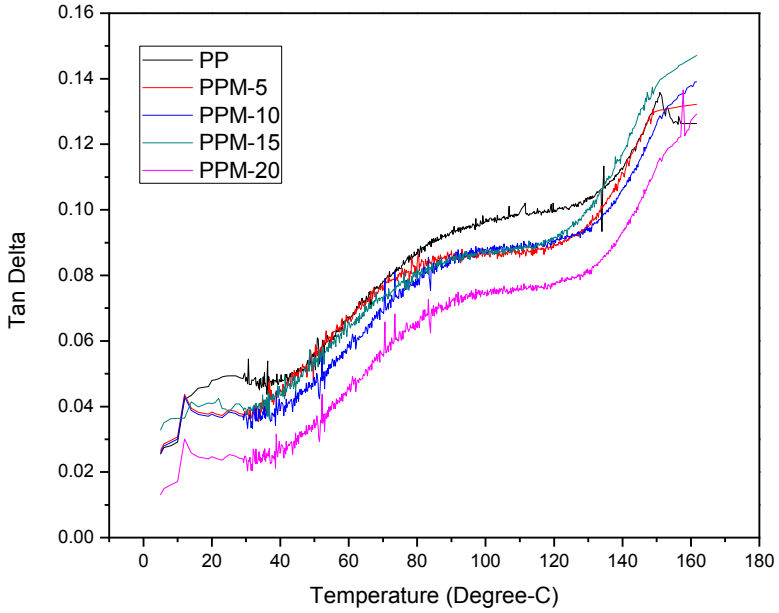

Figure 5.23 Variation of the Tan Delta (Tan δ) as a function of temperature for PP-Marble Composites

The amount of the damping factor (Tan delta) is indicator of a polymer system and it gives equilibrium between elastic-viscous phase in a polymer composite. Tan delta measurements elaborate the practical information related to Tg and presents an indication of strength of a polymer material to store and disperse energy. Tan delta values of injection moulded specimen of PP - Marble composites with temperature at a frequency of 1 Hz has shown in Figure 5.23. It is observed that Tan delta rises with rise in the temperature; it goes at highest level in the transition region and then drops in rubbery region. It was also observed that below T_g , the damping factor was low, in all composites due to the chain-segments which was found in frozen state. For that reason, the higher the Tan delta peak values, the greater is the degree of molecules mobility. As shown in Figure 5.23, Tan delta < 1, reflects fabricated polymer composites behave analogous to solid. In addition, the interaction of marble reduces the peak value of height of Tan delta. It was due to integration of more stiff filler that restrict the random movement of molecules of polymer-filler.

5.3.2.2. Thermo-Gravimetric Analysis (TGA) PP-Marble Powder composites

Thermo-Gravimetric Analysis (TGA) has been used to study the thermal characteristics of all the fabricated PP-Marble composites. Figure 5.24 indicated the thermal behaviour of PP-Marble composite. As temperature rises, the weight of PP-marble composite reduce with different rates. In the beginning, at 200°C, there was some minor loss about 0.05% which was due to dehydration process and removal of unstable impurities etc. After this, the thermal degradation of PP-Marble composite began in the region of 350-450°C in all the curves.

It was observed that composite PPM-5 and PPM-10 have less thermal degradation temperature in comparison to virgin PP. PPM-15 shows highest thermal degradation temperature. According to Ahmetli et al. rise in marble waste rises the thermal stability of composite with much higher char yield.

According to study of Mehta et al. [12] one peak was observed between 350°C to 400°C which corresponds to endothermic peaks at 355°C having weight loss of 2.5% during TGA analysis. Second endothermic peak was observed between 700- 880°C having weight loss 30.3%. The endothermic peaks were observed due to the evolution of CO_2 with the formation of CaO and MgO respectively. The weight loss observed in marble waste powder is accredited to the decomposition of carbonates in two stages.

The study propose that the use of developed marble powder as industrial and agricultural waste is accomplished to provide a cost-effective, industrially prospective, and smart replacement to the currently widely used fillers like calcium carbonate, china-clay and talc.

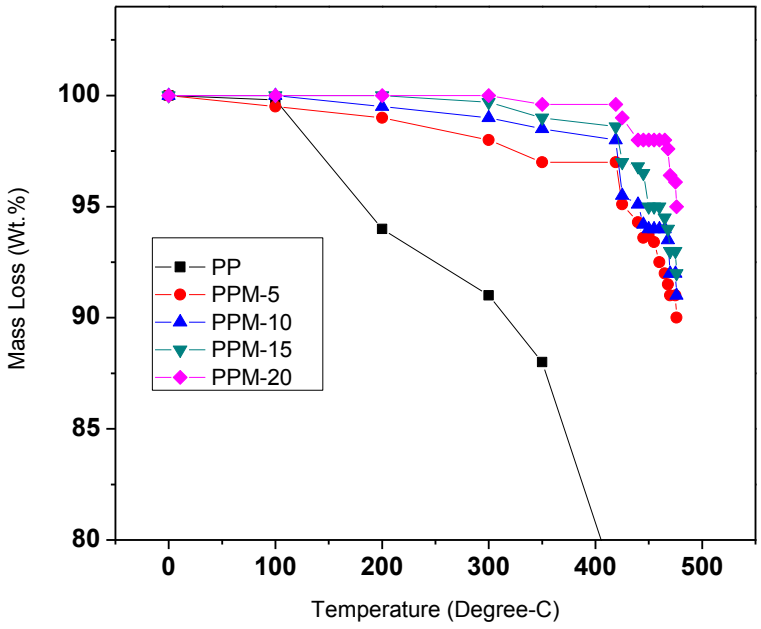

Figure 5.24 TGA of PP-Marble composites

Chapter Summary

This chapter concluded that:

- It was observed that the Shore D hardness values increases significantly as filler loading increases in all the composites. The incorporation of alumina, titanium dioxide and marble powder into the polypropylene lead to an enhancement in hardness. The hardness of PP composites filled with different weight-percentages of alumina, titanium dioxide and marble powder particle are in the range of 58-70, 67-70 and 67-73 respectively. The maximum value of Shore D hardness of PP composite is 73 indicated by PP composite filled with 20 wt.% (PPM-20) marble powder. It is 30.35% higher than Shore D hardness of virgin PP.
- The impact strength of PP composites filled with the different weight-percentage (5, 10, 15 and 20 wt.%) of alumina and titanium dioxide decreases as the filler content increases. In PP-alumina composites, the impact strength decreases from 36 J/m to 21.32 J/m. Similarly, in PP-TiO_2 composites PPT-5, PPT-10, PPT-15 and PPT-20 have Impact strength to be 35, 32, 29 and 24 J/m respectively. On the other hand, adding of marble powder increases impact strength of PP composites. Marble powder

having 5 and 10 wt.% consist impact strength 37 J/m and 38.5 J/m respectively. Marble powder having 15 and 20 wt.% consists impact strength 39.7 and 40.6 J/m respectively.

- The flexural strength of PP composites filled with the different weight-percentage (5, 10, 15 and 20 wt. %) of alumina is in the increasing trend, which is 53.04 -59.26 MPa. On the other hand, titanium dioxide and Marble powder exhibits decreasing trend of flexural strength which is 58.9-50.8 MPa and 64.16-52.56 MPa respectively.
- The compressive strength of PP composites filled with different weight-percentage (5, 10, 15 and 20 wt. %) of alumina, titanium dioxide and Marble powder are in the range of 98.63-121.34 MPa, 113.8-171.6 MPa and 103.4-159.4 MPa respectively. Thus maximum compressive strength was found in PP-TiO_2 composite having 20 wt.%. which is 171.6 MPa.
- The glass transition temperature of PP-composites increased with the increase in micro filler content in the matrix material. Similarly, the thermal stability and degradation temperature are also improved with increase in filler content. The results of glass transition temperature of PP composite using Thermo-gravimetric analysis are in agreement with the results using Dynamic mechanical analysis.
- For PP-alumina composites the storage modulus (E') is in the range of 650-860 MPa at lower temperature (30°C) and remains higher for PPA-10. However, at higher temperature (i.e 150°C) the storage modulus lies in the range of 50-100 MPa.
- For PP-TiO_2 composites the storage modulus (E') is in the range of 630-1030 MPa at lower temperature (30°C) and remains higher for PPT-10. However, at higher temperature (i.e. 150°C) the storage modulus lies in the range of 65-80 MPa.
- For PP-marble powder composites the storage modulus (E') is in the range of 625-855 MPa at lower temperature (30°C) and remains higher for PPM-10. However, at higher temperature (i.e. 150°C) the storage modulus lies in the range of 65-135 MPa.
- Thermo-Gravimetric Analysis (TGA) measurements indicate that both the initial degradation temperature and the end degradation temperature

increase with increasing filler (alumina, titanium dioxide and marble powder) in all the composites.

- The study suggests that the use of marble powder as industrial waste can be accomplished to provide a cost effective and industrially prospective.

The next chapter presents the Morphological Characterizations of Polypropylene Composites under study.

******

Chapter 6

MORPHOLOGICAL CHARACTERIZATIONS OF POLYPROPYLENE COMPOSITES

This chapter discusses the results based on the properties of Polypropylene composites according to the formulations discussed in previous chapter. The Morphological characterization include determination of Scanning Electron Microscopy (SEM) and Atomic force Microscopy (AFM).

The interpretation of the results of various Polypropylene composite samples are also presented. This chapter consists of three parts: part I consists of Polypropylene composite filled with alumina (Al_2O_3), part II consists of Polypropylene composite filled titanium dioxide (TiO_2) and part III consists of Polypropylene composite filled marble powder.

Part I

6.1 Morphological characterization of Alumina filled Polypropylene composites

6.1.1. Scanning Electron Microscopy (SEM) of PP-Al_2O_3 composites

The morphology of PP-Al_2O_3 composites was examined using SEM analysis. SEM images taken from flexural fractured specimens were analyzed and exhibited in Figure 6.1. It is quite clear that the descriptions show good adhesion of PP structure with Al_2O_3 micro particles. Figure 6.1 reflects that virgin PP has a comparatively smooth surface and shows no sign of the plastic deformation. Al_2O_3 appeared to be well dispersed in PP-alumina composite and Aluminates, generally, have elevated surface energy that show the way of relatively strong interaction between the PP matrix and filler. According to Rasheed et al. [184], flexural strength are greatly affected by the interface quality in the composites.

In addition to the interfacial stiffness, the static adhesion strength, work as a main function to raise filler reinforcement. On the other hand, according to Dong et al. [163] deterioration of impact strength can be due to clustering effect of large particles which can impart the stress concentration around the edges which in turn commence the cracks through the epoxy matrix. Some aggregates and agglomerates are identifiable in the composites. The agglomeration of filler particles in composites produces the voids in composites which probably weaken the storage modulus. According to Ngu et al., [65] It was observed that the contributions of the inter-phase

to the storage modulus at lower temperatures, is less than that of others due to high modulus of the matrix and thus storage modulus of polymer matrix is higher than that of the composites. Furthermore, some humps and cavities on a micro-scale are observable on the fracture surface, which can be attributed to the rubber phase (ethylene –propylene) of PP copolymer (Pedrazzoli et al. [106]). SEM observations of the PP-Alumina composites illustrated that fracture surface became rougher by increasing the addition of filler loading. According to Laachachi et al. [28] presence of spherical nodules rich in Al and O in which individual alumina particles are well dispersed, which are responsible for better thermal stability of composites.

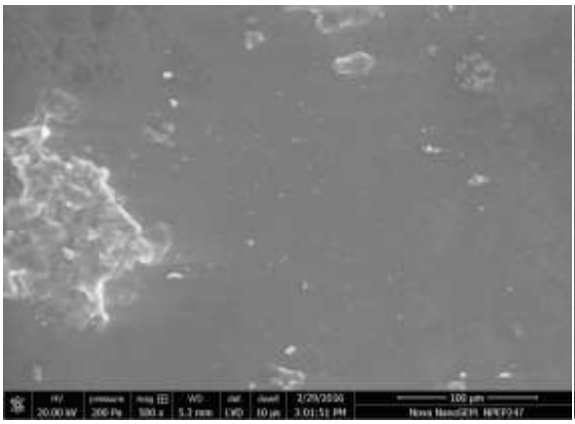

a) PP

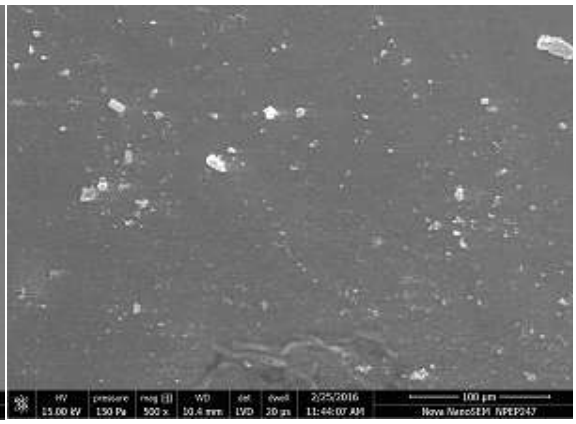

b) PPA-5

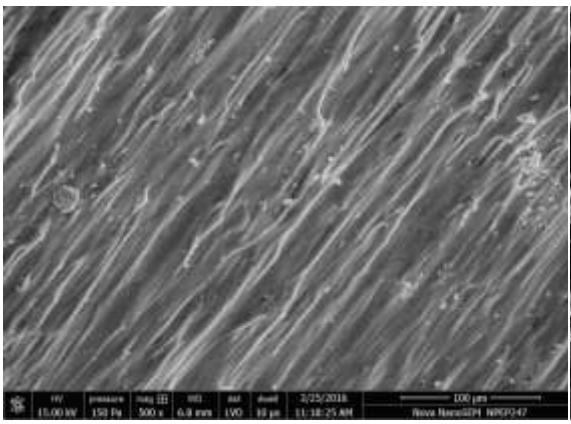

c) PPA-10

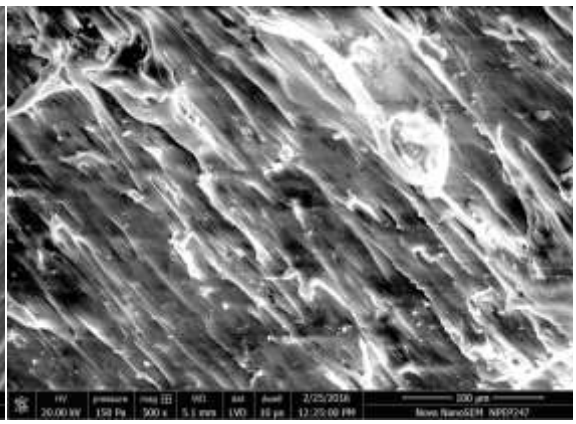

d) PPA-15

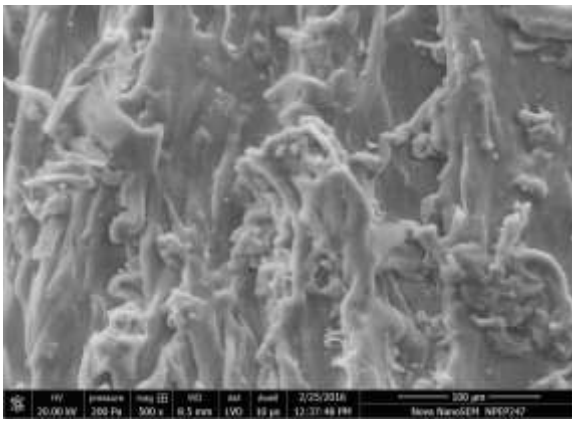

e) PPA-20

Figure 6.1 SEM morphology of virgin PP and PP-Al_2O_3 composites

6.1.2. Atomic Force Microscopy (AFM) of PP-Al_2O_3 composites

The surface morphology for different PP- Al_2O_3 composites are shown in Figure 6.2 at identical scale of 1×1 μm^2. Alumina particles are clearly visible and their mean size is of about 0.6 μm. It indicates that PP-Al_2O_3 composites possesses a high specific area than Al_2O_3 as received. Like other porous ceramic particles, this leads to a higher volume fraction per unit weight of the composite in PP matrix. It is noteworthy that the Al_2O_3 particles are embedded in the continuous PP phase (Zhang et al., [63]). AFM results indicate that morphology of alumina in the PP matrix is characterized by a chainlike branched structure. In some instances the PP seems to skin or wrap around the alumina particles as per investigations of Pötschke, P. et al., [185].

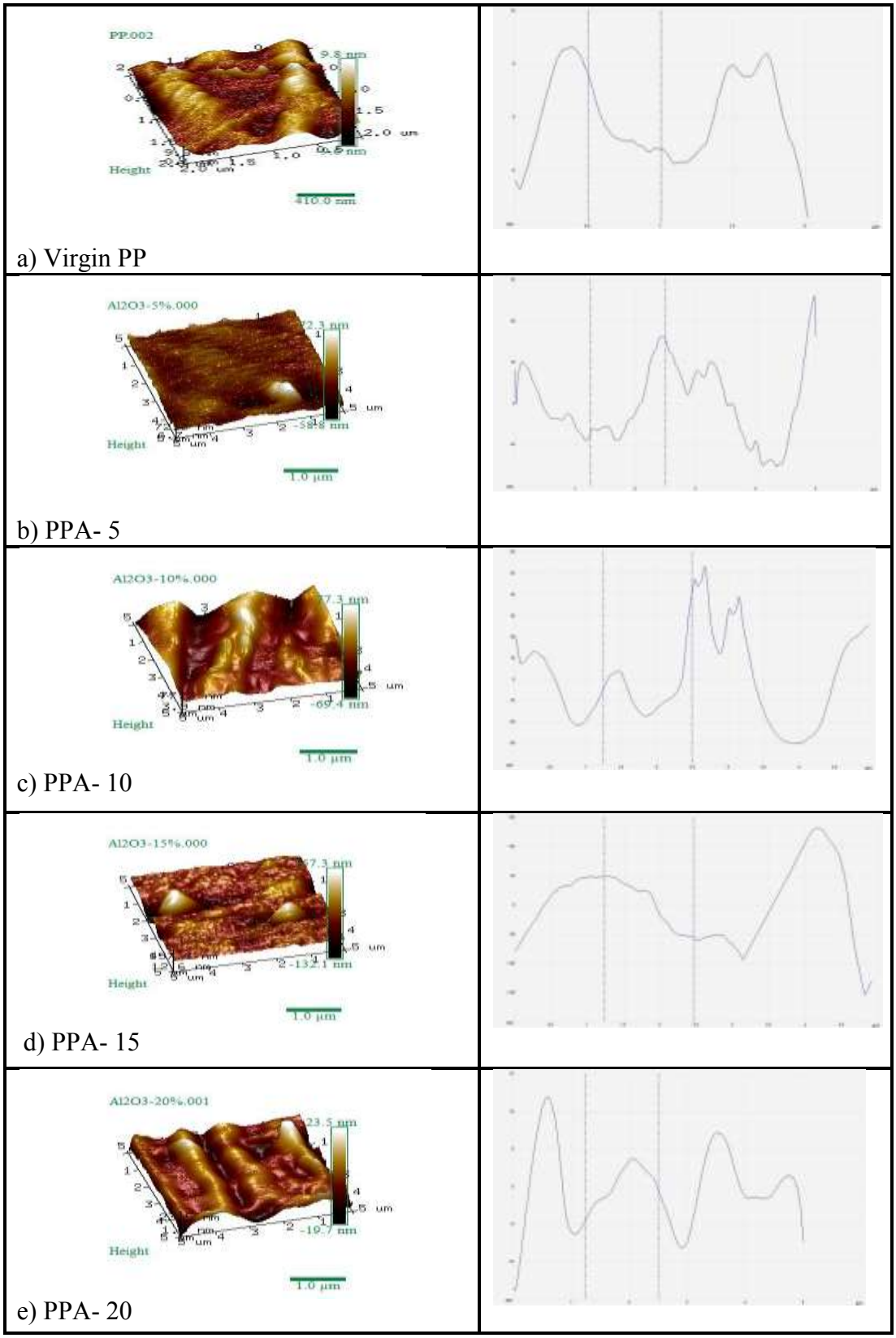

Figure 6.2 **AFM micrographs with their line profiles of the surface of virgin PP and PP-Al_2O_3 composites**

6.2. Morphological characterization of PP-TiO_2 composites

6.2.1. Scanning Electron Microscopy (SEM) of PP-TiO_2 composites

SEM micrographs of impact-fractured surface of PP-TiO_2 composites are shown in Figure 6.3. The properties of composites depend on degree of crystallinity, internal structure and spinning conditions [108]. By the addition of TiO_2, strength of PP is increasing which reveals reinforcing effect of TiO_2 in the composites. Dispersion of TiO_2 particles has a significant effect on the mechanical properties of the composites. A fine distribution and dispersion of TiO_2 particles in the matrix breaks aggregates and agglomerates to present a better interfacial area between TiO_2 particles and the immediate polymer phase. SEM micrographs measurements indicate that the TiO_2 particles are well dispersed in polymer matrixes, especially the anatase particles. However, it is important to notice that the presence of few TiO_2 lumps which increases in the composites due to the increasing wt.% of filler content. Due to agglomeration of filler particles the lumps are formed. Interface between lumps or particles, or between matrix and filler may not be continuous due to their mismatched nature, but in SEM micrographs interfacial gap was not visible within the considered scale. However, as TiO_2 particles are relatively harder than the PP matrix, they may harden the entire material if they create good quality contact with the polymer matrix. It was also observed that TiO_2 particles are spherical and their size was about 100 to 300 nm according to SEM analysis.

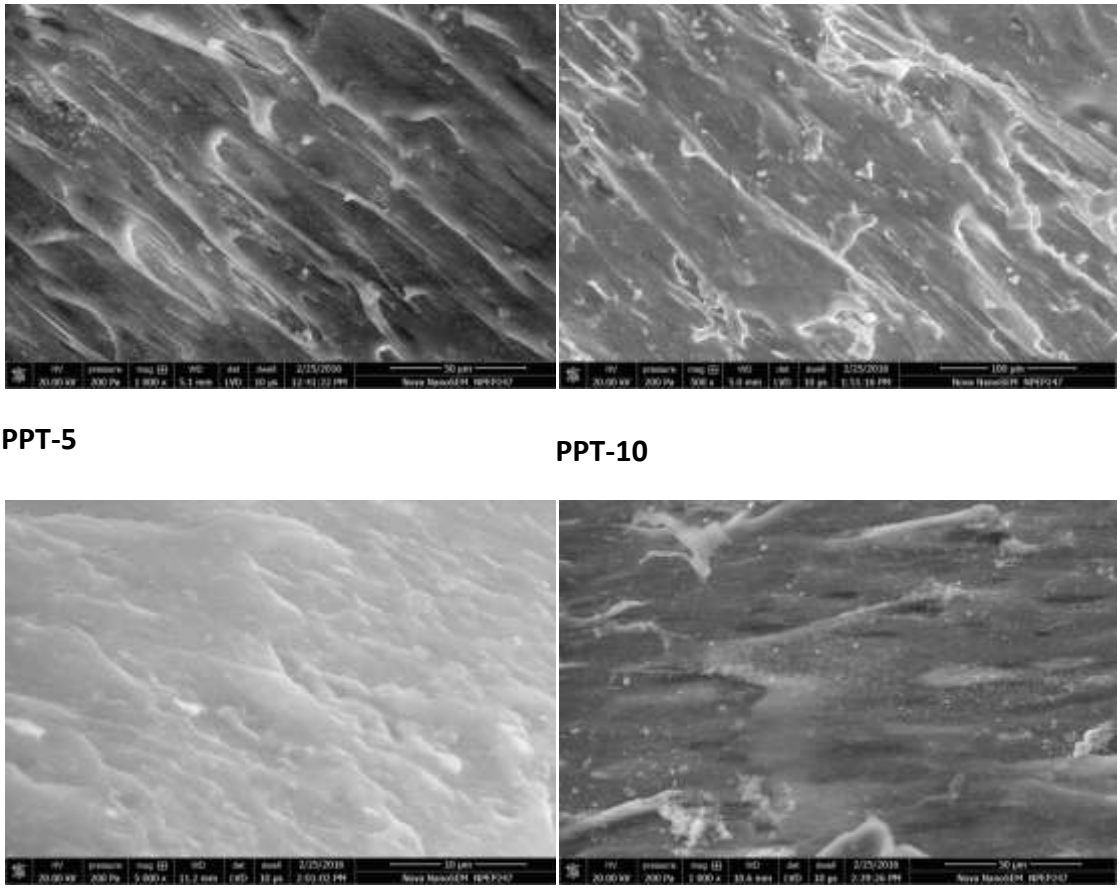

Figure 6.3 SEM morphology of PP-TiO_2 composites

6.2.2. Atomic force Microscopy (AFM) of PP-TiO_2 composites

The surface morphology of PP-TiO_2 composites was examined using an atomic force microscope (AFM) in the tapping mode as shown in Figure 6.4 at identical scale of $2\times2\ \mu m^2$. With mean size of about 0.6 μm TiO_2 particles are clearly visible. From the AFM images the roughness was determined as the arithmetic mean (R_a) of the distribution of heights. It is remarkable that the TiO_2 particles are embedded in the continuous PP phase. The presence of coarse grooves and ridges is the major feature of the surface for all composites as shown in Figure 6.4. The mean size of the observed structures, much larger external layer of PP only removed from the surface after than the size of the TiO_2 particles, indicate they are aggregated particles [186].

Addition of TiO_2 content from 5 wt.% to 20 wt.% has shown increased surface roughness of the composite. It also shows that the height of peaks of lateral grooves reflecting microgroove formation have been increasing as the TiO_2 content increased in the composites.

Figure 6.4 exhibits that the mean surface roughness values of composite are 8 nm, 16.3 nm, 17.4 nm and 18.6 nm in composites PPT-5, PPT-10, PPT-15 and PPT-20, respectively. However virgin PP exhibits mean surface roughness value of 4.2 nm. It can be observed as the filler content rises, surface roughness of PP-TiO_2 also rises. Due to presence of brittle and hard inorganic filler TiO_2 particles maximum roughness was found.

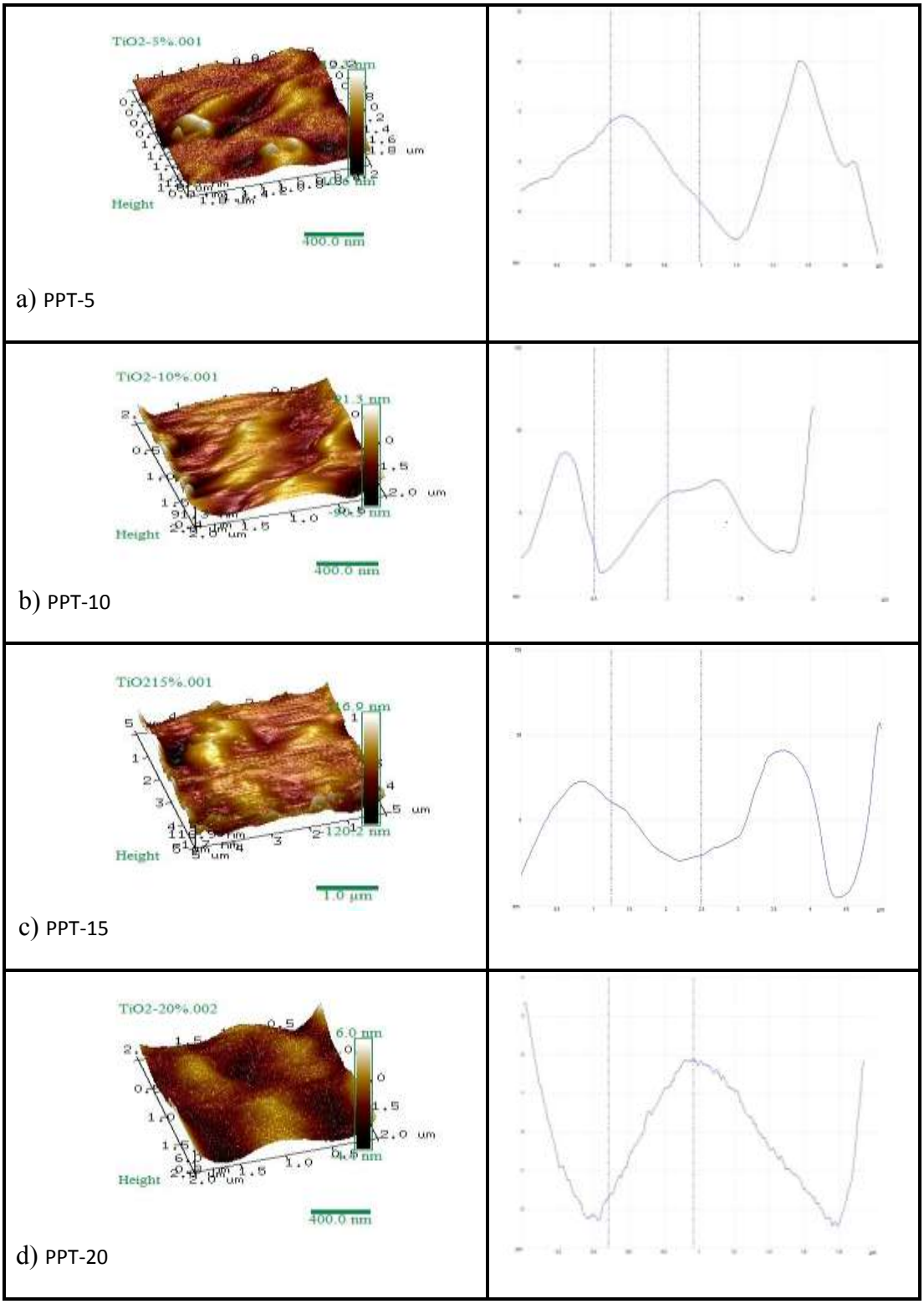

Figure 6.4 AFM micrographs with their line profiles of the surface of PP-TiO_2 composites

6.3. Morphological characterization of PP-Marble Powder composites

6.3.1. Scanning Electron Microscopy (SEM) of PP-Marble Powder composites

To investigate the surface morphology of PP-marble composites, SEM was used. Marble particles exist in the shape of separated grains, as shown in Figure 6.5. Sphere like formation were obtained during calcination process as the temperature was increased to 600^{o}C, this was due to the decomposition of carbonates and formation of new phases (CaO and MgO).

Zuo et al. [187] investigated the failure mechanism and fracture surface of Jinping marble with SEM. For their study, the Yantang and Baishan marbles specimens from Jinping hydropower station were used. Test results exhibited that the fracture toughness and mechanical behaviors of Yantang marble were higher than Baishan marble. It was due to the fact that Baishan marble contains a large percentage of dolomite and minor mica.

Mehta et al. [12] examined the surface morphology of calcined and uncalcined samples of marble. It was observed that the marble particles are in the form of separated grains. It was perceived that during calcinations process as the temperature raised from 600^{0}C to 800^{0}C, sphere like structures were obtained. The presence of the compositional elements of marble samples such as Si, Mg, Ca, and O were detected.

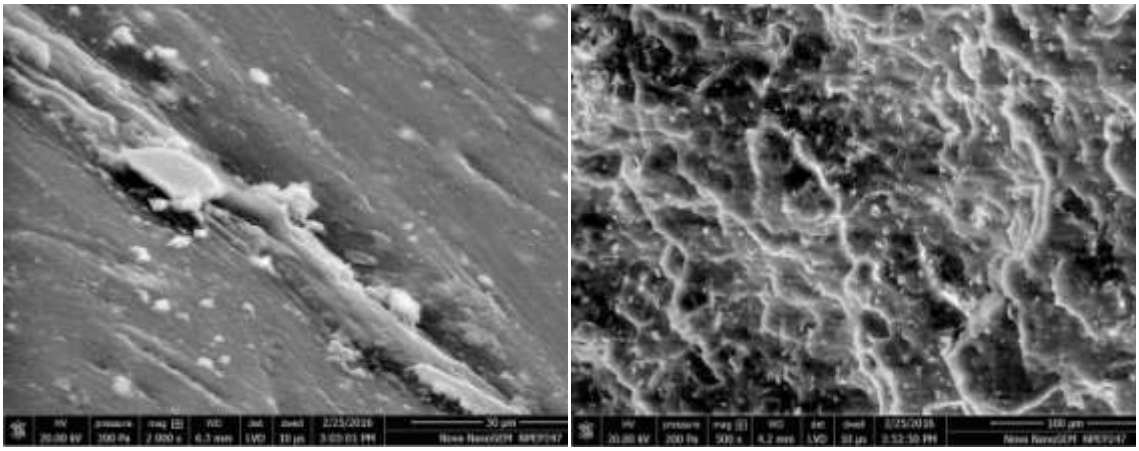

a) PPM-5 **b) PPM-10**

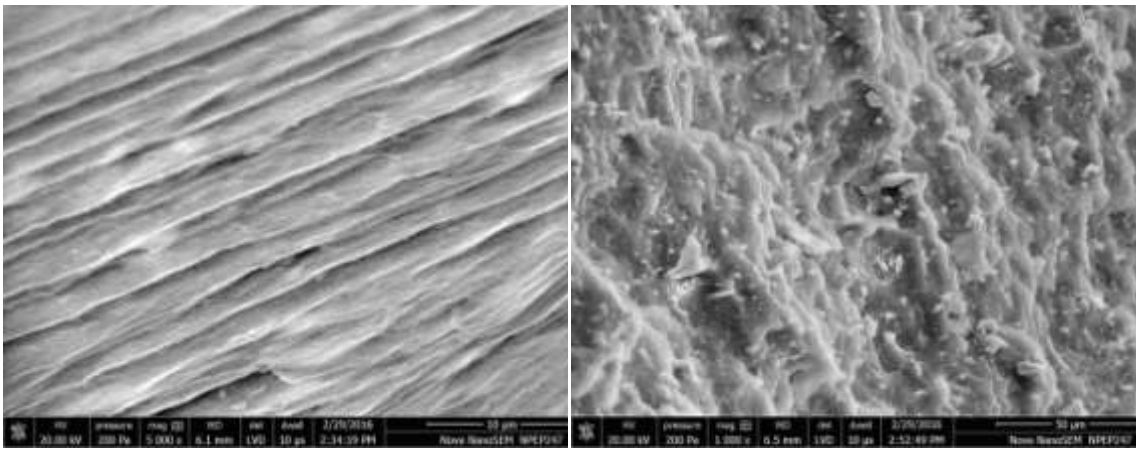

c) PPM-15 **d) PPM-20**

Figure 6.5 SEM morphology of PP-Marble composites

6.3.2. Atomic force Microscopy (AFM) of PP-Marble Powder composites

The surface morphology of PP-marble composites was examined and it was observed that with mean size of about 0.7 μm marble particles are clearly visible. From the AFM images, the roughness was determined as the arithmetic mean (R_a) of the distribution of heights. The presence of coarse grooves and ridges is the major feature of the surface for all composites as shown in Figure 6.6.

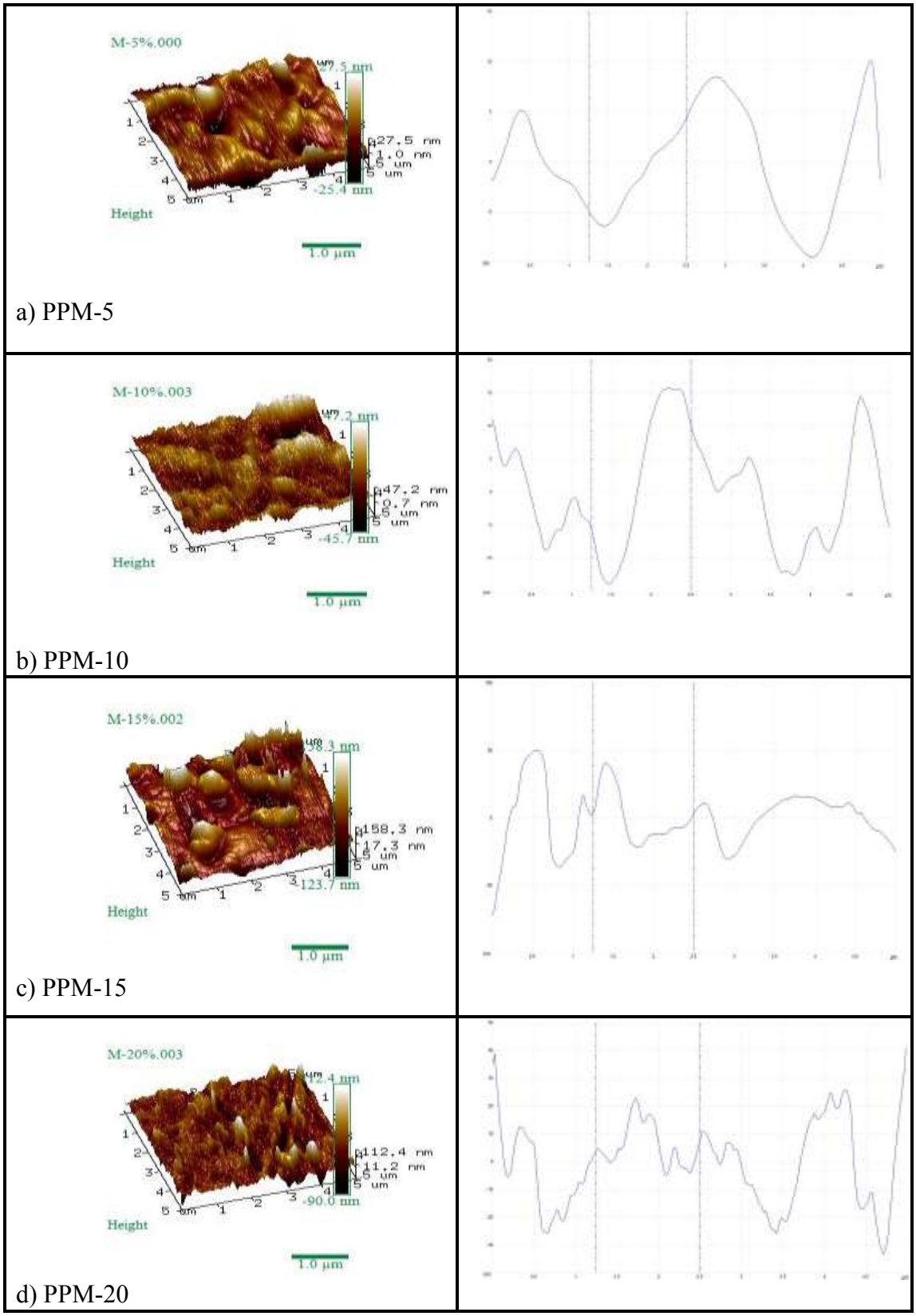

Figure 6.6 AFM micrographs with their line profiles of the surface of PP-Marble composites

Chapter Summary

This chapter concluded that:

- This chapter presents the morphological study of PP composites.
- The filler particles such as alumina, titanium dioxide and marble powder are successfully dispersed with polypropylene.
- SEM observations of the PP-Alumina composites show that fracture surface became rougher by increasing the filler loading. The presence of spherical nodules rich in Al and O in which individual alumina particles are well dispersed, which provides better thermal stability of composites.
- It was also observed that in PP-Al_2O_3 composite large particles of alumina creates stress concentration. The mean size of alumina particles was about 0.6 μm.
- For PP- TiO_2, SEM micrographs, it was observed that the presence of few TiO_2 lumps increase in the composites due to the increasing wt.% of filler content. Due to agglomeration of filler particles, the lumps are formed. Interface between lumps or between matrix and filler may not be continuous due to their mismatched nature. Addition of TiO_2 content from 5 wt.% to 20 wt.% increased the surface roughness of the composite.
- The morphological characterization of PP-marble composites shows the mean size of 0.7 μm marble particles with its clear appearance. From the AFM images, the roughness was determined as the arithmetic mean (R_a) of the distribution of heights. The presence of the compositional elements of marble samples such as Si, Mg, Ca, and O were detected.

The next chapter describes the optimization of the process parameters in injection moulding for minimization of shrinkage - warpage and maximization of impact strength of virgin PP and virgin PC with the help of Taguchi method.

*****

Chapter-7

OPTIMIZATION OF PROCESS PARAMETERS

7.1. Selection of Optimal Formulation by Using Taguchi Technique

Determining and optimization of process parameters in plastic injection moulding (PIM) are very essential to produce good quality of plastic parts. From literature survey, it was found that shrinkage and warpage in plastic parts are most prominent defects and affects the quality of plastic parts. No literature was found which shows the methodology for minimization of defects viz., shrinkage, warpage and maximization of impact strength. Impact strength is desirable property in the parts under consideration.

In this chapter, Design of experiment (DOE) technique Taguchi orthogonal array was used to determine the optimum values of process parameters in injection moulding. To determine the initial range of parameters, steady state experiments were performed for virgin Polypropylene (PP) and virgin Polycarbonate (PC). The modified linear graph was used with the line- separation method to assign the parameters and to take care of interactions between the parameters. To know the significance of parameters ANOVA technique was adopted.

Six process parameters viz., mould temperature, melt temperature, injection pressure, packing time, packing pressure and cooling time were considered for minimization of shrinkage, warpage and maximization of impact strength of virgin Polypropylene (PP) and virgin Polycarbonate (PC). With this approach, prediction equations and mathematical models for shrinkage, warpage and impact strength of virgin Polypropylene (PP) and virgin Polycarbonate (PC) were developed successfully which are useful for industrial applications.

7.2. Measurement

7.2.1. Shrinkage Measurement

The shrinkage may be measured as the difference between the size of mould cavity and the size of finished part divided by the size of a mould cavity. The relative shrinkage of selected characteristics were calculated with following equation:

$$S = (L_{cavity} - L_{Part})/ L_{Cavity} \times 100\%$$

where, S denotes the linear shrinkage in percentage, L_{cavity} denotes the long length of cavity and L_{Part} denotes the long length of specimen. The percentage of shrinkage of PP and PC are being used in experiment, which is taken through the output of mean linear shrinkage.

7.2.2. Warpage Measurement

Warpage of specimen of PP and PC were measured on a Coordinate Measuring Machine (CMM). It was observed that warpage occurs at the ribs, where cross sectional area changes. On the specimen, reference points were marked on the ribs and warpage of PP and PC were measured on these points. Maximum warpage value of all reference points have been taken as the warpage value of the whole model in this study.

7.2.3. Impact Strength Measurement

For impact strength measurement of specimen of PP and PC, a hardened steel striker was selected mounted in pendulum and it was having the radius of curvature 0.80±0.20 mm with its axis horizontal and perpendicular to the plane of swing of the pendulum. The specimens were prepared with a milled notch. The size of specimens was 63.5×10×3 mm. The notch angle was kept 45 ± 1^0. Moulded specimens were prepared for each experiment run. The line of contact of the striker was located at the centre of the percussion of pendulum within ± 2.54 mm. The distance from axis of support to the centre of the percussion was determined experimentally from period of small amplitude oscillations of the pendulum with following equation:

$$L = (g/4\pi^2)\, p^2$$

where

L distance from the axis of support to the centre of percussion in meter
g gravitational acceleration in m/s^2
π 3.1416
p period of a single complete swing (to and fro)

The position of the swinging pendulum releasing mechanism was aligned in such a manner that vertical height of fall of the striker was 615±2 mm, so that a velocity of the striker at the moment of impact of 3.5 m. The effective length of the pendulum

was maintained at 0.33 m, so that the required elevation can be obtained by raising pendulum to an angle between 60^0 and 30^0 above the horizontal.

7.3. Experimental Investigation

The experiments were performed on plastic injection moulding machine having capacity of 80 ton. The basic parts of machine are hopper, barrel, screw, nozzle and part cavity with arrangement of ejector pins. To determine the ranges of injection machine's process parameters, steady state experiments were performed for both PP and PC. In steady state experiments, one process parameter was varied while all other parameters remained constant. For virgin PP, by varying mould temperature in the range of 50-90^0C, it was found that mould temperature below 60^0C and above 80^0C results in more shrinkage and warpage of PP specimen as shown in Figure 7.1. So the range of mould temperature was decided between 60^0C and 80^0C. Similarly, melt temperature was varied between 225^0C and 295^0C as shown in Figure 7.2. It was found that below 235^0C, the flow of plastic is not possible, as frozen layer forms. Heating of PP above 275^0C was not able to produce good quality of part. So the range for melt temperature was decided between 235^0C and 275^0C.

During steady state experiments, regarding injection pressure, it was found that below 110 MPa short shot defect increases in the PP specimen. It was the major factor to fill the part cavity completely. Thus, the range for injection pressure was decided between 110 and 130 MPa. Figure 7.3 shows the variation of shrinkage and warpage in PP with change in injection pressure. Similarly, the range of packing pressure was decided between 60 and 100 MPa. Below 60 MPa and above 100 MPa, shrinkage and warpage of the PP increases, as shown in Figure 7.4.

Similarly, steady state experiments were performed for virgin Polycarbonate (PC) and its shrinkage and warpage behaviour were observed. The results of these experiments are shown in Figure 7.5 to Figure 7.8.

Thus, final ranges of parameters of injection moulding, for virgin PP and virgin PC, are decided and shown in Table 7.1. Taguchi method uses the signal-to-noise (S/N) ratio, which reveals both the average and the variation of quality characteristics. The S/N ratio is a measure of the response aimed at developing the products and processes insensitive to the noise factors. In this study lower value of shrinkage and warpage are expected and higher values of impact strength are expected. The characteristic that lower value represents better process response, such

as for shrinkage and warpage, is called, 'Lower is Better (LB)'. Inversely, the characteristic that higher value represents better process response, such as impact strength, is called 'Higher is Better, (HB)'. Thus S/N ratios for 'LB' and 'HB' are defined as follows:

$$S/N_{LB} = -10\ Log_{10} \frac{1}{n} \quad (\sum y_i^2) \tag{1}$$

$$S/N_{HB} = -10\ Log_{10} \frac{1}{n} \quad (\sum 1/y_i^2) \tag{2}$$

where y_i is the value of the quality characteristics for the i^{th} trials, n is number of repetitions.

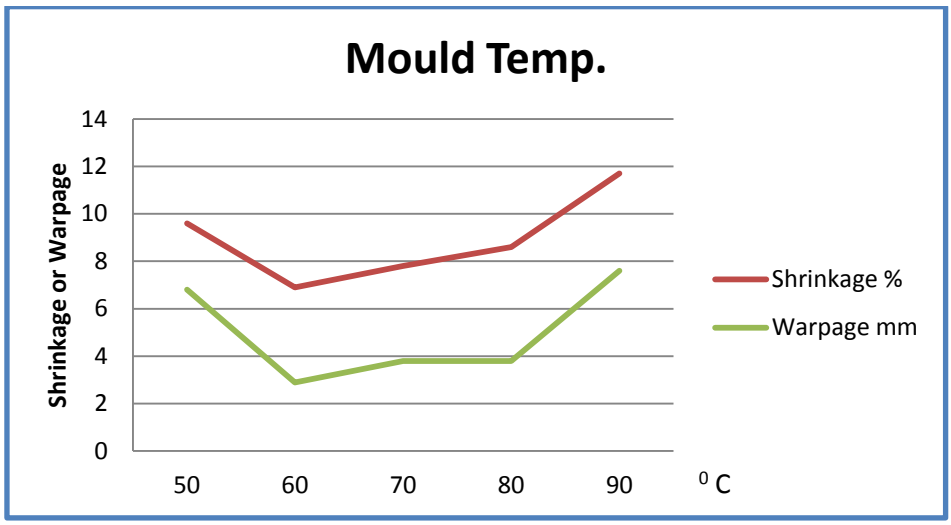

Figure 7.1 Steady state experiment for Mould Temperature for PP

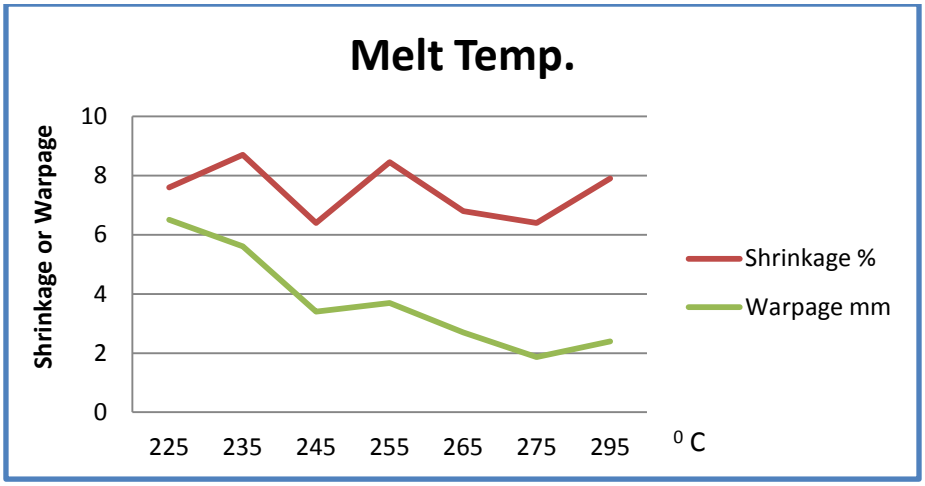

Figure 7.2 Steady state experiment for Melt Temperature for PP

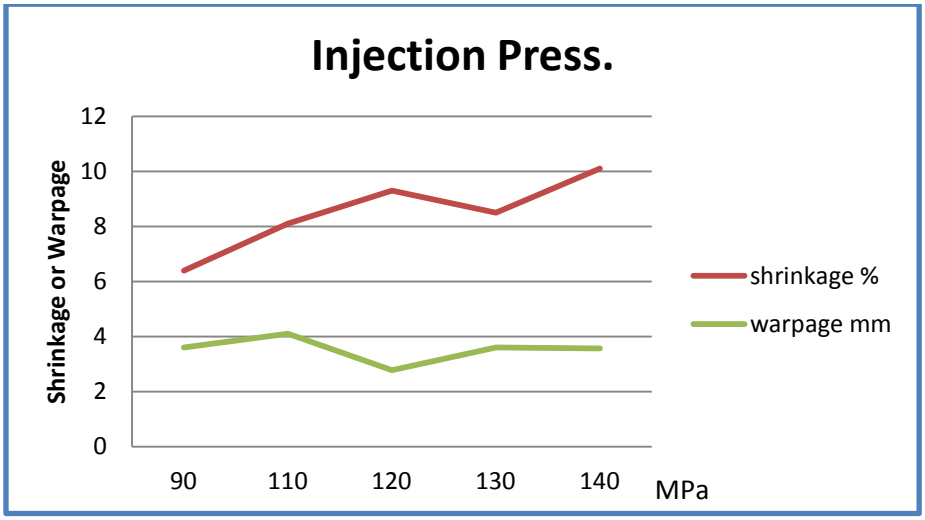

Figure 7.3 Steady state experiment for Injection Pressure for PP

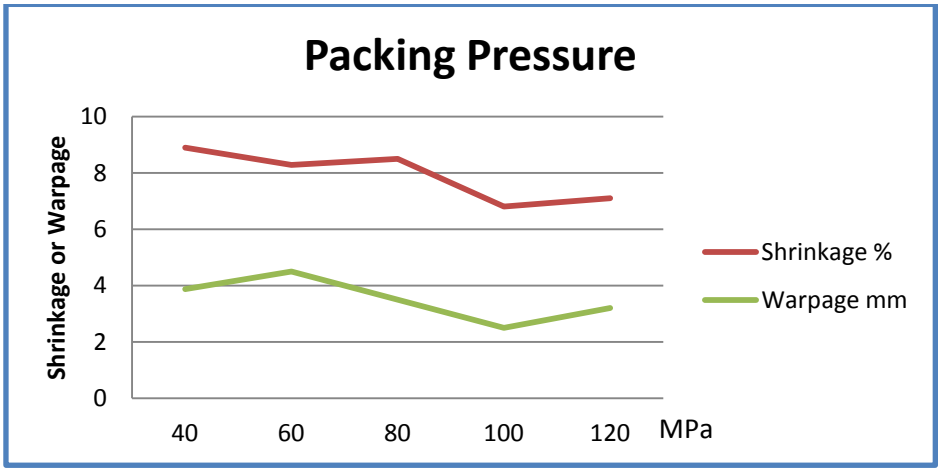

Figure 7.4 Steady state experiment for Packing Pressure for PP

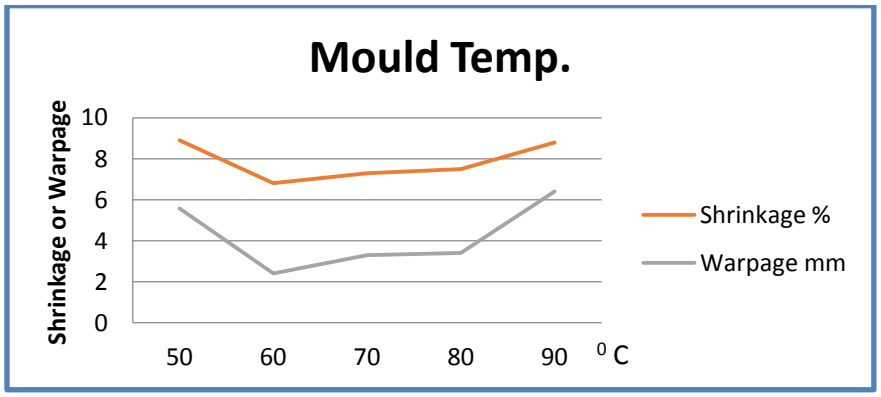

Figure 7.5 Steady state experiment for Mould Temperature for PC

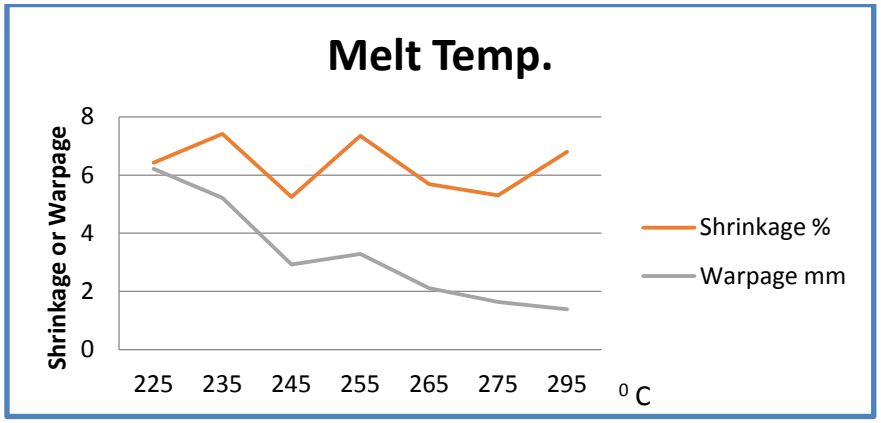

Figure 7.6 Steady state experiment for Melt Temperature for PC

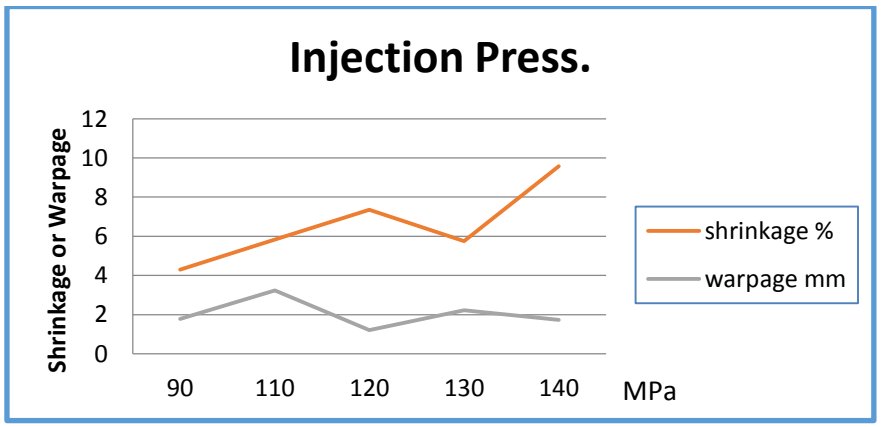

Figure 7.7 Steady state experiment for Injection Pressure for PC

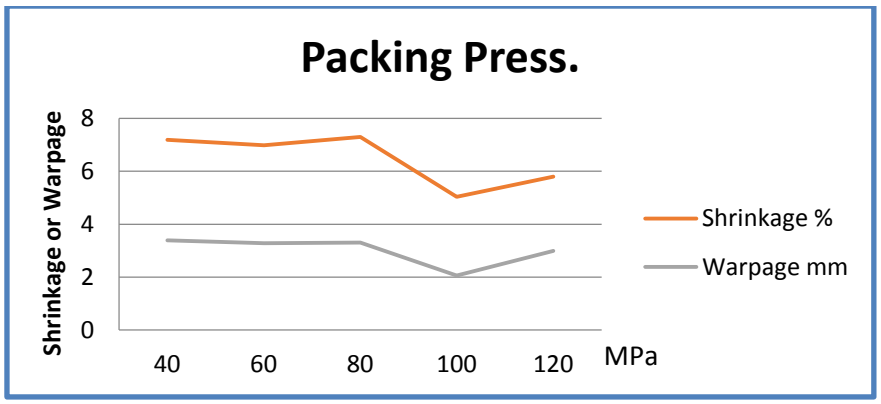

Figure 7.8 Steady state experiment for Packing Pressure for PC

Table 7.1 Range of parameters for virgin PP and virgin PC

Parameters	Level-1	Level-2	Level-3	Unit
Mould Temperature (A)	60	70	80	^{0}C
Melt Temperature (B)	235	255	275	^{0}C
Injection Pressure (C)	110	120	130	MPa
Packing Time (D)	4	5	6	sec
Packing Pressure (E)	60	80	100	MPa
Cooling Time (F)	10	12	14	sec

7.4. Orthogonal Array

The standard liner-graph was modified by means of the line-separation method as exhibited in the Figure 7.9 to designate the parameters and their interactions to different columns of the orthogonal array (OA). The array selected was L_{27} (3^{13}), consists 27 rows corresponding to the number of experiments (runs) with 13 columns with 3 levels, as shown in the Table 7.2. By adapting the standard linear –graph, the parameters and their interactions were assigned in the columns. The experiments were designed as follows, the very first column was assigned to mould temperature (A), second column to melt temperature (B), fifth column to injection pressure (C), ninth column to packing time (D), tenth column to packing pressure (E), the twelfth column to mould cooling time (F), the third column and fourth column assigned to $(AxB)_1$ and $(AxB)_2$ respectively, to estimate interaction between mould temperature and melt temperature. Sixth and seventh column are assigned to $(AxC)_1$ and $(AxC)_2$ respectively, to estimate possible interaction between mould temperature and injection pressure. Eighth and Eleventh column are assigned to $(BxC)_1$ and $(BxC)_2$ respectively, to estimate interaction between melt temperature and injection pressure.

Thus, according to the Taguchi design, a L_{27} orthogonal array was selected for the experiments of PP and PC are exhibited in the Table 7.2.

The experiments were performed for each combination of parameters (rows) as per the selected orthogonal array and as per modified linear graph (Figure 7.9). For each experiment of PP and PC, shrinkage (%), warpage (mm) and impact strength (J/m) were measured and S/N ratios were calculated.

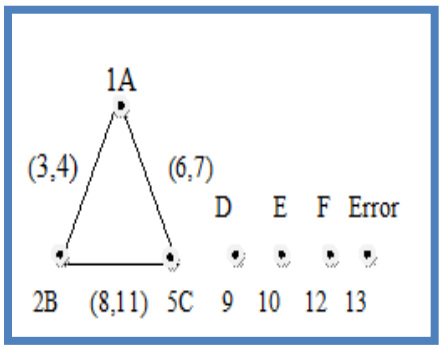

Figure 7.9 Modified liner graph for L_{27} [30]

Table 7.2 Orthogonal array for L_{27} (3^{13})Taguchi Design for PP and PC [30]

L_{27} Run	A	B	$(AxB)_1$	$(AxB)_2$	C	$(AxC)_1$	$(AxC)_2$	$(BxC)_1$	D	E	$(BxC)_2$	F	Error
	(1)	(2)	(3)	(4)	(5)	(6)	(7)	(8)	(9)	(10)	(11)	(12)	(13)
1	1	1	1	1	1	1	1	1	1	1	1	1	1
2	1	1	1	1	2	2	2	2	2	2	2	2	2
3	1	1	1	1	3	3	3	3	3	3	3	3	3
4	1	2	2	2	1	1	1	2	2	2	3	3	3
5	1	2	2	2	2	2	2	3	3	3	1	1	1
6	1	2	2	2	3	3	3	1	1	1	2	2	2
7	1	3	3	3	1	1	1	3	3	3	2	2	2
8	1	3	3	3	2	2	2	1	1	1	3	3	3
9	1	3	3	3	3	3	3	2	2	2	1	1	1
10	2	1	2	3	1	2	3	1	2	3	1	2	3
11	2	1	2	3	2	3	1	2	3	1	2	3	1
12	2	1	2	3	3	1	2	3	1	2	3	1	2
13	2	2	3	1	1	2	3	2	3	1	3	1	2
14	2	2	3	1	2	3	1	3	1	2	1	2	3
15	2	2	3	1	3	1	2	1	2	3	2	3	1
16	2	3	1	2	1	2	3	3	1	2	2	3	1
17	2	3	1	2	2	3	1	1	2	3	3	1	2
18	2	3	1	2	3	1	2	2	3	1	1	2	3
19	3	1	3	2	1	3	2	1	3	2	1	3	2
20	3	1	3	2	2	1	3	2	1	3	2	1	3
21	3	1	3	2	3	2	1	3	2	1	3	2	1
22	3	2	1	3	1	3	2	2	1	3	3	2	1
23	3	2	1	3	2	1	3	3	2	1	1	3	2
24	3	2	1	3	3	2	1	1	3	2	2	1	3
25	3	3	2	1	1	3	2	3	2	1	2	1	3
26	3	3	2	1	2	1	3	1	3	2	3	2	1
27	3	3	2	1	3	2	1	2	1	3	1	3	2

7.5. Shrinkage, Warpage and Impact Strength of PP

From Table 7.3, the overall mean for the S/N ratio of shrinkage, warpage and impact strength of PP are found to be -18.68 dB, -12.51 dB and 31.12 dB respectively. Figure 7.10 –Figure 7.12 show graphically the main effect plots for S/N ratios for shrinkage, warpage and impact strength of PP for the six process parameters, respectively.

The analysis was performed using the software for Design of Experiments (DOE) applications known as MiniTab-17. Before any effort was made to employ this simple model as a predictor for the measures of response, the possibility of interactions between the parameters were considered. Thus factorial design integrates a simple means of testing for the presence of the possible interaction effects. The S/N

ratio Response Table for shrinkage, warpage and impact strength for PP, are shown in Table 7.4, 7.5 and 7.6 respectively.

Analysis of the results leads to the conclusion that parameters at level A_2, B_1, C_2, D_3, E_3, and F_2 gives minimum shrinkage for PP. From Table 7.4, in order of priority, melt temperature, injection pressure and mould temperature were dominant parameters to minimize the shrinkage in PP. Similarly, levels A_1, B_3, C_2, D_1, E_3, and F_3 gives minimum warpage. From Table 7.5, in order of priority, melt temperature, injection pressure and packing pressure are dominant parameters to minimize the warpage. Similarly, from Table 7.6, levels A_3, B_3, C_2, D_3, E_2 and F_3 gives maximum impact strength of PP.

Thus, for all the three responses, parameters mould temperature (A), melt temperature (B) and injection pressures (C) are effective parameters and their interactions are also important for reducing shrinkage, warpage and to increase impact strength of PP. These interactions are shown in Figure 7.13, 7.14 and 7.15.

Table 7.3 L_{27} Orthogonal Array for PP

L_{27} Run	A	B	C	D	E	F	Shrinkage (%)	Shrinkage S/N ratio (dB)	Warpage (mm)	Warpage S/N ratio (dB)	Impact Strength (J/m)	Impact Strength S/N ratio (dB)
1	1	1	1	1	1	1	8.89	-18.978	6.632	-16.4067	30.4	29.7
2	1	1	2	2	2	2	7.375	-17.3552	6.282	-15.9343	35	30.9
3	1	1	3	3	3	3	7.34	-17.3139	6.506	-16.2395	36.6	31.3
4	1	2	1	2	2	3	8.37	-18.4545	3.58	-11.029	35.8	31.1
5	1	2	2	3	3	1	8.116	-18.1868	3.664	-11.2316	34	30.6
6	1	2	3	1	1	2	9.4	-19.4626	3.91	-11.799	35.5	31.0
7	1	3	1	3	3	2	11.45	-21.1761	2.733	-8.669	34.8	30.8
8	1	3	2	1	1	3	12.5	-21.9382	2.787	-8.84018	38.7	31.8
9	1	3	3	2	2	1	12.8	-22.1442	2.96	-9.36695	36.3	31.2
10	2	1	1	2	3	2	9.007	-19.0916	6.6	-16.3645	35.2	30.9
11	2	1	2	3	1	3	4.948	-13.8886	4.37	-12.7698	36.5	31.2
12	2	1	3	1	2	1	8.552	-18.6414	6.398	-16.0937	34.7	30.8
13	2	2	1	3	1	1	8.976	-19.0617	3.605	-11.0898	35.8	31.1
14	2	2	2	1	2	2	7.62	-17.6391	3.724	-11.3734	38.3	31.7
15	2	2	3	2	3	3	10.67	-20.5633	3.43	-10.6551	35.7	31.1
16	2	3	1	1	2	3	8.528	-18.6169	3.5	-10.8316	39.3	31.9
17	2	3	2	2	3	1	7.347	-17.3222	3.528	-10.9012	37.8	31.5
18	2	3	3	3	1	2	8.397	-18.4825	3.603	-11.0849	37.6	31.5
19	3	1	1	3	2	3	8.322	-18.4046	6.266	-15.912	35.3	31.0
20	3	1	2	1	3	1	6.264	-15.937	4.77	-13.5339	34.6	30.8
21	3	1	3	2	1	2	7.471	-17.4676	6.126	-15.7151	36.3	31.2
22	3	2	1	1	3	2	6.661	-16.4708	3.826	-11.6094	38.4	31.7
23	3	2	2	2	1	3	8.444	-18.531	4.64	-13.2928	38.8	31.8
24	3	2	3	3	2	1	9.414	-19.4755	6.18	-15.7916	37.4	31.5
25	3	3	1	2	1	1	11.056	-20.872	3.246	-10.1733	37.7	31.5
26	3	3	2	3	2	2	11.583	-21.2764	3.261	-10.2136	42.8	32.6
27	3	3	3	1	3	3	11.89	-21.5036	3.19	-10.0212	38.2	31.6

Table 7.4 Response table for Signal to Noise Ratios for Shrinkage of PP

Level	A	B	C	D	E	F
1	-19.45	-17.45	-19.01	-18.8	-18.74	-18.96
2	-18.15	-18.65	-18.01	-19.09	-19.11	-18.71
3	-18.88	-20.37	-19.45	-18.59	-18.62	-18.8
Delta	1.3	2.92	1.44	0.5	0.49	0.24
Rank	**3**	**1**	**2**	**4**	**5**	**6**

Table 7.5 Response table for Signal to Noise Ratios for Warpage of PP

Level	A	B	C	D	E	F
1	-12.17	-15.44	-12.45	-12.28	-12.35	-12.73
2	-12.35	-11.99	-12.01	-12.6	-12.95	-12.53
3	-12.92	-10.01	-12.97	-12.56	-12.14	-12.18
Delta	0.75	5.43	0.96	0.32	0.81	0.56
Rank	**4**	**1**	**2**	**6**	**3**	**5**

Table 7.6 Response table for Signal to Noise Ratios for Impact Strength of PP

Level	A	B	C	D	E	F
1	30.92	30.86	31.07	31.21	31.19	30.97
2	31.3	31.27	31.43	31.24	31.4	31.37
3	31.52	31.61	31.24	31.29	31.15	31.41
Delta	0.59	0.76	0.36	0.08	0.24	0.44
Rank	**2**	**1**	**4**	**6**	**5**	**3**

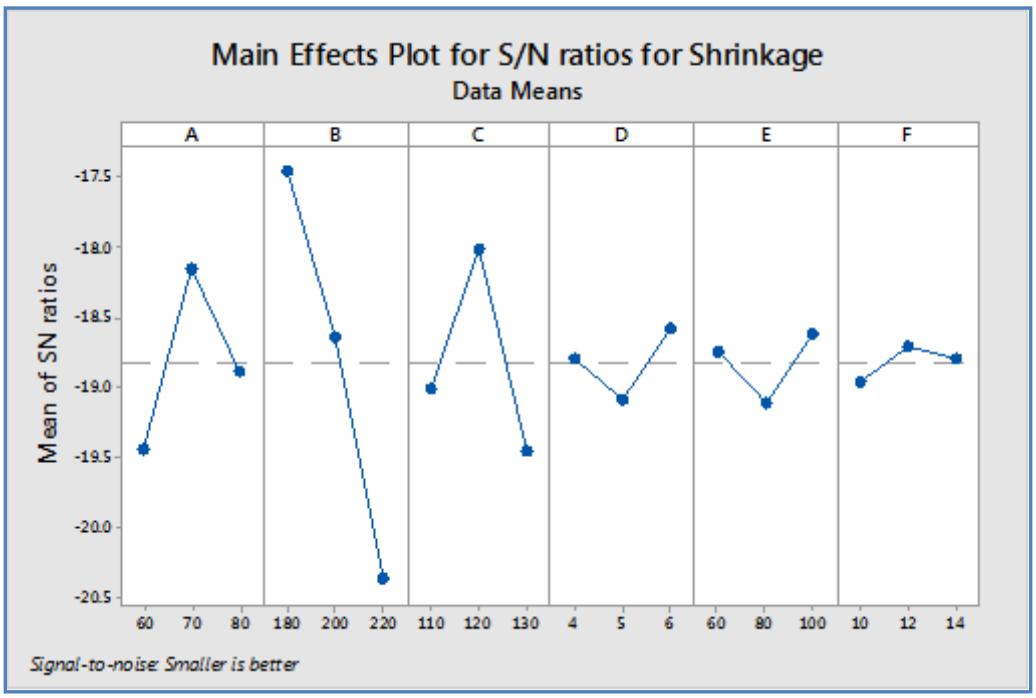

Figure 7.10 Main Effects Plot for S/N Ratios for Shrinkage of PP

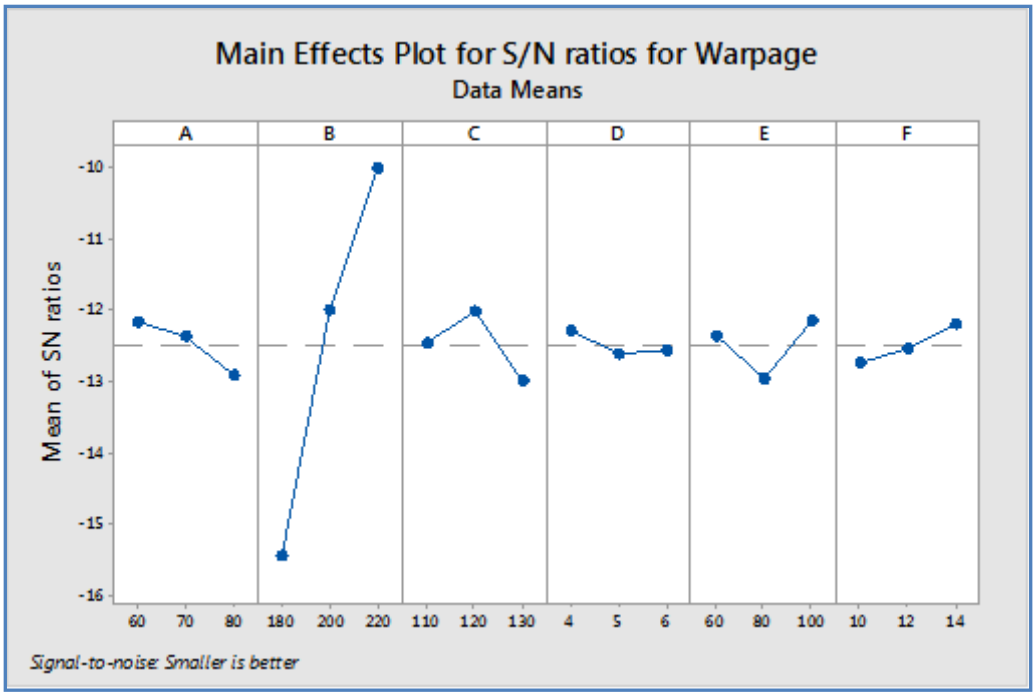

Figure 7.11 Main Effects Plot for S/N Ratios for Warpage of PP

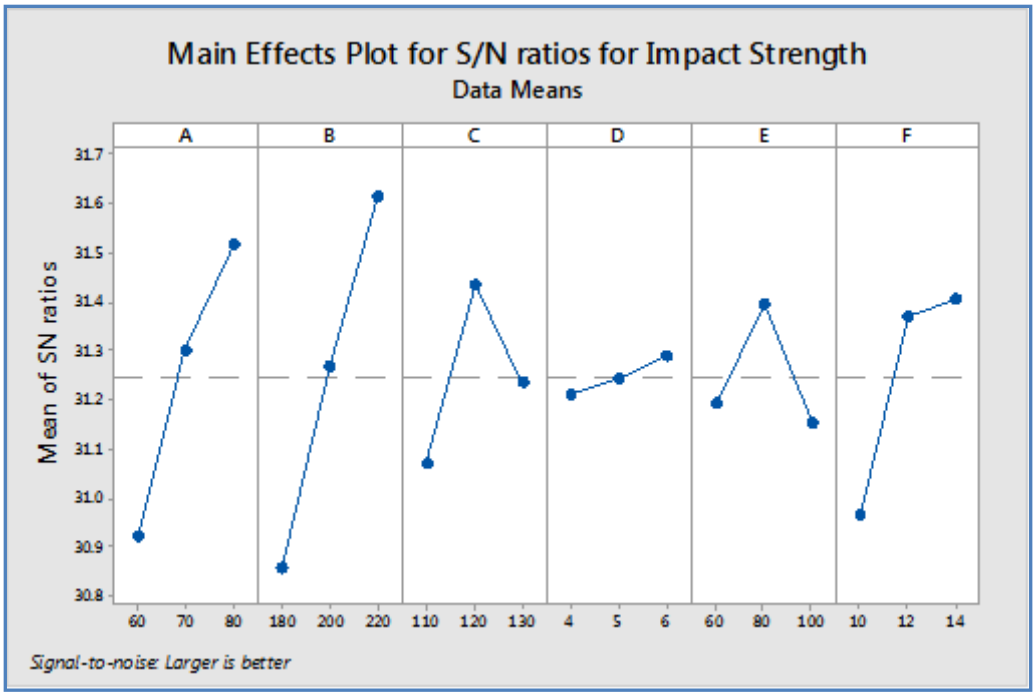

Figure 7.12 Main Effects Plot for S/N Ratios for Impact Strength of PP

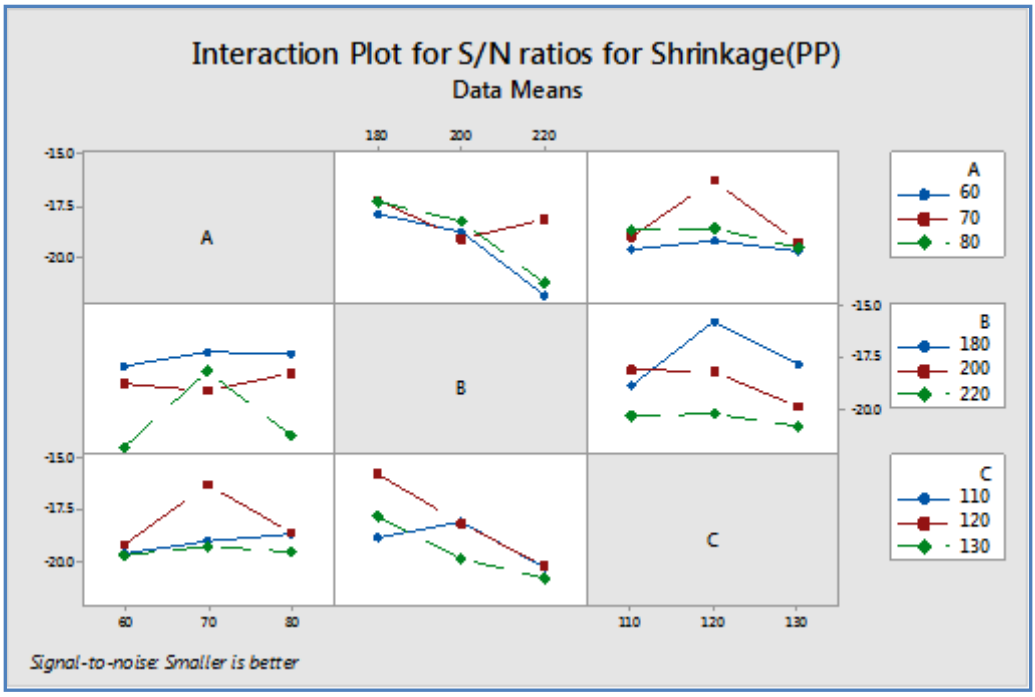

Figure 7.13 Interaction plots between parameters for Shrinkage of PP

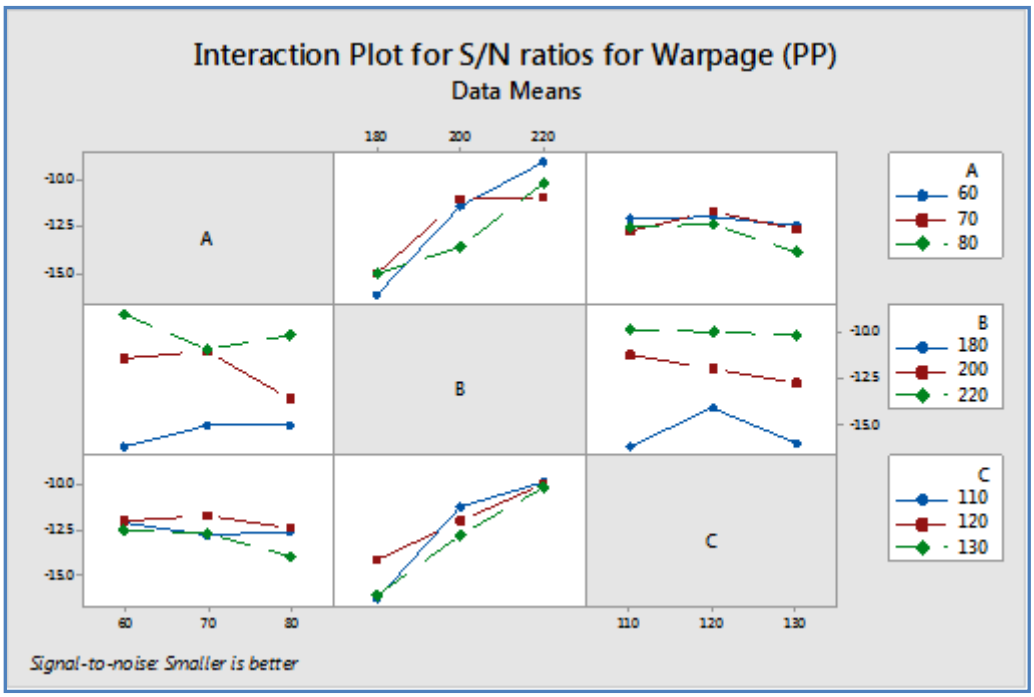

Figure 7.14 Interaction plots between parameters for Warpage of PP

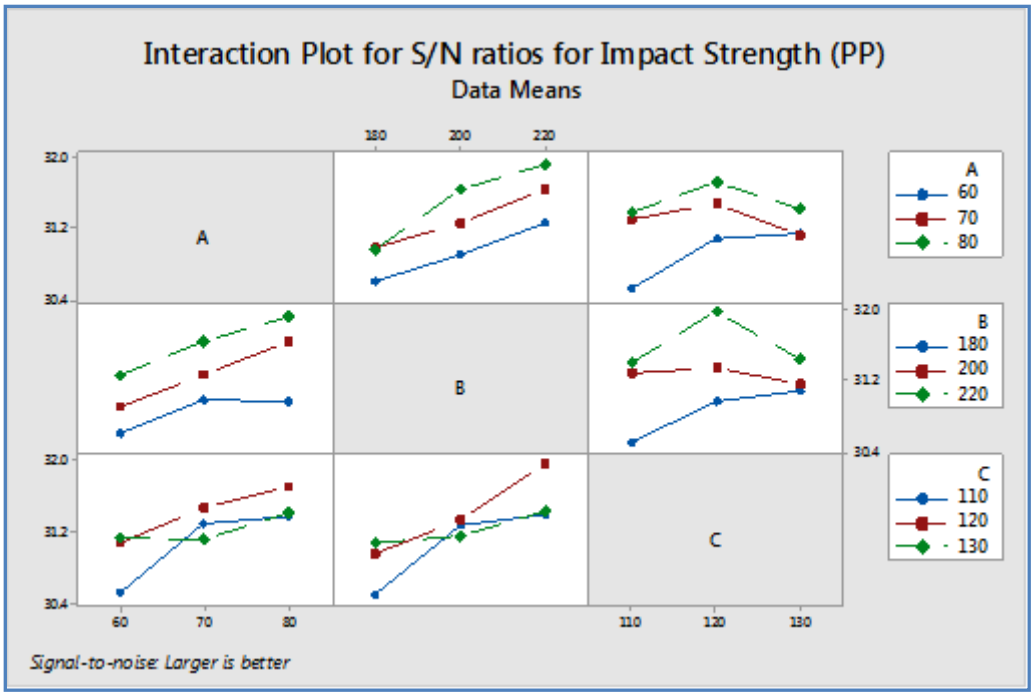

Figure 7.15 Interaction plots between parameters for Impact Strength of PP

7.6. Shrinkage, Warpage and Impact Strength of PC

From Table 7.7 (L_{27}), the overall mean for the S/N ratio of shrinkage, warpage and impact strength of PC are found to be -17.12 dB, -8.58 dB and 34.85 dB, respectively.

The S/N ratio Response Table for shrinkage, warpage and impact strength of PC are shown in Table 7.8, 7.9 and 7.10 respectively. Similarly, main effect plots of S/N ratio (response graphs) for shrinkage, warpage and impact strength of PC are shown graphically in Figure 7.16, 7.17 and 7.18, respectively.

For the PC material, levels A_2, B_1, C_2, D_3, E_1, and F_3 gives minimum shrinkage. From Table 7.8, in order of priority, melt temperature, mould temperature and injection pressure were dominant parameters to minimize the shrinkage in PC.

Similarly, levels A_2, B_3, C_2, D_3, E_1, and F_3 gives minimum warpage in PC. From Table 7.9, in order of priority, melt temperature, injection pressure and mould temperature were dominant parameters to minimize the warpage in PC.

Similarly, levels A_3, B_3, C_2, D_3, E_3 and F_3 gives maximum impact strength of PC. From Table 7.10, in order of priority, melt temperature, mould temperature and injection pressure were dominant parameters to maximum the impact strength.

Table 7.7 L_{27} Orthogonal Array for PC

L_{27} Run	A	B	C	D	E	F	Shrinkage (%)	Shrinkage S/N ratio (dB)	Warpage (mm)	Warpage S/N ratio (dB)	Impact Strength (J/m)	Impact Strength S/N ratio (dB)
1	1	1	1	1	1	1	7.59	-17.605	5.448	-14.72	50.4	34.0486
2	1	1	2	2	2	2	6.075	-15.671	5.032	-14.03	53	34.4855
3	1	1	3	3	3	3	5.91	-15.432	5.256	-14.41	54	34.6479
4	1	2	1	2	2	3	7.057	-16.972	2.376	-7.517	54.4	34.7120
5	1	2	2	3	3	1	6.816	-16.671	2.414	-7.655	56.4	35.0256
6	1	2	3	1	1	2	7.379	-17.36	2.619	-8.363	53.8	34.6156
7	1	3	1	3	3	2	10.38	-20.324	1.483	-3.423	54.4	34.7120
8	1	3	2	1	1	3	10.52	-20.44	1.537	-3.733	56	34.9638
9	1	3	3	2	2	1	10.57	-20.481	1.514	-3.603	54.8	34.7756
10	2	1	1	2	3	2	7.337	-17.31	5.13	-14.2	54.7	34.7597
11	2	1	2	3	1	3	3.278	-10.312	1.7	-4.609	54.2	34.6800
12	2	1	3	1	2	1	6.882	-16.754	4.928	-13.85	53.7	34.5995
13	2	2	1	3	1	1	7.306	-17.274	2.135	-6.588	54.5	34.7279
14	2	2	2	1	2	2	5.95	-15.49	2.254	-7.059	56	34.9638
15	2	2	3	2	3	3	9.00	-19.085	1.96	-5.845	54.5	34.7279
16	2	3	1	1	2	3	6.858	-16.724	2.03	-6.15	57.8	35.2386
17	2	3	2	2	3	1	5.677	-15.082	2.058	-6.269	56.5	35.0410
18	2	3	3	3	1	2	6.727	-16.556	2.133	-6.58	56.8	35.0870
19	3	1	1	3	2	3	6.652	-16.459	4.796	-13.62	53.3	34.5345
20	3	1	2	1	3	1	4.594	-13.244	3.379	-10.58	53.6	34.5833
21	3	1	3	2	1	2	5.801	-15.27	4.65	-13.35	54	34.6479
22	3	2	1	1	3	2	4.991	-13.964	2.35	-7.421	57	35.1175
23	3	2	2	2	1	3	6.774	-16.617	3.164	-10.00	57.8	35.2386
24	3	2	3	3	2	1	7.744	-17.779	4.68	-13.4	57.4	35.1782
25	3	3	1	2	1	1	9.386	-19.45	1.77	-4.959	56.9	35.1022
26	3	3	2	3	2	2	9.913	-19.924	1.785	-5.033	58.7	35.3728
27	3	3	3	1	3	3	9.928	-19.937	1.741	-4.816	58.2	35.2985

Table 7.8 Response table for Signal to Noise Ratios for Shrinkage of PC

Level	A	B	C	D	E	F
1	-17.88	-15.34	-17.34	-16.84	-16.76	-17.15
2	-16.07	-16.8	-15.94	-17.33	-17.36	-16.87
3	-16.96	-18.77	-17.63	-16.75	-16.78	-16.89
Delta	1.82	3.43	1.69	0.58	0.6	0.27
Rank	**2**	**1**	**3**	**5**	**4**	**6**

Table 7.9 Response table for Signal to Noise Ratios for Warpage of PC

Level	A	B	C	D	E	F
1	-8.607	-12.598	-8.734	-8.522	-8.101	-9.07
2	-7.906	-8.206	-7.664	-8.865	-9.364	-8.829
3	-9.242	-4.952	-9.359	-8.369	-8.291	-7.856
Delta	1.336	7.646	1.695	0.496	1.262	1.214
Rank	**3**	**1**	**2**	**6**	**4**	**5**

Table 7.10 Response table for Signal to Noise Ratios for Impact Strength of PC

Level	A	B	C	D	E	F
1	34.67	34.55	34.77	34.83	34.79	34.79
2	34.87	34.92	34.93	34.83	34.87	34.86
3	35.01	35.07	34.84	34.89	34.88	34.89
Delta	0.34	0.51	0.16	0.06	0.09	0.11
Rank	**2**	**1**	**3**	**6**	**5**	**4**

Thus, parameters mould temperature (A), melt temperature (B) and injection pressures (C) are effective parameters and their interactions are also important, which are shown in Figure 7.19, 20, 21.

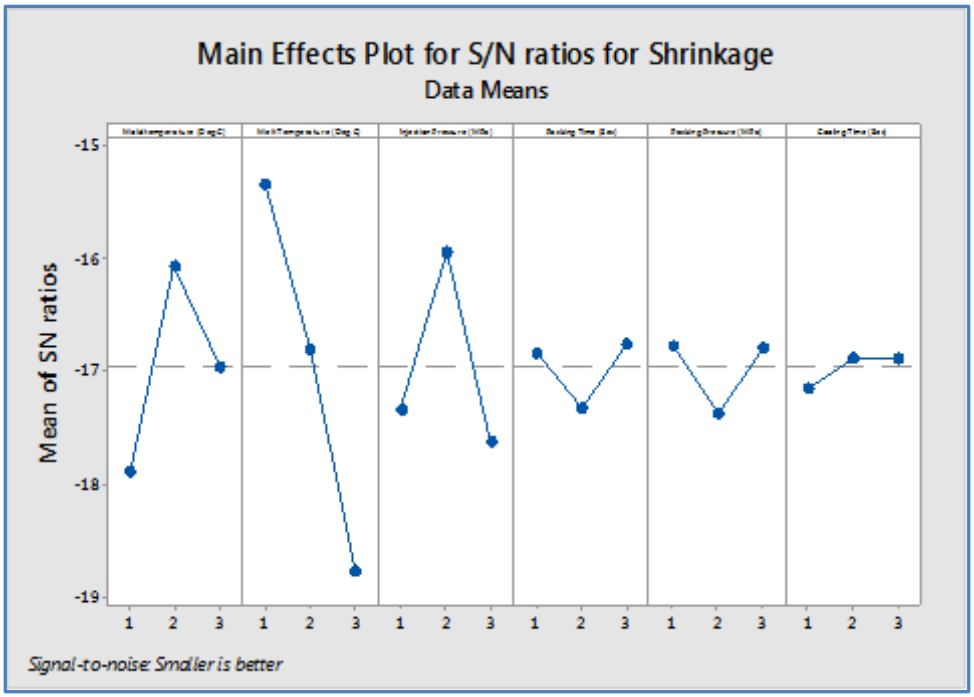

Figure 7.16 Main Effects Plot for S/N Ratios for Shrinkage of PC

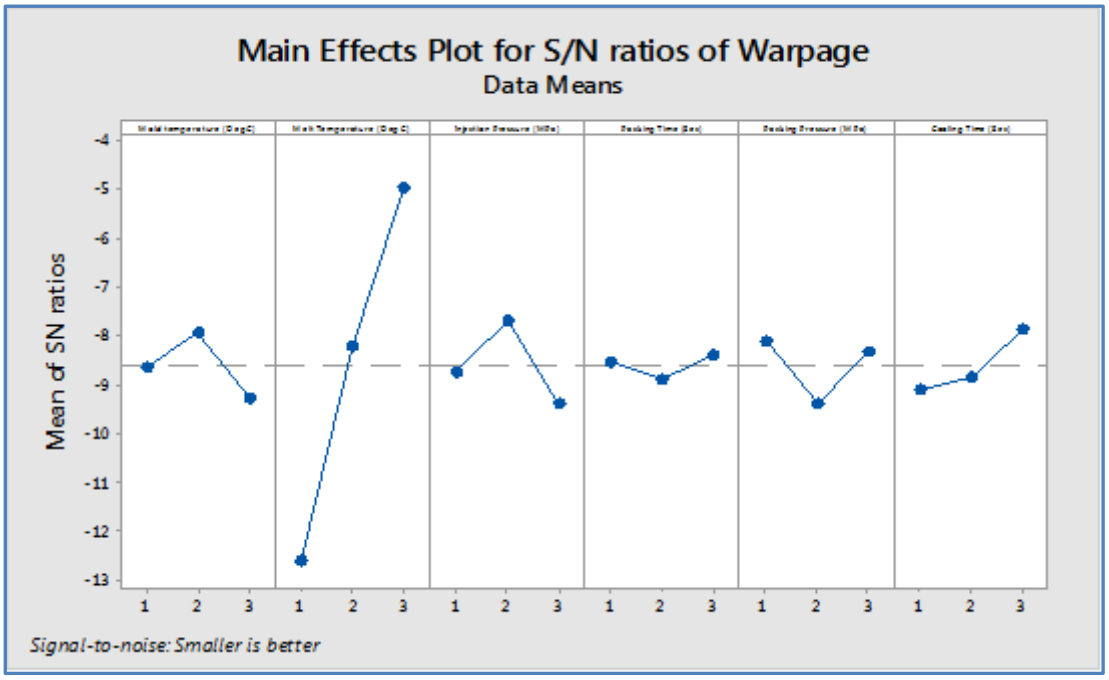

Figure 7.17 Main Effects Plot for S/N Ratios for Warpage of PC

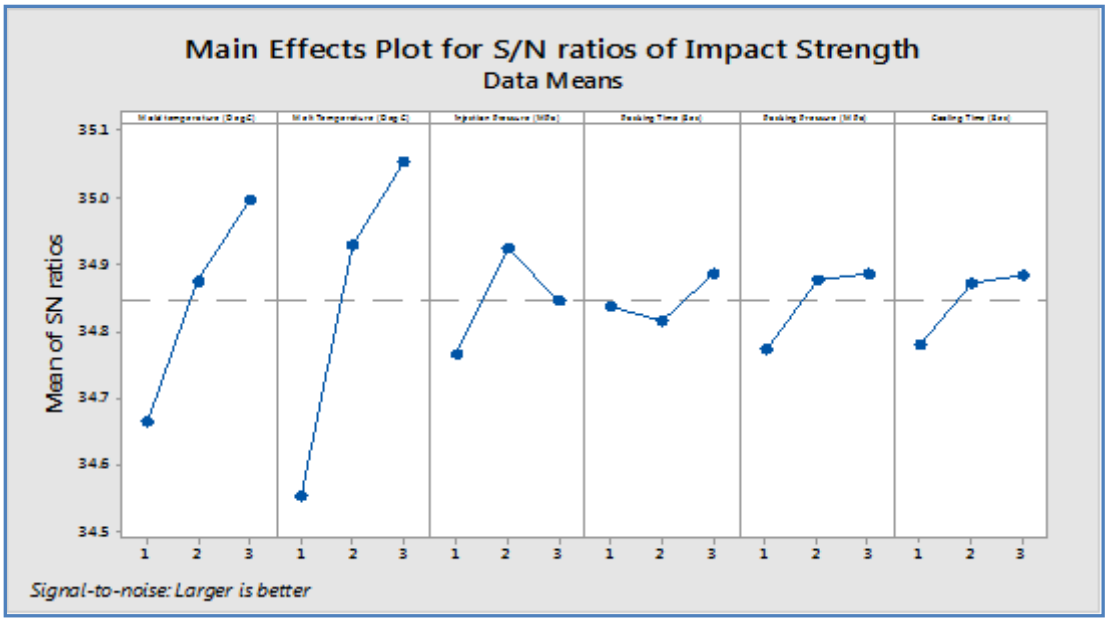

Figure 7.18 Main Effects Plot for S/N Ratios for Impact Strength of PC

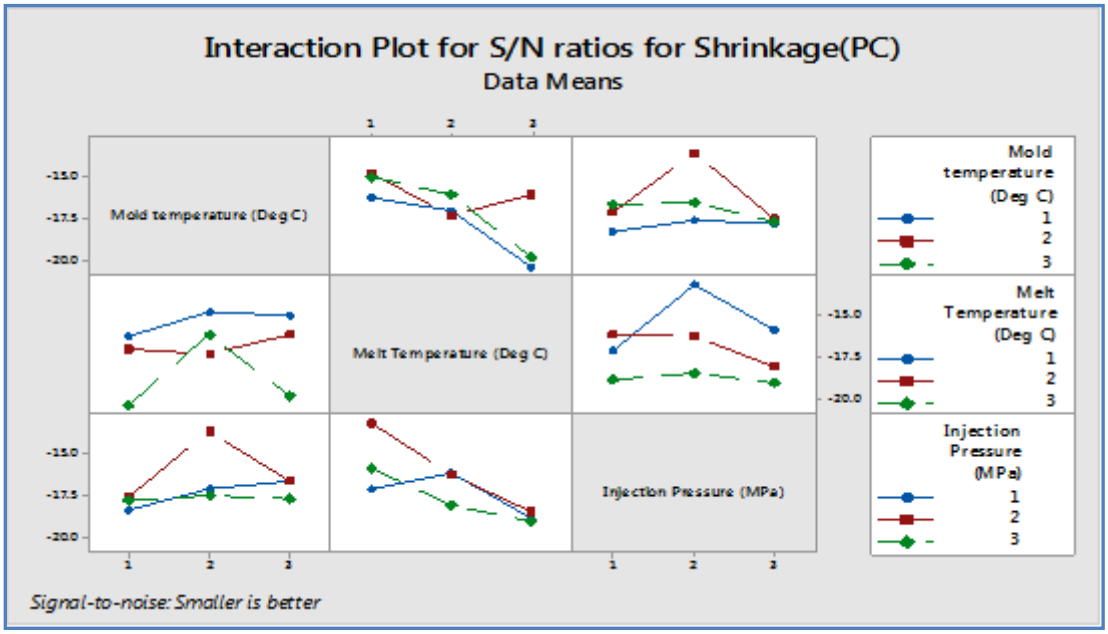

Figure 7.19 Interaction plot between parameters for Shrinkage of PC

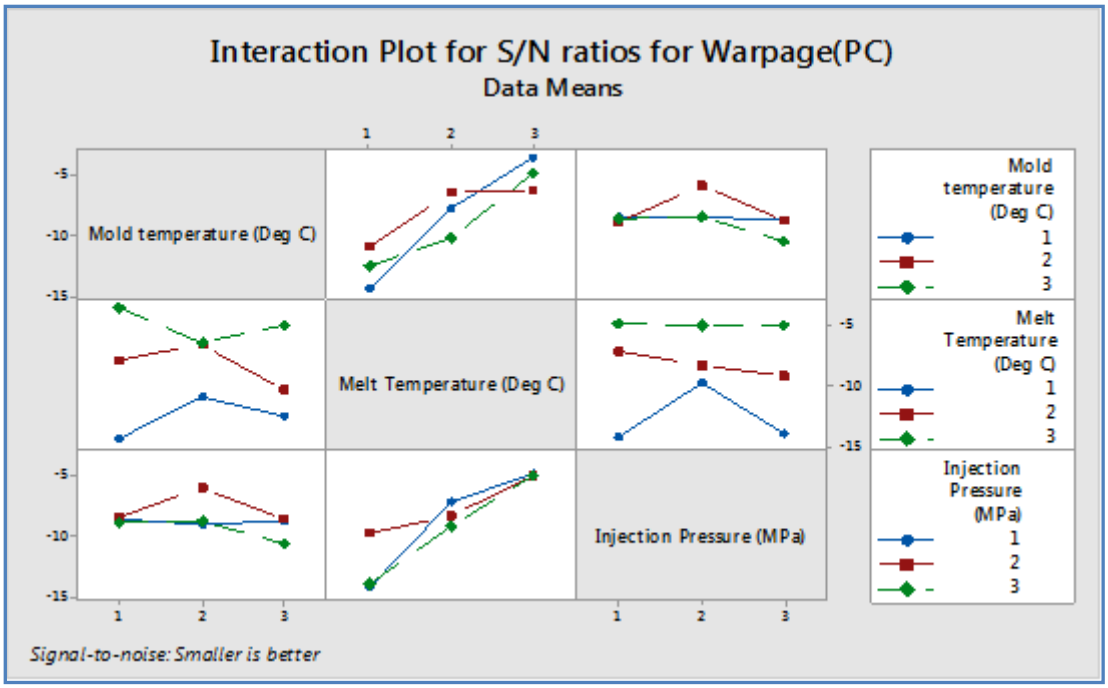

Figure 7.20 Interaction plot between parameters for Warpage of PC

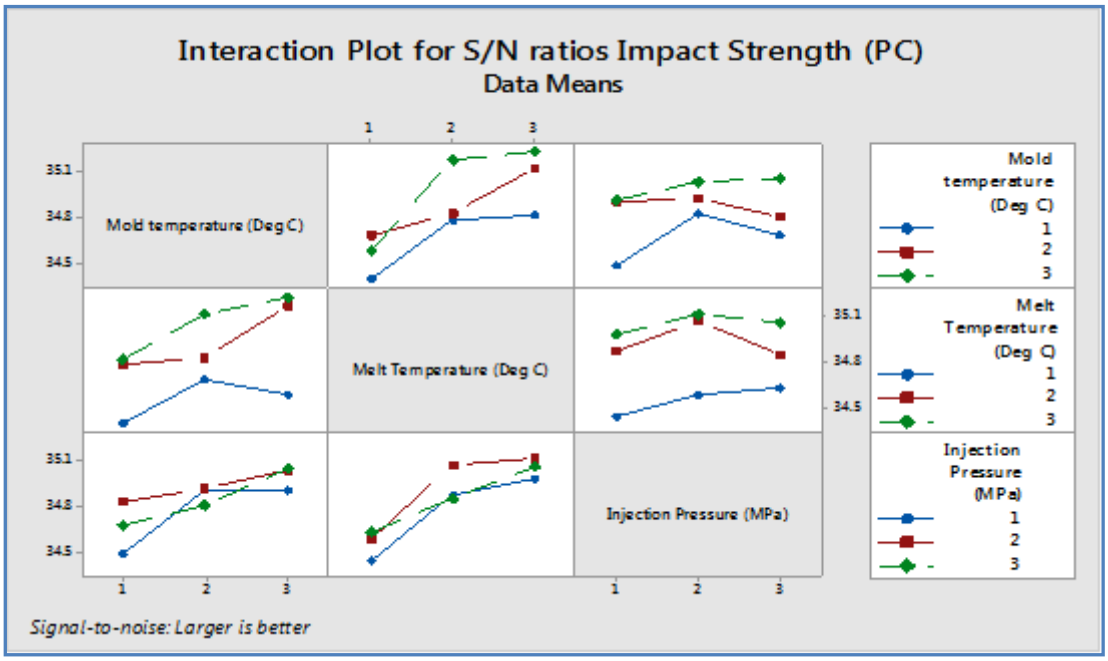

Figure 7.21 Interactions plot between parameters for Impact Strength of PC

7.7. ANOVA and the effects of parameters

7.7.1. ANOVA of PP

The ANOVA test was adopted to determine the significance of each parameter in the designed experimental study. The ANOVA results for PP, are shown in Table 7.11 to Table 7.13 for shrinkage, warpage and impact strength, respectively. ANOVA at 95% confidence interval also shows the same results for shrinkage, warpage and impact strength as obtained by analysis of S/N ratios. Interactions between mould temperature, melt temperature and injection pressure were also considered in the ANOVA. In the analysis of ANOVA of shrinkage of PP, Table 7.11 also shows the p-values. Since the p-values of three parameters viz. mould temperature, melt temperature and injection pressure are less than 0.05, which reflects these parameters are statistically significant. Two interactions viz., mould temperature with melt temperature and melt temperature with injection pressure also have p-values less than 0.05, which reflects their statistically significant effect on the part shrinkage at the 95% confidence level. The R^2 value and adjusted R^2 value for shrinkage model are 90.21% and 87.45% respectively.

Similarly, Table 7.12 shows the ANOVA for warpage. The p-values of five parameters viz., mould temperature, melt temperature, injection pressure, packing pressure and mould cooling time are less than 0.05, which reflects these parameters are statistically significant. Two interactions viz., mould temperature with melt temperature and melt temperature with injection pressure also have p-values less than 0.05, which reflects their statistically significant effect on the warpage of PP. The R^2 value and adjusted R^2 value for warpage model are 92.17% and 88.56% respectively.

Similarly, Table 7.13 shows the ANOVA for impact strength of PP. The p-values of five parameters viz., mould temperature, melt temperature, injection pressure, packing pressure and mould cooling time are less than 0.05, which reflects these parameters are statistically significant. All the three interactions viz., mould temperature with melt temperature, melt temperature with injection pressure and mould temperature with injection pressure also have p-values less than 0.05, which reflects their statistically significance on the impact strength of PP. The R^2 value and adjusted R^2 value for warpage model are 95.16% and 91.27% respectively.

Table 7.11 ANOVA for Shrinkage of PP

Source	DF	Adj SS	Adj MS	F-value	p-value	
Mould temperature	2	16.69	8.345	19.5948	0	Significant
Melt Temperature	2	91.34	45.67	107.257	0	Significant
Injection Pressure	2	18.78	9.39	22.0526	0	Significant
Packing Time	2	1.091	0.5455	1.28112	0.391	Not significant
Packing Pressure	2	1.06	0.53	1.24472	0.341	Not significant
Cooling Time	2	0.362	0.181	0.42508	0.557	Not significant
Mould temperature ×Melt Temperature	4	40.838	10.2095	23.9772	0	Significant
Melt Temperature × Injection Pressure	4	16.214	4.0535	9.51973	0	Significant
Error	33	14.054	0.4258788			
R^2	90.21%					
Adjusted R^2	87.45%					

Table 7.12 ANOVA for Warpage of PP

Source	DF	Adj SS	Adj MS	F-value	p-value	
Mould temperature	2	3.68	1.84	10.5626	0.007	Significant
Melt Temperature	2	73.092	36.546	209.793	0	Significant
Injection Pressure	2	4.398	2.199	12.6234	0	Significant
Packing Time	2	0.349	0.1745	1.00172	0.483	Not significant
Packing Pressure	2	1.832	0.916	5.25832	0.004	Significant
Cooling Time	2	1.722	0.861	4.94259	0.013	Significant
Mould temperature ×Melt Temperature	4	9.824	2.456	14.0987	0	Significant
Melt Temperature × Injection Pressure	4	8.724	2.181	12.5201	0	Significant
Error	33	5.751	0.1742727			
R^2	92.17%					
Adjusted R^2	88.56%					

Table 7.13 ANOVA for Impact Strength of PP

Source	DF	Adj SS	Adj MS	F-value	p-value	
Mould temperature	2	56.75	28.375	350.309	0	Significant
Melt Temperature	2	90.979	45.4895	112.61	0	Significant
Injection Pressure	2	21.41	10.705	50.44	0	Significant
Packing Time	2	1.471	0.7355	9.02	0.072	Not significant
Packing Pressure	2	11.4	5.7	20.96	0	Significant
Cooling Time	2	36.62	18.31	25.84	0	Significant
Mould temperature ×Melt Temperature	4	18.5	4.625	49.16	0	Significant
Melt Temperature × Injection Pressure	4	8.67	2.1675	27.45	0	Significant
Mould temperature× Injection Pressure	4	6.67	1.6675	16.45	0	Significant
Error	29	2.364	0.0815172			
R^2	95.16%					
Adjusted R^2	91.27%					

7.7.2. ANOVA of PC

The ANOVA results for PC, are shown in Table 7.14 to Table 7.16 for shrinkage, warpage and impact strength, respectively. ANOVA at 95% confidence interval also shows the same results for shrinkage, warpage and impact strength as obtained by analysis of S/N ratios. Interactions between mould temperatures, melt temperature and injection pressure were also considered in the ANOVA. In the analysis of ANOVA of shrinkage, Table 7.14 also shows the p-values. Since the p-values of three parameters viz. mould temperature, melt temperature and injection pressure are less than 0.05, which reflects these parameters are statistically significant. Two interactions viz., mould temperature with melt temperature and melt temperature with injection pressure also have p-values less than 0.05, which reflects their statistically significant effect on the shrinkage at the 95% confidence level. The R^2 value and adjusted R^2 value for shrinkage model are 94.42% and 91.04% respectively.

Similarly, Table 7.15 shows the ANOVA for warpage of PC. The p-values of five parameters viz., mould temperature, melt temperature, injection pressure, packing pressure and mould cooling time are less than 0.05, which reflects these parameters are statistically significant. Two interactions viz., mould temperature with melt temperature and melt temperature with injection pressure also have p-values less than

0.05, which reflects their statistically significant effect on the warpage of PC. The R^2 value and adjusted R^2 value for warpage model are 93.35% and 91.56% respectively.

Similarly, Table 7.16 shows the ANOVA for impact strength of PC. The p-values of five parameters viz., mould temperature, melt temperature, injection pressure, packing pressure and mould cooling time are less than 0.05, which reflects these parameters are statistically significant. All the three interactions viz., mould temperature with melt temperature, melt temperature with injection pressure and mould temperature with injection pressure also have p-values less than 0.05, which reflects their statistically significance on the impact strength of PC. The R^2 value and adjusted R^2 value for warpage model are 97.26% and 95.23% respectively.

Table 7.14 ANOVA for Shrinkage of PC

Source	DF	Adj SS	Adj MS	F-value	p-value	
Mould temperature	2	18.679	9.3394	21.93	0.000	Significant
Melt Temperature	2	75.73	37.8649	88.91	0.000	Significant
Injection Pressure	2	12.574	6.287	14.76	0.000	Significant
Packing Time	2	1.091	0.5454	1.28	0.291	Not significant
Packing Pressure	2	1.09	0.5451	1.28	0.291	Not significant
Cooling Time	2	0.362	0.1809	0.42	0.657	Not significant
Mould temperature ×Melt Temperature	4	40.838	10.2094	23.97	0.000	Significant
Melt Temperature × Injection Pressure	4	16.214	4.0535	9.52	0.000	Significant
Error	33	14.054	0.4259			
R^2	94.42%					
Adjusted R^2	91.04%					

Table 7.15 ANOVA for Warpage of PC

Source	DF	Adj SS	Adj MS	F-value	p-value	
Mould temperature	2	2.039	1.0196	5.85	0.007	Significant
Melt Temperature	2	68.092	34.0459	195.36	0.000	Significant
Injection Pressure	2	4.398	2.199	12.62	0.000	Significant
Packing Time	2	0.259	0.1296	0.74	0.483	Non-Significant
Packing Pressure	2	2.332	1.166	6.69	0.004	Significant
Cooling Time	2	1.722	0.861	4.94	0.013	Significant
Mould temperature ×Melt Temperature	4	9.824	2.4559	14.09	0.000	Significant
Melt Temperature × Injection Pressure	4	8.724	2.1809	12.51	0.000	Significant
Error	33	5.751	0.1743			
R^2	93.35%					
Adjusted R^2	91.56%					

Table 7.16 ANOVA for Impact Strength of PC

Source	**DF**	**Adj SS**	**Adj MS**	**F-value**	**p-value**	
Mould temperature	2	16.838	8.41911	103.26	0.00	Significant
Melt Temperature	2	18.364	9.18178	112.61	0.00	Significant
Injection Pressure	2	8.225	4.11244	50.44	0.00	Significant
Packing Time	2	1.471	0.73556	9.02	0.072	Non-Significant
Packing Pressure	2	3.418	1.70889	20.96	0.00	Significant
Cooling Time	2	4.213	2.10667	25.84	0.00	Significant
Mould temperature ×Melt Temperature	4	16.031	4.00778	49.16	0.00	Significant
Melt Temperature × Injection Pressure	4	8.951	2.23778	27.45	0.00	Significant
Mould temperature× Injection Pressure	4	5.364	1.34111	16.45	0.00	Significant
Error	29	2.364	0.08153			
R^2	97.26%					
Adjusted R^2	95.23%					

Results of S/N ratios can be compared to previous research. Altan [121] and Öktem [124] had investigated that melt temperature as the most significant parameter to minimize the shrinkage and warpage in PP and PC part. Similarly, Chen et al. [144] found with simulation and experiments that melt temperature and packing pressure were the most significant parameters to reduce the warpage in thin-shell plastic parts. Ozcelik and Sonat [188] used Taguchi orthogonal array for the thin shell phone cover with polycarbonate/acrylonitrile butadiene styrene (PC/ABS) thermoplastic as a

model. The result for PC/ABS material was the most influential parameters on warpage were packing pressure and melt temperature. Ozcelik et al. [189] optimized injection parameters and found that melt temperature as the important parameter, which affected the elasticity module, tensile strength-strain at the yield and tensile strain at the break. Wang et al. [118] found that the resin temperature has a great effect on the resin viscosity for brake booster valve body. Similarly, the moulding temperature was found a very remarkable effect on increasing curing percentage and improving compression strength of valve body.

7.8. Confirmation Experiment

7.8.1. Confirmation Experiment for PP

The optimal combination of process parameters has been determined in the earlier analysis. The final step is to predict and verify the improvement of the observed values through the use of optimal combination level of parameters. The estimated S/N ratio for part shrinkage, warpage and impact strength for PP can be determined with the help of following prediction equation:

$$\hat{\eta}_1 = \overline{A}_2\overline{B}_3 + \overline{A}_2\overline{C}_2 + \overline{B}_3\overline{C}_2 - \overline{B}_3 - \overline{A}_2 + \overline{C}_2 + \overline{D}_1 + \overline{E}_1 + \overline{F}_1 - 2\overline{T}$$

$$\hat{n}_2 = \overline{A}_3\overline{B}_3 + \overline{A}_3\overline{C}_3 + \overline{B}_3\overline{C}_3 - \overline{A}_3 - \overline{B}_3 - \overline{C}_3 + \overline{D}_2 + \overline{E}_3 - \overline{F}_3 - 2\overline{T}$$

$$\hat{n}_3 = \overline{A}_3\overline{B}_3 + \overline{A}_3\overline{C}_3 + \overline{B}_3\overline{C}_3 - \overline{A}_2 - \overline{B}_3 - \overline{C}_3 + \overline{D}_1 + \overline{E}_2 - \overline{F}_2 - 2\overline{T}$$

A new combination of parameter levels $A_2B_3C_2D_3E_1F_2$ was used for prediction of Shrinkage of PP through prediction equation and it was found to be $\hat{\eta}_1$ = -11.785 dB.

A new combination of parameter levels $A_3B_3C_2D_3E_1F_1$ was used for prediction of Warpage of PP through prediction equation and it was found to be $\hat{\eta}_2$ = -6.736 dB.

A new combination of parameter levels $A_1B_2C_2D_3E_1F_2$ was used for prediction of impact strength of PP through prediction equation and it was found to be $\hat{\eta}_3$ = 29.38 dB.

Table 7.17 Results of the confirmation experiment for Shrinkage for PP

	Optimal parameters		
	Prediction	Experimental	Error
Level	$A_2B_3C_2D_3E_1F_2$	$A_2B_3C_2D_3E_1F_2$	
S/N ratio for shrinkage	-11.785	-12.575	6.28%

Table 7.18 Results of the confirmation experiment for Warpage for PP

	Optimal parameters		
	Prediction	Experimental	Error
Level	$A_3B_3C_2D_3E_1F_1$	$A_3B_3C_2D_3E_1F_1$	
S/N ratio for warpage	-6.836	-6.361	7.46%

Table 7.19 Results of the confirmation experiment for Impact Strength for PP

	Optimal parameters		
	Prediction	Experimental	Error
Level	$A_1B_2C_2D_3E_1F_2$	$A_1B_2C_2D_3E_1F_2$	
S/N ratio for impact strength	29.38	29.78	1.34%

For each response measures viz. shrinkage, warpage and impact strength of PP, an experiment was performed for a set of different parameter combination and evaluated with the result obtained from the predictive- equations, which is exhibited in Tables 7.17 - 7.19 respectively. The resulting model appears to be competent of predicting shrinkage, warpage and impact strength to a realistic precision. An error of 6.28% for the prediction of S/N ratio of shrinkage, error of 7.46% for the prediction of S/N ratio of warpage and error of 1.34% for the prediction of impact strength of PP were observed.

7.8.2 Confirmation Experiment for PC

Similarly, the estimated S/N ratio for part shrinkage, warpage and impact strength for PC can be calculated with the help of following prediction equation:

$$\hat{\eta}_4 = \overline{A}_2\overline{B}_3 + \overline{A}_2\overline{C}_2 + \overline{B}_3\overline{C}_2 - \overline{B}_3 - \overline{A}_2 + \overline{C}_2 + \overline{D}_3 + \overline{E}_2 + \overline{F}_1 - 2\overline{T}$$

$$\hat{n}_5 = \overline{A}_2\overline{B}_3 + \overline{A}_2\overline{C}_3 + \overline{B}_3\overline{C}_3 - \overline{A}_2 - \overline{B}_3 - \overline{C}_3 + \overline{D}_2 + \overline{E}_3 - \overline{F}_3 - 2\overline{T}$$

$$\hat{n}_6 = \overline{A}_3\overline{B}_3 + \overline{A}_3\overline{C}_3 + \overline{B}_3\overline{C}_3 - \overline{A}_2 - \overline{B}_3 - \overline{C}_3 + \overline{D}_2 + \overline{E}_2 - \overline{F}_2 - 2\overline{T}$$

A new combination of parameter levels $A_2B_3C_2D_3E_1F_2$ was used for prediction of shrinkage of PC through prediction equation and it was found to be $\hat{\eta}_4$ = -13.9055dB

A new combination of parameter levels $A_2B_3C_3D_2E_3F_3$ was used for prediction of warpage of PC through prediction equation and it was found to be $\hat{\eta}_5$ = -5.7695 dB.

A new combination of parameter levels $A_3B_3C_3D_2E_2F_2$ was used for prediction of impact strength of PC through prediction equation and it was found to be $\hat{\eta}_6$ =35.237 dB.

For each response measures viz. shrinkage, warpage and impact strength, an experiment was performed for a set of different parameter combination and evaluated with the result obtained from the predictive-equations which is exhibited in Tables 7.20-22, respectively. The resulting model appears to be competent of predicting shrinkage, warpage and impact strength of PC to a realistic precision. An error of 5.11% for the prediction of S/N ratio of shrinkage, error of 5.91% for the prediction of S/N ratio of warpage and error of 1.17% for the prediction of impact strength of PC were observed.

Table 7.20 Results of the confirmation experiment for shrinkage for PC

	Optimal parameters		
	Prediction	Experimental	Error
Level	$A_2B_3C_2D_3E_1F_2$	$A_2B_3C_2D_3E_1F_2$	
S/N ratio for shrinkage	-13.9055	-14.6545	5.11%

Table 7.21 Results of the confirmation experiment for warpage for PC

	Optimal parameters		
	Prediction	Experimental	Error
Level	$A_2B_3C_3D_2E_3F_3$	$A_2B_3C_3D_2E_3F_3$	
S/N ratio for warpage	-5.7695	-6.1321	5.91%

Table 7.22 Results of the confirmation experiment for impact strength for PC

	Optimal parameters		
	Prediction	Experimental	Error
Level	$A_3B_3C_3D_2E_2F_2$	$A_3B_3C_3D_2E_2F_2$	
S/N ratio for impact strength	35.237	35.656	1.17%

7.9. Mathematical models for PP and PC

By increasing the number of measurements, the errors in prediction of response (shrinkage, warpage and impact strength) can be further reduced for both the materials. This validates the successfully development of the mathematical model for predicting the shrinkage, warpage and impact strength based on knowledge of the input parameters.

Parameters setting that satisfy multiple objectives of minimization of shrinkage and warpage and maximization of impact strength need to be determined. The mathematical model suggested here is in the following form:

$$Z = K_0 + K_1 \times A + K_2 \times B + K_3 \times C + K_4 \times D + K_5 \times E + K_6 \times F + K_7 \times A \times B + K_8 \times A \times C + K_9 \times B \times C$$

Here, Z is the response output and K_i (i=0,1,2…..9) are the model constants. With the help of MiniTab -17 software, the constants can be calculated by using non-linear regression analysis.

Thus, based on the predictive equations, the following mathematical models (in coded forms) can be proposed for determining the values of shrinkage (%), warpage (mm) and impact strength (J/m) for PP and PC. The calculated coefficients were used and the following relations were developed for PP and PC.

Mathematical model for virgin PP

$$\text{Shrinkage} = 229.7 - 1.686\,A + 0.0788\,B - 2.766\,C - 0.338\,D + 0.01187\,A^2 + 0.01070\,C^2 + 0.00278\,C\times D \quad (8)$$

$$\text{Warpage} = 138.7 - 0.499\,A - 0.788\,B - 0.802\,C + 2.598\,E + 0.001348\,B^2 + 0.00451\,C^2 + 0.002563\,A\times B - 0.02229\,C\times E \quad (9)$$

$$\text{Impact Str.} = -262.6 + 0.813A - 0.0576B + 3.367C + 0.3767\,D + 7.46\,E - 0.0122\,C^2 - 0.00239\times D2 - 0.1972\times E^2 + 0.00195\,A\times B - 0.00575\,A\times C - 0.0325\,A\times E \quad (10)$$

Mathematical model for virgin PC

$$\text{Shrinkage} = 15.66 - 3.23\,A - 0.05\,B - 5.64\,C - 0.496\,D - 1.971\,E + 0.535\,A^2 + 0.437\,B^2 + 1.008\,C^2 + 0.661\,A\times C + 0.558\,B\times C - 0.689\,B\times E - 0.892\,C\times D + 0.528\,C\times E + 1.137\,D\times E \quad (11)$$

$$\text{Warpage} = 13.08 - 0.002\,A - 4.233\,B - 3.311\,C - 2.295\,D + 0.063\,E + 0.470\,B^2 + 0.575\,C^2 - 0.437\,E^2 + 0.233\,A\times B + 0.269\,B\times C + 0.291\,C\times D + 0.859\,D\times E \quad (12)$$

$$\text{Impact Str.} = 42.82 + 0.078\,A + 2.622\,B + 0.861\,C + 3.672\,E + 2.167\,F - 0.700\,B^2 + 1.008A\times B - 0.500\,A\times E - 0.358\,B\times E + 0.250\,B\times F - 0.325\,C\times F - 0.842\,E\times F \quad (13)$$

Chapter summery

This chapter briefly presents/discusses following things:

- Shrinkage, warpage and impact strength of virgin PP and PC were successfully analyzed by using Taguchi technique. It provides an organized and efficient methodology for the optimization of the parameters. The standard liner graph was modified using the line-separation method to assign the parameters and various interactions in the orthogonal array.

- Melt temperature, mould temperature and injection pressure with their interactions was found to perform significant role in minimization for shrinkage, warpage and maximization of impact strength for both virgin PP and virgin PC.
- The confirmation experiment reveals that the errors linked with prediction of shrinkage, warpage and impact strength are 6.28%, 7.46%, and 1.34% respectively for virgin PP. Similarly, the confirmation experiment shows that the errors associated with prediction of shrinkage, warpage and impact strength are 5.11%, 5.91%, and 1.17% respectively for virgin PC. In order to minimize shrinkage and warpage and to maximize impact strength, mathematical-models were determined by using the non-linear regression method.

The next chapter discusses the Summary, Conclusions and Scope for Future Work.

*****

Chapter-8

SUMMARY, CONCLUSIONS AND SCOPE FOR FUTURE WORK

This chapter contains the summary of the work done along with objectives, composite fabrication, analysis of results and conclusions based on the research work are presented in this thesis systematically followed by the scope for future work in this field.

8.1. Background to the research work

The work in this thesis is initiated with a goal to find the influence of reinforcement of micro sized filler (alumina, TiO_2, and marble powder) on the performance properties of Polypropylene. Following three types of composites were developed:

Type-1: Polypropylene-composite filled with Al_2O_3 filler (PPA series)

Type-2: Polypropylene-composite filled with TiO_2 filler (PPT series)

Type-3: Polypropylene-composite filled with marble powder filler (PPM series)

The selected three types of PP composites were prepared under identical processing conditions and were studied for the following properties:

- Physical and chemical properties (Chapter-4)
- Mechanical and thermo-mechanical properties (Chapter-5)
- Morphological properties (Chapter-6)
- Performance optimization of virgin PP and PC using Taguchi method (Chapter-7)

8.2. Summary of the research findings

The summary based on the studies conducted in this research work are presented chapter wise.

8.2.1. Summary of research finding of Physical, Chemical, Mechanical and Thermo-Mechanical characteristics of the Polypropylene composites

The studies on the evaluation of physical, chemical, mechanical and thermo-mechanical properties on the developed composites have been summarized as:

- The void content of PP composites filled with different weight-percentage of Alumina, Titanium dioxide and marble powder are in the range of 0.30 - 8.25%, 0.28 - 2.38% and 0.53 - 6.38% respectively.

- The incorporation of alumina, titanium dioxide and marble powder into the PP led to an enhancement in hardness. The hardness of PP composites filled with different weight-percentages of Alumina, Titanium dioxide and marble powder particle were in the range of 58-70, 67 - 70 and 67 - 73 respectively. The maximum value of Shore D hardness of PP composite was 73 indicated by PP composite filled with 20 wt.% marble powder. It is 30.35% higher than Shore D hardness of virgin PP.
- The impact strength of PP composites filled with different weight-percentage (0, 5, 10, 15 and 20 wt. %) of alumina and titanium dioxide decreases as the filler content increases. In PP-alumina composites, the impact strength decreases from 36 J/m to 21.32 J/m which was due to the increasing void content. Similarly, in PP-TiO_2 composites PPT-5, PPT-10, PPT-15 and PPT-20 have Impact strength to be 35, 32, 29 and 24 J/m respectively. On the other hand, adding of marble powder increases impact strength of PP composites. Marble powder having 5 and 10 wt.% consist impact strength to be 37 J/m and 38.5 J/m. Marble powder having 15 and 20 wt.% consists increasing trend of impact strength from 39.7 to 40.6 J/m respectively. Thus, PPM-20 has 11.33 % higher impact strength than virgin PP.
- The flexural strength of PP-Al_2O_3 composites, having different weight-percentage (5, 10, 15 and 20 wt. %), is in the increasing trend, which is 53.04 - 59.26 MPa.

  In PP-TiO_2 composites, initially flexural strength increases and further addition of filler decreases flexural strength. Thus, PPT-5 shows maximum flexural strength in PPT series. Same trend was obtained in PP-Marble powder composites, as they also exhibit decreasing trend of flexural strength which is 64.16 - 52.56 MPa respectively.

  Thus, in all the three series of composites, maximum flexural strength was obtained in PPM-5 which is 64.16 MPa.
- The compressive strength of PP composites filled with different weight-percentage (5, 10, 15 and 20 wt. %) of alumina, titanium dioxide and Marble powder are in the range of 98.63 - 121.34 MPa, 113.8 - 171.6 MPa and 103.4 – 159.4 MPa respectively. Thus maximum compressive strength was 87.8%, higher than virgin PP which is found in PP-TiO_2 composite having 20 wt.%.

- The glass transition temperature of PP-composites increased with the increase in micro filler content in the matrix material. Similarly, the thermal stability and degradation temperature also improved with increase in filler content. The results of glass transition temperature of PP composite using Thermo-gravimetric analysis were in agreement with the results using Dynamic mechanical analysis.
- For PP-alumina composites the storage modulus (E') is in the range of 650-860 MPa at lower temperature (30°C) and remains higher for PPA-10. However, at higher temperature (i.e. 150°C) the storage modulus lies in the range of 50-100 MPa.
- For PP-TiO_2 composites the storage modulus (E') is in the range of 630-1030 MPa at lower temperature (30°C) and remains higher for PPT-10. However, at higher temperature (i.e. 150°C) the storage modulus lies in the range of 65-80 MPa.
- For PP-marble powder composites the storage modulus (E') is in the range of 625-855 MPa at lower temperature (30°C) and remains higher for PPM-10. However, at higher temperature (i.e. 150°C) the storage modulus lies in the range of 65-135 MPa.

8.2.2. Summary of research findings of Morphological characterizations of PP composites

The research findings of PP-Alumina composites are summarized as:

- Good adhesion was observed of PP matrix with alumina filler.
- It was also observed that clustering effect of large particles of alumina creates stress concentration. The mean size of alumina particles was about 0.6 μm.

The research findings of PP-TiO_2 composites are summarized as:

- During SEM micrographs, it was observed that the TiO_2 particles are well dispersed in PP matrix, especially the anatase particles. However, it is important to notice that the presence of few TiO_2 lumps increase in the composites due to the increasing wt.% of filler content. Due to agglomeration of filler particles, the lumps are formed. Interface between lumps or between matrix and filler may not be continuous due to their mismatched nature. As TiO_2 particles are relatively harder than the PP matrix, they may harden the

entire material if they create good quality contact with the polymer matrix. It was also observed that TiO_2 particles are spherical and their size was about 100 to 300 nm according to SEM analysis. Addition of TiO_2 content from 5 wt.% to 20 wt.% increased the surface roughness of the composite.

The research findings of PP-Marble Powder composites are summarized as:

- The surface morphology of PP-marble composites was examined and it was observed that with mean size of about 0.7 μm marble particles are clearly visible. From the AFM images, the roughness was determined as the arithmetic mean (R_a) of the distribution of heights. The presence of the compositional elements of marble samples such as Si, Mg, Ca, and O were detected.

8.2.3. Summary of research on optimization of shrinkage, warpage and impact strength characteristics of the virgin PP and virgin PC

In this study, an attempt was made to determine the important process parameters for minimization of defects, viz., shrinkage, warpage and maximization of impact strength of virgin PP and virgin PC with plastic injection moulding process. To determine the range of parameters steady state experiments were performed for both the virgin PP and virgin PC.

Shrinkage, warpage and impact strength of plastic parts can be successfully analyzed by using Taguchi experimental design. Taguchi method provides organized and efficient methodology for the optimization of the parameters. The standard linear graph was modified using the line-separation method to assign the parameters and interactions to various columns of the orthogonal array. The array selected was the L_{27} (3^{13}), which has 27 rows corresponding to the number of experiments with 13 columns at three levels. By modifying the standard linear graph, the parameters and their interactions were assigned to the columns.

Melt temperature, mould temperature and injection pressure with their interactions have been found to perform a significant role in minimization of shrinkage, warpage and maximization of impact strength for both the virgin PP and virgin PC. In the process of plastic injection moulding, when the melt temperature was increased, unoriented molecules were fixed in a frozen layer and the material has

to remain hot for a longer time, thus allowing relaxation of molecules and thereby reducing the orientation effect, which helps to reduce the shrinkage and warpage.

The confirmation experiment shows that the errors associated with prediction of shrinkage, warpage and impact strength were 6.21%, 7.46%, and 1.34%, respectively for virgin PP. Similarly, the confirmation experiment shows that the errors associated with prediction of shrinkage, warpage and impact strength were 5.11%, 5.91%, and 1.171%, respectively for virgin PC. In order to minimize shrinkage and warpage and to maximize impact strength, mathematical models were developed by using the non-linear regression method.

8.3. Conclusions of the research work

Following salient conclusions were drawn based on the studies on the evaluation of physical, chemical, mechanical, thermo-mechanical and morphological behaviour of these experimental PP composites.

1. Fabrication of injection-moulded composites with micro fillers has been performed.
2. The physical, chemical and mechanical properties were found to be well within the ASTM standards.
3. The fillers (alumina, titanium dioxide, and marble powder) were successfully characterized by using FTIR spectroscopy and Scanning Electron Microscope.
4. The inclusion of fillers content led to increase in the density and void content of the PP composites.
5. The higher magnitude of mechanical properties in all the PP composites noticed may be attributed to the presence of hard and brittle phase inorganic oxide alumina, titanium dioxide, and marble powder as filler because of higher degree of exfoliation and higher adhesion at the particle-matrix interface leads to higher load transfer.
6. The Izod impact strength for alumina and titanium dioxide filled PP composite decreased as filler content increased. In contrast, reverse trends were seen with PP composite filled with marble powder.
7. The flexural strength of PP composites filled with alumina showed an increasing trend, while titanium dioxide and Marble powder exhibited a decreasing trend.

8. The glass transition temperature increased with increase in filler content in the composites. Addition of fillers also lead to improvement in thermal stability and degradation temperature of PP composite materials.
9. Melt temperature, mould temperature and injection pressure with their interactions have been found to perform a significant role in minimization for shrinkage, warpage and maximization of impact strength for both the virgin PP and virgin PC.

8.4. Scope for future work

Because of time limit, the research work accomplished in this project is still in initial stage. Following aspects could not be addressed in this thesis work and hence should be taken up in the future work.

1. The studies are mainly focused on mechanical and thermo mechanical performance of particulate filled PP composites. However, few more parameters can be introduced in future scope such as effect of change in particle size and shape, effect on thermal conductivity etc. can be performed.
2. In future study, the effect of different treatments like Silane treatment can be performed and its effect on composite properties can be determined.
3. The friction and wear study of PP composites in the different working condition can be conducted for future.

*****

References

[1] U. Szeluga, B. Kumanek, and B. Trzebicka, "Synergy in hybrid polymer/nanocarbon composites. A review," *Compos. Part A Appl. Sci. Manuf.*, vol. 73, pp. 204–231, 2015.

[2] F. Hussain, "Polymer-matrix Nanocomposites, Processing, Manufacturing, and Application: An Overview," *J. Compos. Mater.*, vol. 40, no. 17, pp. 1511–1575, 2006.

[3] T. Kuilla, S. Bhadra, D. H. Yao, N. H. Kim, S. Bose, and J. H. Lee, "Recent advances in graphene based polymer composites," *Prog. Polym. Sci.*, vol. 35, no. 11, pp. 1350–1375, 2010.

[4] S. Kango, S. Kalia, A. Celli, J. Njuguna, Y. Habibi, and R. Kumar, "Surface modification of inorganic nanoparticles for development of organic-inorganic nanocomposites - A review," *Prog. Polym. Sci.*, vol. 38, no. 8, pp. 1232–1261, 2013.

[5] A. Akinci, S. Sen, and U. Sen, "Friction and wear behavior of zirconium oxide reinforced PMMA composites," *Compos. Part B*, vol. 56, pp. 42–47, 2014.

[6] S. Omar, H. Bin, N. Abbas, A. El-aziz, Z. Arifin, and B. Ahmad, "Effect of alumina particles loading on the mechanical properties of light-cured dental resin composites," *Mater. Des.*, vol. 54, pp. 430–435, 2014.

[7] M. Turnšek, P. Krajnc, R. Liska, and T. Koch, "Macroporous alumina with cellular interconnected morphology from emulsion templated polymer composite precursors," *J. Eur. Ceram. Soc.*, vol. 36, no. 4, pp. 1045–1051, 2016.

[8] S. Mallakpour and E. Khadem, "Recent development in the synthesis of polymer nanocomposites based on nano-alumina," *Prog. Polym. Sci.*, vol. 51, pp. 74–93, 2014.

[9] T. Sathishkumar, S. Satheeshkumar, and J. Naveen, "Glass fiber-reinforced polymer composites - a review," *J. Reinf. Plast. Compos.*, vol. 33, no. 13, pp. 1258–1275, 2014.

[10] Y. L. Thuyavan, N. Anantharaman, G. Arthanareeswaran, A. F. Ismail, and R. V. Mangalaraja, "Preparation and characterization of TiO_2-sulfonated polymer embedded polyetherimide membranes for effective desalination application," *Desalination*, vol. 365, pp. 355–364, 2015.

[11] A. Razmjou, J. Mansouri, and V. Chen, “The effects of mechanical and chemical modification of TiO_2 nanoparticles on the surface chemistry, structure and fouling performance of PES ultrafiltration membranes,” *J. Memb. Sci.*, vol. 378, no. 1–2, pp. 73–84, 2011.

[12] D. Mehta, P. Mondal, and S. George, “Utilization of marble waste powder as a novel adsorbent for removal of fluoride ions from aqueous solution,” *J. Environ. Chem. Eng.*, vol. 4, no. 1, pp. 932–942, 2016.

[13] A. O. Mashaly, B. A. El-Kaliouby, B. N. Shalaby, A. M. El - Gohary, and M. A. Rashwan, “Effects of marble sludge incorporation on the properties of cement composites and concrete paving blocks,” *J. Clean. Prod.*, vol. 112, pp. 731–741, 2015.

[14] S. D. Kore and A. K. Vyas, “Impact of Marble Waste as Coarse Aggregate on properties of lean cement concrete,” *Case Stud. Constr. Mater.*, 2016.

[15] M. K. Karasu, M. Cakmakci, M. B. Cakiroglu, and E. Ayva, “Improvement of changeover times via Taguchi empowered SMED / case study on injection molding production,” *Measurement*, vol. 47, pp. 741–748, 2014.

[16] Y. Arao, S. Yumitori, H. Suzuki, T. Tanaka, K. Tanaka, and T. Katayama, “Mechanical properties of injection-molded carbon fiber/polypropylene composites hybridized with nanofillers,” *Compos. Part A*, vol. 55, no. May, pp. 19–26, 2013.

[17] D. Li, Y. Yan, and H. Wang, “Recent advances in polymer and polymer composite membranes for reverse and forward osmosis processes,” *Prog. Polym. Sci.*, vol. 61, pp. 104–155, 2015.

[18] M. Forhad Mina, S. Seema, R. Matin, M. Jellur Rahaman, R. Bijoy Sarker, M. Abdul Gafur, and M. Abu Hashan Bhuiyan, “Improved performance of isotactic polypropylene/titanium dioxide composites: Effect of processing conditions and filler content,” *Polym. Degrad. Stab.*, vol. 94, no. 2, pp. 183–188, 2009.

[19] Y. W. Leong, M. B. Abu Bakar, Z. A. Mohd Ishak, and A. Ariffin, “Characterization of talc/calcium carbonate filled polypropylene hybrid composites weathered in a natural environment,” *Polym. Degrad. Stab.*, vol. 83, no. 3, pp. 411–422, 2004.

[20] N. Chisholm, H. Mahfuz, V. K. Rangari, A. Ashfaq, and S. Jeelani, “Fabrication and mechanical characterization of carbon/SiC-epoxy nanocomposites,” *Compos. Struct.*, vol. 67, no. 1, pp. 115–124, 2005.

[21] T. Yanagishita and H. Masuda, “Carbon nano fiber arrays from high-aspect ratio polymer pillar prepared by nanoimprinting using anodic porous alumina,” *Mater. Lett.*, vol. 160, pp. 235–237, 2015.

[22] Q. Wang, W. L. Song, L. Z. Fan, and Y. Song, “Facile fabrication of polyacrylonitrile/alumina composite membranes based on triethylene glycol diacetate-2-propenoic acid butyl ester gel polymer electrolytes for high-voltage lithium-ion batteries,” *J. Memb. Sci.*, vol. 486, pp. 21–28, 2015.

[23] M. F. Ashby and Y. J. M. Bréchet, “Designing hybrid materials,” *Acta Materialia*, vol. 51, no. 19. pp. 5801–5821, 2003.

[24] S. R. Kumar, A. Patnaik and I. K. Bhat, “Physical and thermo-mechanical characterizations of resin-based dental composite reinforced with silane-modified nanoalumina filler particle,” *J. Mater. Des. Appl.*, pp. 1–11, 2015.

[25] F. Mirjalili, L. Chuah and E. Salahi, “Mechanical and Morphological Properties of Polypropylene/Nano -Al_2O_3 Composites,” *Sci. J.*, vol. 2014, pp. 1–12, 2014.

[26] B. Peron, A. Lowe, and C. Bailliet, “The effect of transcrystallinity on the interfacial characteristics of polypropylene / alumina single fibre composites,” *Compos. Part A Appl. Sci. Manuf.*, vol. 3, pp. 839–845, 1996.

[27] S. Nath, S. Bodhak, and B. Basu, “HDPE- Al_2O_3-HAp composites for biomedical applications: Processing and characterizations,” *J. Biomed. Mater. Res. - Part B Appl. Biomater.*, vol. 88, no. 1, pp. 1–11, 2009.

[28] A. Laachachi, M. Cochez, E. Leroy, P. Gaudon, M. Ferriol, and J. M. Lopez Cuesta, “Effect of Al_2O_3 and TiO_2 nanoparticles and APP on thermal stability and flame retardance of PMMA,” *Polym. Adv. Technol.*, vol. 17, no. 4, pp. 327–334, 2006.

[29] J. Abenojar, M. a. Martínez, M. Pantoja, F. Velasco, and J. C. Del Real, “Epoxy Composite Reinforced with Nano and Micro SiC Particles: Curing Kinetics and Mechanical Properties,” *J. Adhes.*, vol. 88, no. 4–6, pp. 418–434, 2012.

[30] S. S. Mahapatra and A. Patnaik, “Study on mechanical and erosion wear behavior of hybrid composites using Taguchi experimental design,” *Mater. Des.*, vol. 30, no. 8, pp. 2791–2801, 2009.

[31] R. Maleki Moghadam, S. A. Hosseini, and M. Salehi, “The influence of Stone–Thrower–Wales defect on vibrational characteristics of single-walled carbon nanotubes incorporating Timoshenko beam element,” *Phys. E Low-dimensional Syst. Nanostructures*, vol. 62, pp. 80–89, 2014.

[32] M. Razlan, H. Akil, M. Helmi, A. Kudus, and M. Bisyrul, “Compressive properties and thermal stability of hybrid carbon nanotube-alumina fi lled epoxy nanocomposites,” vol. 91, pp. 235–242, 2016.

[33] E. M. Nascimento, Daniel Eiras, and L. A. Pessan, “Effect of thermal treatment on impact resistance and mechanical properties of polypropylene / calcium carbonate nanocomposites ” vol. 91, pp. 228–234, 2016.

[34] D. Eiras and L. A. Pessan, “Influence of calcium carbonate nanoparticles on the crystallization of polypropylene,” *Mater. Res.*, vol. 12, no. 4, pp. 523–527, 2009.

[35] J. Gu, G. Wu, and Q. Zhang, “Preparation and damping properties of fly ash filled epoxy composites,” *Mater. Sci. Eng. A*, vol. 453, no. August 2006, pp. 614–618, 2007.

[36] B. K. Satapathy, A. Patnaik, N. Dadkar, D. K. Kolluri, and B. S. Tomar, “Influence of vermiculite on performance of flyash-based fibre-reinforced hybrid composites as friction materials,” *Mater. Des.*, vol. 32, no. 8–9, pp. 4354–4361, 2011.

[37] N. Dadkar, B. S. Tomar, B. K. Satapathy, and A. Patnaik, “Performance assessment of hybrid composite friction materials based on flyash-rock fibre combination,” *Mater. Des.*, vol. 31, no. 2, pp. 723–731, 2010.

[38] M. Barczewski, D. Matykiewicz, J. Andrzejewski, and K. Skrczewska, “Application of waste bulk moulded composite (BMC) as a filler for isotactic polypropylene composites,” *J. Adv. Res.*, vol. 7, no. 3, pp. 373–380, 2016.

[39] L. Zuniga, V. Agubra, D. Flores, H. Campos, J. Villareal, and M. Alcoutlabi, “Multichannel hollow structure for improved electrochemical performance of TiO_2/Carbon composite nanofibers as anodes for lithium ion batteries,” *J. Alloys Compd.*, vol. 686, pp. 733–743, 2016.

[40] J. K. Pi, H. C. Yang, L. S. Wan, J. Wu, and Z. K. Xu, "Polypropylene microfiltration membranes modified with TiO_2 nanoparticles for surface wettability and antifouling property," *J. Memb. Sci.*, vol. 500, pp. 8–15, 2016.

[41] A. Fujishima, X. Zhang, and D. A. Tryk, "TiO_2 photocatalysis and related surface phenomena," *Surf. Sci. Rep.*, vol. 63, no. 12, pp. 515–582, 2008.

[42] S. M. Gupta and M. Tripathi, "A review of TiO_2 nanoparticles," *Chinese Sci. Bull.*, vol. 56, no. 16, pp. 1639–1657, 2011.

[43] A. M. Jastrze, J. Karcz, and D. Zabost, "Synthesis of RGO / TiO_2 nanocomposite fl akes and characterization of their unique electrostatic properties using zeta potential measurements," *J. Alloys Compd.*, vol. 679, pp. 470–484, 2016.

[44] C. K. Huang and F. S. Cheng, "Study on kneading and molding of PP/TiO_2 nanocomposite," *Int. Polym. Process.*, vol. 24, no. 3, pp. 267–271, 2009.

[45] Y. Zhao, P. Ding, C. Ba, A. Tang, N. Song, Y. Liu, and L. Shi, "Preparation of TiO_2 coated silicate micro-spheres for enhancing the light diffusion property of polycarbonate composites," *Displays*, vol. 35, no. 4, pp. 220–226, 2014.

[46] C. G. Kuo, C. Y. Hsu, S. S. Wang, and D. C. Wen, "Photocatalytic characteristics of TiO_2 films deposited by magnetron sputtering on polycarbonate at room temperature," *Appl. Surf. Sci.*, vol. 258, no. 18, pp. 6952–6957, 2012.

[47] S. Singh, AnshumanTiwari, R. Nagar, and V. Agrawal, "Feasibility as a Potential Substitute for Natural Sand: A Comparative Study between Granite Cutting Waste and Marble Slurry," *Procedia Environ. Sci.*, vol. 35, pp. 571–582, 2016.

[48] M. J. Pawar, A. Patnaik, and R. Nagar, "Mechanical and Thermo-Mechanical Analysis Based Numerical Simulation of Granite Powder Filled Polymer Composites for Wind Turbine Blade," *Fibers Polym.*, vol. 17, no. 7, pp. 1078–1089, 2016.

[49] N. F. Medina and M. M. Barbero-Barrera, "Mechanical and physical enhancement of gypsum composites through a synergic work of polypropylene fiber and recycled isostatic graphite filler," *Constr. Build. Mater.*, vol. 131, pp. 165–177, 2017.

[50] G. H. Michler and H. K. Von Schmeling, “The physics and micro-mechanics of nano-voids and nano-particles in polymer combinations,” *Polymer (Guildf).*, vol. 54, no. 13, pp. 3131–3144, 2013.

[51] X.L. García, A. Martinez, S. V asquez, L. Torres, "Photo-Oxidative degradation of TiO2/polypropylene films", *Mat. Res. Bull.* vol. 51 pp 56-62, 2014.

[52] A. M. Díez-Pascual and M. Naffakh, “Mechanical and thermal behaviour of isotactic polypropylene reinforced with inorganic fullerene-like WS2 nanoparticles: Effect of filler loading and temperature,” *Mater. Chem. Phys.*, vol. 141, no. 2–3, pp. 979–989, 2013.

[53] N. M. Stark and L. M. Matuana, “Characterization of weathered wood-plastic composite surfaces using FTIR spectroscopy, contact angle, and XPS,” *Polym. Degrad. Stab.*, vol. 92, no. 10, pp. 1883–1890, 2007.

[54] R. N. Darie, C. Popescu, C. Vasile, and E. Pa, “Structure – morphology – mechanical properties relationship of some polypropylene / lignocellulosic composites,” *Mater. Des.*, vol. 56, pp. 763–772, 2014.

[55] M. M. Motsa, B. B. Mamba, J. M. Thwala, and T. A. M. Msagati, “Preparation, characterization, and application of polypropylene-clinoptilolite composites for the selective adsorption of lead from aqueous media,” *J. Colloid Interface Sci.*, vol. 359, no. 1, pp. 210–219, 2011.

[56] R. Xu, M. Chen, F. Zhang, X. Huang, X. Luo, C. Lei, S. Lu, and X. Zhang, “High thermal conductivity and low electrical conductivity tailored in carbon nanotube (carbon black)/polypropylene (alumina) composites,” *Compos. Sci. Technol.*, vol. 133, pp. 111–118, 2016.

[57] P. A. Zapata, A. Zenteno, N. Amigó, F. M. Rabagliati, F. Sepúlveda, F. Catalina, and T. Corrales, “Study on the photodegradation of nanocomposites based on polypropylene and TiO_2 nanotubes,” *Polym. Degrad. Stab.*, vol. 133, pp. 101–107, 2016.

[58] L. F. A. Bernardo, A. P. B. M. Amaro, D. G. Pinto, and S. M. R. Lopes, “Modeling and simulation techniques for polymer nanoparticle composites – A review,” *Comput. Mater. Sci.*, vol. 118, pp. 32–46, 2016.

[59] Soon Poh Yap, U. Johnson Alengaram and Mohd Zamin Jumaat, “Enhancement of mechanical properties in polypropylene – and nylon – fibre reinforced oil palm shell concrete,” *Mater. Des.*, vol. 49, pp. 1034–1041, 2013.

[60] U. A. Handge, M. F. H. Wolff, V. Abetz, and S. Heinrich, “Viscoelastic and dielectric properties of composites of poly(vinyl butyral) and alumina particles with a high filling degree,” *Polym. (United Kingdom)*, vol. 82, pp. 337–348, 2016.

[61] A. Chandra, L. Turng, P. Gopalan, and R. M. Rowell, “Study of utilizing thin polymer surface coating on the nanoparticles for melt compounding of polycarbonate / alumina nanocomposites and their optical properties,” vol. 68, pp. 768–776, 2008.

[62] E. Mohseni, M. M. Khotbehsara, F. Naseri, M. Monazami, and P. Sarker, “Polypropylene fiber reinforced cement mortars containing rice husk ash and nano-alumina,” *Constr. Build. Mater.*, vol. 111, pp. 429–439, 2016.

[63] S. Zhang, X. Y. Cao, Y. M. Ma, Y. C. Ke, J. K. Zhang, and F. S. Wang, “The effects of particle size and content on the thermal conductivity and mechanical properties of Al 2 O 3 / high density polyethylene (HDPE) composites,” *Polym. Lett.*, vol. 5, no. 7, pp. 581–590, 2011.

[64] V. M. Khumalo, J. Karger-Kocsis, and R. Thomann, “Polyethylene/synthetic boehmite alumina nanocomposites: Structure, mechanical, and perforation impact properties,” *J. Mater. Sci.*, vol. 46, no. 2, pp. 422–428, 2011.

[65] J. Ngu, I. Noshida, M. Akmil, a. L. Chuah, and R. C. Thevy, “Thermal properties of low-density polyethylene/ALPHA- alumina nanocomposites,” *J. Thermoplast. Compos. Mater.*, vol. 25, no. 4, pp. 415–426, 2011.

[66] S. Y. Fu, X. Q. Feng, B. Lauke, and Y. W. Mai, “Effects of particle size, particle/matrix interface adhesion and particle loading on mechanical properties of particulate-polymer composites,” *Compos. Part B Eng.*, vol. 39, no. 6, pp. 933–961, 2008.

[67] S. Daneshpayeh, F. Ashenai, I. Ghasemi, and M. Ayaz, “Predicting of mechanical properties of PP / LLDPE / TiO_2 nano- composites by response surface methodology,” *Compos. Part B*, vol. 84, pp. 109–120, 2016.

[68] V. K. Patel and A. Dhanola, “Influence of CaCO3, Al_2O_3, and TiO_2 microfillers on physico-mechanical properties of Luffa cylindrica/polyester composites,” *Eng. Sci. Technol. an Int. J.*, vol. 19, no. 2, pp. 0–7, 2015.

[69] P. Threepopnatkul, C. Wongnarat, W. Intolo, S. Suato, and C. Kulsetthanchalee, “Effect of TiO_2 and ZnO on thin film properties of PET/PBS blend for food packaging applications,” *Energy Procedia*, vol. 56, no. C, pp. 102–111, 2014.

[70] K. Ahmed, N. Z. Raza, F. Habib, M. Aijaz, and M. H. Afridi, “An investigation on the influence of filler loading and compatibilizer on the properties of polypropylene/marble sludge composites,” *J. Ind. Eng. Chem.*, vol. 19, no. 6, pp. 1805–1810, 2013.

[71] J. Peng, G. Rong, M. Cai, M. Yao, and C. Zhou, “Comparison of mechanical properties of undamaged and thermal-damaged coarse marbles under triaxial compression,” *Int. J. Rock Mech. Min. Sci.*, vol. 83, pp. 135–139, 2016.

[72] M. E. Achaby, F. E. Arrakhiz, S. Vaudreuil, A. K. Qaiss, M. Bousmina, and O. F. Fehri “Mechanical, thermal, and rheological properties of graphene-based polypropylene nanocomposites,” *Polym. Compos.*, vol. 33, pp. 733–744, 2012.

[73] M. J. Pawar, A. Patnaik and R. Nagar “Investigation on Mechanical and Thermo-Mechanical Properties of Granite Powder Filled Treated Jute Fiber Reinforced Epoxy Composite,” *Polym. Compos.*, 2015.

[74] C. Özdilek, K. Kazimierczak, and S. J. Picken, “Preparation and characterization of titanate-modified Boehmite-polyamide-6 nanocomposites,” *Polymer (Guildf).*, vol. 46, no. 16, pp. 6025–6034, 2005.

[75] F. Mirjalili, L. Chuah, M. Khalid, and M. Hasmaliza, “Effects of nano - Al_2O_3fillers and dispersant on thermal and dynamic mechanical properties of polypropylene/nano - Al_2O_3 composite,” *J. Thermoplast. Compos. Mater.*, vol. 25, no. 4, pp. 453–467, 2012.

[76] H. Xie, W. Yang, A. C. Y. Yuen, C. Xie, J. Xie, H. Lu, and G. H. Yeoh, “Study on flame retarded flexible polyurethane foam/alumina aerogel composites with improved fire safety,” *Chem. Eng. J.*, 2016.

[77] Z. Cui, B. Nelson, Y. Peng, K. Li, S. Pilla, W. J. Li, L. S. Turng, and C. Shen, “Fabrication and characterization of injection molded poly (Ɛ-caprolactone) and poly (Ɛ-caprolactone)/hydroxyapatite scaffolds for tissue engineering,” *Mater. Sci. Eng. C*, vol. 32, no. 6, pp. 1674–1681, 2012.

[78] H. M. Akil, “Effect of Various Coupling Agents on Properties of Alumina-filled PP Composites,” *J. Reinf. Plast. Compos.*, vol. 25, no. 7, pp. 745–759, 2006.

[79] S. Kango, S. Kalia, A. Celli, J. Njuguna, Y. Habibi, and R. Kumar, “Surface modification of inorganic nanoparticles for development of organic-inorganic nanocomposites - A review,” *Prog. Polym. Sci.*, vol. 38, no. 8, pp. 1232–1261, 2013.

[80] N. Saba, M. Jawaid, O. Y. Alothman, and M. T. Paridah, “A review on dynamic mechanical properties of natural fibre reinforced polymer composites,” *Constr. Build. Mater.*, vol. 106, pp. 149–159, 2016.

[81] F. Duc, P. E. Bourban, C. J. G. Plummer, and J. E. Månson, “A Damping of thermoset and thermoplastic flax fibre composites,” *Compos. PART A*, vol. 64, pp. 115–123, 2014.

[82] H. P. S. Abdul Khalil, I. U. H. Bhat, M. Jawaid, A. Zaidon, D. Hermawan, and Y. S. Hadi, “Bamboo fibre reinforced biocomposites: A review,” *Mater. Des.*, vol. 42, pp. 353–368, 2012.

[83] K. Wang and N. Bahlouli, “Dynamic behavior and flame retardancy of HDPE / hemp short fiber composites : Effect of coupling agent and fiber loading,” no. April, 2016.

[84] A. Etaati, S. Pather, Z. Fang, and H. Wang, “The study of fibre / matrix bond strength in short hemp polypropylene composites from dynamic mechanical analysis,” *Compos. Part B*, vol. 62, pp. 19–28, 2014.

[85] N. Lu and S. Oza, “Thermal stability and thermo-mechanical properties of hemp-high density polyethylene composites: Effect of two different chemical modifications,” *Compos. Part B*, vol. 44, no. 1, pp. 484–490, 2013.

[86] H. Essabir, A. Elkhaoulani, K. Benmoussa, R. Bouhfid, F. Z. Arrakhiz, and A. Qaiss, “Dynamic mechanical thermal behavior analysis of doum fibers reinforced polypropylene composites,” *Mater. Des.*, vol. 51, pp. 780–788, 2013.

[87] S. A. S. Alariqi, A. P. Kumar, B. S. M. Rao, and R. P. Singh, “Effect of gamma-dose rate on crystallinity and morphological changes of gamma-sterilized biomedical polypropylene,” *Polym. Degrad. Stab.*, vol. 94, no. 2, pp. 272–277, 2009.

[88] S. Kudilil, S. Kumbamala, and R. Joseph, “Effect of titanium dioxide on the thermal ageing of polypropylene,” *Polym. Degrad. Stab.*, vol. 97, no. 4, pp. 615–620, 2012.

[89] M. Botev and C. P. H. Betchev, D. Bikiaris, “Mechanical properties and viscoelastic behavior of basalt fiber-reinforced polypropylene,” *J. Appl. Polym. Sci.*, vol. 74, no. September, pp. 19–21, 1999.

[90] S. K. Esthappan, S. K. Kuttappan, and R. Joseph, “Thermal and mechanical properties of polypropylene/titanium dioxide nanocomposite fibers,” *Mater. Des.*, vol. 37, pp. 537–542, 2012.

[91] P. Organophilic, “Preparation of Recycled Nanocomposites Part I : The Recycling Process of Polypropylene and the Mechanical Properties of Recycled Polypropylene/Organoclay Nanocomposites,” *J. Reinf. Plast. Compos.*, vol. 27, pp. 1–20, 2008.

[92] M. Magioli, A. S. Sirqueira, and B. G. Soares, “The effect of dynamic vulcanization on the mechanical , dynamic mechanical and fatigue properties of TPV based on polypropylene and ground tire rubber,” *Polym. Test.*, vol. 29, no. 7, pp. 840–848, 2010.

[93] A. Saffar, P. J. Carreau, M. R. Kamal, and A. Ajji, “Hydrophilic modification of polypropylene microporous membranes by grafting TiO_2 nanoparticles with acrylic acid groups on the surface,” *Polym. (United Kingdom)*, vol. 55, no. 23, pp. 6069–6075, 2014.

[94] T. Hosoda, “Effect of TiO_2 on morphology and mechanical properties of PVDF/PMMA blend films prepared by melt casting process,” *J. Appl. Polym.*, vol. 131, no. 13, pp. 2–32, 2013.

[95] M. S. Mohagheghian Majid, Ebadi-Dehaghani Hassan, Ashouri Davoud, “A study on the effect of nano-ZnO on rheological and dynamic mechanical properties of polypropylene: Experiments and models,” *Compos. Part B*, vol. 30, pp. 2038–46, 2011.

[96] P. Meloni, F. Manca, and G. Carcangiu, “Marble protection: An inorganic electrokinetic approach,” *Appl. Surf. Sci.*, vol. 273, pp. 377–385, 2013.

[97] G. Martínez-Barrera, F. Ureña-Nuñez, O. Gencel, and W. Brostow, “Mechanical properties of polypropylene-fiber reinforced concrete after gamma irradiation,” *Compos. Part A Appl. Sci. Manuf.*, vol. 42, no. 5, pp. 567–572, 2011.

[98] O. Keleştemur, E. Arıcı, S. Yıldız, and B. Gökçer, "Performance evaluation of cement mortars containing marble dust and glass fiber exposed to high temperature by using Taguchi method," *Constr. Build. Mater.*, vol. 60, pp. 17–24, 2014.

[99] X. Liu, X. Dong, D. Wang, and C. C. Han, "Synergistic effect of nanofiller geometry and shear flow on the morphology evolution in SSBR/LPI/filler ternary system," *Polymer (Guildf).*, vol. 72, pp. 193–201, 2015.

[100] K. Kalaitzidou, H. Fukushima, and L. T. Drzal, "A new compounding method for exfoliated graphite-polypropylene nanocomposites with enhanced flexural properties and lower percolation threshold," *Compos. Sci. Technol.*, vol. 67, no. 10, pp. 2045–2051, 2007.

[101] F. Fenouillot, P. Cassagnau, and J. C. Majesté, "Uneven distribution of nanoparticles in immiscible fluids: Morphology development in polymer blends," *Polymer (Guildf).*, vol. 50, no. 6, pp. 1333–1350, 2009.

[102] P. Rajeshwari and T. K. Dey, "Finite element modelling and experimental investigation on effective thermal conductivity of AlN (nano) particles reinforced HDPE polymer nanocomposites," *Thermochim. Acta*, vol. 638, pp. 103–112, 2016.

[103] X. Xu, X. P. Li, B. Q. Jin, Q. Sheng, T. Wang, and J. Zhang, "Influence of morphology evolution on the mechanical properties of beta nucleated isotactic polypropylene in presence of polypropylene random copolymer," *Polym. Test.*, vol. 51, pp. 13–19, 2016.

[104] M. Kersch, H.-W. Schmidt, and V. Altstädt, "Influence of different beta-nucleating agents on the morphology of isotactic polypropylene and their toughening effectiveness," *Polymer (Guildf).*, vol. 98, pp. 320–326, 2016.

[105] D. Pedrazzoli, F. Tuba, V. Khumalo, A. Pegoretti, and J. Karger-Kocsis, "Mechanical and rheological response of polypropylene/boehmite nanocomposites," *J. Reinf. Plast. Compos.*, vol. 33, no. 3, pp. 252–265, 2013.

[106] D. Pedrazzoli, V. M. Khumalo, J. Karger-Kocsis, and A. Pegoretti, "Thermal, viscoelastic and mechanical behavior of polypropylene with synthetic boehmite alumina nanoparticles," *Polym. Test.*, vol. 35, pp. 92–100, 2014.

[107] S. Siengchin and J. Karger-kocsis, “Mechanical and stress relaxation behavior of Santoprene Ò thermoplastic elastomer / boehmite alumina nanocomposites produced by water-mediated and direct melt compounding,” *Compos. Part A*, vol. 41, no. 6, pp. 768–773, 2010.

[108] S. Cao, T. Liu, Y. Tsang, and C. Chen, “Role of hydroxylation modification on the structure and property of reduced graphene oxide / TiO_2 hybrids,” *Appl. Surf. Sci.*, vol. 382, pp. 225–238, 2016.

[109] J. Velásquez, S. Valencia, L. Rios, G. Restrepo, and J. Marín, “Characterization and photocatalytic evaluation of polypropylene and polyethylene pellets coated with P25 TiO_2 using the controlled-temperature embedding method,” *Chem. Eng. J.*, vol. 203, pp. 398–405, 2012.

[110] I. Tekin, “Properties of NaOH activated geopolymer with marble, travertine and volcanic tuff wastes,” *Constr. Build. Mater.*, vol. 127, pp. 607–617, 2016.

[111] M. Sardinha, J. de Brito, and R. Rodrigues, “Durability properties of structural concrete containing very fine aggregates of marble sludge,” *Constr. Build. Mater.*, vol. 119, pp. 45–52, 2016.

[112] K.C. Jung and S.H. Chang, “Evaluation of shrinkage-induced stress in a runway repaired using compliant polymer concrete,” *Compos. Struct.*, vol. 158, pp. 217–226, 2016.

[113] G. Martínez-Barrera, C. Menchaca-Campos, and O. Gencel, “Polyester polymer concrete: Effect of the marble particle sizes and high gamma radiation doses,” *Constr. Build. Mater.*, vol. 41, pp. 204–208, 2013.

[114] Z. Cao, M. Daly, L. Clémence, L. M. Geever, I. Major, C. L. Higginbotham, and D. M. Devine, “Chemical surface modification of calcium carbonate particles with stearic acid using different treating methods,” *Appl. Surf. Sci.*, vol. 378, pp. 320–329, 2016.

[115] D. Kusic, J. M. Slabe, R. Sve, and J. Grum, “The impact of process parameters on test specimen deviations and their correlation with AE signals captured during the injection moulding cycle,” vol. 32, pp. 583–593, 2013.

[116] H. S. Park and T. T. Nguyen, “Optimization of injection molding process for car fender in consideration of energy efficiency and product quality,” *J. Comput. Des. Eng.*, vol. 1, no. 4, pp. 256–265, 2014.

[117] N. C. Fei, N. M. Mehat, and S. Kamaruddin, “Practical Applications of Taguchi Method for Optimization of Processing Parameters for Plastic Injection Moulding: A Retrospective Review,” *Hindawi Publ. Co, ISRN Ind. Eng.*, vol. 2013, pp. 1–11, 2013.

[118] Y. Wang, J. Kim, and J. Song, “Optimization of plastic injection molding process parameters for manufacturing a brake booster valve body,” *J. Mater.*, vol. 56, pp. 313–317, 2014.

[119] Á. Oroszlány and J. G. Kovács, “Gate type influence on thermal characteristics of injection molded biodegradable interference screws for ACL reconstruction,” *Int. Commun. Heat Mass Transf.*, vol. 37, no. 7, pp. 766–769, Aug. 2010.

[120] A. Etxabide, K. de la Caba, and P. Guerrero, “A novel approach to manufacture porous biocomposites using extrusion and injection moulding,” *Eur. Polym. J.*, vol. 82, pp. 324–333, 2016.

[121] M. Altan, “Reducing shrinkage in injection moldings via the Taguchi, ANOVA and neural network methods,” *Mater. Des.*, vol. 31, no. 1, pp. 599–604, 2010.

[122] M. D. Azaman, S. M. Sapuan, S. Sulaiman, E. S. Zainudin, and A. Khalina, “Shrinkages and warpage in the processability of wood-filled polypropylene composite thin-walled parts formed by injection molding,” *Mater. Des.*, vol. 52, pp. 1018–1026, 2013.

[123] F. Yin, H. Mao, and L. Hua, “A hybrid of back propagation neural network and genetic algorithm for optimization of injection molding process parameters,” *Mater. Des.*, vol. 32, no. 6, pp. 3457–3464, Jun. 2011.

[124] H. Öktem, “Modeling and Analysis of Process Parameters for Evaluating Shrinkage Problems During Plastic Injection Molding of a DVD-ROM Cover,” *J. Mater. Eng. Perform.*, vol. 21, no. 1, pp. 25–32, Apr. 2012.

[125] B. Ozcelik, E. Kuram, and M. M. Topal, “Investigation the effects of obstacle geometries and injection molding parameters on weld line strength using experimental and finite element methods in plastic injection molding,” *Int. Commun. Heat Mass Transf.*, vol. 39, no. 2, pp. 275–281, Feb. 2012.

[126] X. Dang, “General frameworks for optimization of plastic injection molding process parameters,” *Simul. Model. Pract. Theory*, vol. 41, pp. 15–27, 2014.

[127] P. Niu, B. Liu, X. Wei, X. Wang, and J. Yang, “Study on mechanical properties and thermal stability of polypropylene/hemp fiber composites,” *J. Reinf. Plast. Compos.*, vol. 30, no. 1, pp. 36–44, 2011.

[128] A. Suplicz, F. Szabo, and J. G. Kovacs, “Injection molding of ceramic filled polypropylene: The effect of thermal conductivity and cooling rate on crystallinity,” *Thermochim. Acta*, vol. 574, pp. 145–150, 2013.

[129] A. Krairi, I. Doghri, and G. Robert, “Multiscale high cycle fatigue models for neat and short fiber reinforced thermoplastic polymers,” *Int. J. Fatigue*, vol. 92, pp. 179–192, 2016.

[130] S. Mathurosemontri, P. Uawongsuwan, S. Nagai, and H. Hamada, “The Effect of Processing Parameter on Mechanical Properties of Short Glass Fiber Reinforced Polyoxymethylene Composite by Direct Fiber Feeding Injection Molding Process,” *Energy Procedia*, vol. 89, pp. 255–263, 2016.

[131] S. H. Chang, J.R. Hwang, and J.L. Doong, “Optimization of the injection molding process of short glass fiber reinforced polycarbonate composites using grey relational analysis,” *J. Mater. Process. Technol.*, vol. 97, no. 1–3, pp. 186–193, 2000.

[132] M. Altan and H. Yildirim, “Mechanical and Antibacterial Properties of Injection Molded Polypropylene/TiO_2 Nano-Composites: Effects of Surface Modification,” *J. Mater. Sci. Technol.*, vol. 28, no. 8, pp. 686–692, 2012.

[133] V. L. Wiesner, L. M. Rueschhoff, A. I. Diaz-cano, R. W. Trice, and J. P. Youngblood, “Producing dense zirconium diboride components by room-temperature injection molding of aqueous ceramic suspensions,” *Ceram. Int.*, vol. 42, no. 2, pp. 2750–2760, 2016.

[134] B. Ou, D. Li, and Y. Liu, “Compatibilizing effect of maleated polypropylene on the mechanical properties of injection molded polypropylene / polyamide,” *Composites Sc. and Tech*., vol. 69 pp 421–426, 2009.

[135] H. Y. Juang and M. H. Hon, “Effect of Solid Content on Processing Stability for Injection-Molding of Alumina Evaluated by Weibull Statistics,” *J. Ceram. Soc. Japan*, vol. 103, no. 5, pp. 430–433, 1995.

[136] P. Thomas, B. Levenfeld, A. Várez, and A. Cervera, “Production of alumina microparts by powder injection molding,” *Int. J. Appl. Ceram. Technol.*, vol. 8, no. 3, pp. 617–626, 2011.

[137] J. J. Tierney and J. W. Gillespie, “Crystallization kinetics behavior of PEEK based composites exposed to high heating and cooling rates,” *Compos. Part A Appl. Sci. Manuf.*, vol. 35, no. 5, pp. 547–558, 2004.

[138] S. L. Gao and J. K. Kim, “Cooling rate influences in carbon fibre/PEEK composites. Part 1. Crystallinity and interface adhesion,” *Compos. Part A Appl. Sci. Manuf.*, vol. 31, no. 6, pp. 517–530, 2000.

[139] A. Lopez, J. Aisa, A. Martinez, and D. Mercado, “Injection moulding parameters influence on weight quality of complex parts by means of DOE application: Case study,” *Meas. J. Int. Meas. Confed.*, vol. 90, pp. 349–356, 2016.

[140] B. Kc, O. Faruk, J. A. M. Agnelli, A. L. Leao, J. Tjong, and M. Sain, “Sisal-glass fiber hybrid biocomposite: Optimization of injection molding parameters using Taguchi method for reducing shrinkage,” *Compos. Part A Appl. Sci. Manuf.*, vol. 83, pp. 152–159, 2016.

[141] E. Oliaei, B. S. Heidari, S. M. Davachi, M. Bahrami, S. Davoodi, I. Hejazi, and J. Seyfi, “Warpage and Shrinkage Optimization of Injection-Molded Plastic Spoon Parts for Biodegradable Polymers Using Taguchi, ANOVA and Artificial Neural Network Methods,” *J. Mater. Sci. Technol.*, vol. 32, no. 8, pp. 1–11, 2016.

[142] G. Berti and M. Monti, “A virtual prototyping environment for a robust design of an injection moulding process,” *Comput. Chem. Eng.*, vol. 54, pp. 159–169, Jul. 2013.

[143] T. Erzurumlu and B. Ozcelik, “Minimization of warpage and sink index in injection-molded thermoplastic parts using Taguchi optimization method,” *Mater. Des.*, vol. 27, pp. 853–861, 2006.

[144] W. C. Chen, M. W. Wang, G. L. Fu, and C. T. Chen, “Optimizatiion of Plastic Injection Molding Process via Taguchi’s Parameter Design Method, BPNN and DFP,” *Proc. Seventh Int. Conf. Mach. Learn. Cybern. Kunming, 12-15 July 2008*, no. July, pp. 12–15, 2008.

[145] N. M. Mehat and S. Kamaruddin, “Optimization of mechanical properties of recycled plastic products via optimal processing parameters using the Taguchi method,” *J. Mater. Process. Technol.*, vol. 211, no. 12, pp. 1989–1994, Dec. 2011.

[146] L. Guglani and G. S. Dangayach, “Application of Moldflow and Taguchi technique in improving the productivity of injection moulded energy meter base,” *Int. J. Process Manag. Benchmarking,* vol. 5, no. 3, 2015.

[147] K. T. Chiang and F.-P. Chang, “Application of grey-fuzzy logic on the optimal process design of an injection-molded part with a thin shell feature,” *Int. Commun. Heat Mass Transf.*, vol. 33, no. 1, pp. 94–101, Jan. 2006.

[148] K. T. Chiang, “The optimal process conditions of an injection-molded thermoplastic part with a thin shell feature using grey-fuzzy logic: A case study on machining the PC/ABS cell phone shell,” *Mater. Des.*, vol. 28, no. 6, pp. 1851–1860, Jan. 2007.

[149] D. Kumar, G. S. Dangayach and P. N. Rao, “An Experimental Investigation to Optimize Injection Moulding Process Parameters for Plastic Parts by Using Taguchi Method and Multi-Objective Genetic Algorithm,” *Int. J. Process Manag. Benchmarking* (Article in Press), 2016.

[150] E. Pérez, V. Alvarez, C. J. Pérez, and C. Bernal, “A comparative study of the effect of different rigid fillers on the fracture and failure behavior of polypropylene based composites,” *Compos. Part B Eng.*, vol. 52, pp. 72–83, 2013.

[151] A. L. Yesgat and R. Kitey, “Effect of filler geometry on fracture mechanisms in glass particle filled epoxy composites,” *Eng. Fract. Mech.*, vol. 160, pp. 22–41, 2016.

[152] S. D. Kore and A. K. Vyas, “Case Studies in Construction Materials Impact of marble waste as coarse aggregate on properties of lean cement concrete,” *Case Stud. Constr. Mater.*, vol. 4, pp. 85–92, 2016.

[153] S. El-Sherbiny, S. M. El-Sheikh, and A. Barhoum, “Preparation and modification of nano calcium carbonate filler from waste marble dust and commercial limestone for papermaking wet end application,” *Powder Technol.*, vol. 279, pp. 290–300, 2015.

[154] Y. Lagabrielle, C. Clerc, A. Vauchez, A. Lahfid, P. Labaume, B. Azambre, S. Fourcade, and J. Dautria, “Very high geothermal gradient during mantle exhumation recorded in mylonitic marbles and carbonate breccias from a Mesozoic Pyrenean palaeomargin (Lherz area , North Pyrenean,” *Comptes rendus - Geosci.*, vol. 348, no. 3–4, pp. 290–300, 2016.

[155] M. M. M. G. P. G. Mantilaka, R. M. G. Rajapakse, D. G. G. P. Karunaratne, and H. M. T. G. A. Pitawala, “Preparation of amorphous calcium carbonate nanoparticles from impure dolomitic marble with the aid of poly(acrylic acid) as a stabilizer,” *Adv. Powder Technol.*, vol. 25, no. 2, pp. 591–598, 2014.

[156] B. D. Agarwal and L. J. Broutman, *Analysis and Performance of Fiber Composites*. 3rd Edition, Wiley, 1990.

[157] ASTM D2240-15, "Standard Test Method for Rubber Property—Durometer Hardness," *ASTM Stand.*, 2015.

[158] ASTM D790, “Standard Test Method for Flexural Properties of Unreinforced and Reinforced Plastics and Electrical Insulation Materials,” *ASTM Stand.*, 2003.

[159] M. Pracella, D. Chionna, I. Anguillesi, Z. Kulinski, and E. Piorkowska, “Functionalization, compatibilization and properties of polypropylene composites with Hemp fibres,” *Compos. Sci. Technol.*, vol. 66, no. 13, pp. 2218–2230, 2006.

[160] J. K. Pandey, K. Raghunatha Reddy, A. Pratheep Kumar, and R. P. Singh, “An overview on the degradability of polymer nanocomposites,” *Polym. Degrad. Stab.*, vol. 88, no. 2, pp. 234–250, 2005.

[161] L. J. Bonderer, K. Feldman, and L. J. Gauckler, “Platelet-reinforced polymer matrix composites by combined gel-casting and hot-pressing. Part I: Polypropylene matrix composites,” *Compos. Sci. Technol.*, vol. 70, no. 13, pp. 1958–1965, 2010.

[162] K. Miyazaki, K. Shibata, and H. Nakatani, “Preparation of degradable polypropylene by an addition of poly(ethylene oxide) microcapsule containing TiO_2,” *Polym. Degrad. Stab.*, vol. 96, no. 5, pp. 1039–1046, 2011.

[163] C. Dong, “Effects of Process-Induced Voids on the Properties,” *J. Mater. Sci. Technol.*, pp. 1-9, 2016.

[164] S. R. Kumar, I. K. Bhat, and A. Patnaik, “Novel Dental Composite Material Reinforced With Silane Functionalized Microsized Gypsum Filler Particles,” *Polym. Compos.,* no. 1, pp. 1–12, 2015.

[165] S. R. Kumar, A. Patnaik, and I. K. Bhat, “Analysis of polymerization shrinkage and thermo-mechanical characterizations of resin-based dental composite reinforced with silane modified nanosilica filler particle,” *J. Mater. Des. Appl.*, vol. 230, no. 2, pp. 492–503, 2016.

[166] K. Masouras, N. Silikas, and D. C. Watts, “Correlation of filler content and elastic properties of resin-composites,” *Dent. Mater.*, vol. 24, no. 7, pp. 932–939, 2008.

[167] E. G. Mota, A. Weiss, A. M. Spohr, H. M. S. Oshima, and L. M. N. De Carvalho, “Relationship between filler content and selected mechanical properties of six microhybrid composites,” *Rev. Odonto Cienc.*, vol. 26, no. 2, pp. 151–155, 2011.

[168] D. Kumar, G. S. Dangayach and P. N. Rao, “Experimental Investigation on Mechanical and Thermo-Mechanical Properties of Alumina Filled Polypropylene Composites Using Injection Molding Process,” *Int. Polymer Processing*, (Accepted), 2016.

[169] M. F. Omar, H. M. Akil, and Z. A. Ahmad, “Static and dynamic compressive properties of mica/polypropylene composites,” *Mater. Sci. Eng. A*, vol. 528, no. 3, pp. 1567–1576, 2011.

[170] M. Khalid, a. Salmiaton, T. G. Chuah, C. T. Ratnam, and S. Y. T. Choong, “Effect of MAPP and TMPTA as compatibilizer on the mechanical properties of cellulose and oil palm fiber empty fruit bunch–polypropylene biocomposites,” *Compos. Interfaces*, vol. 15, no. 2–3, pp. 251–262, 2008.

[171] M. S. Vishkaei, M. A. Mohd Salleh, R. Yunus, D. R. Awang Biak, F. Danafar, and F. Mirjalili, “Effect of short carbon fiber surface treatment on composite properties,” *J. Compos. Mater.*, vol. 45, no. 18, pp. 1885–1891, 2011.

[172] M. Zanetti, G. Camino, P. Reichert, and R. Mulhaupt, “Thermal behaviour of poly(propylene) layered silicate nanocomposites,” *Macromol. Rapid Commun.*, vol. 22, no. 3, pp. 176–180, 2001.

[173] Siddhartha, A. Patnaik, and A. D. Bhatt, “Mechanical and dry sliding wear characterization of epoxy-TiO_2 particulate filled functionally graded composites materials using Taguchi design of experiment,” *Mater. Des.*, vol. 32, no. 2, pp. 615–627, 2011.

[174] A. Zohrevand, A. Ajji, and F. Mighri, “Morphology and properties of highly filled iPP/TiO_2 nanocomposites,” *Polym. Eng. Sci.*, vol. 54, no. 4, pp. 874–886, 2014.

[175] P. Duan, C. Yan, W. Luo, and W. Zhou, “Effects of adding nano-TiO_2 on compressive strength, drying shrinkage, carbonation and microstructure of fluidized bed fly ash based geopolymer paste,” *Construction and Building Materials*, vol. 106. pp. 115–125, 2016.

[176] Z. Zu-hua, Y. A. O. Xiao, and Z. H. U. Hua-jun, “Preparation and mechanical properties of polypropylene fiber reinforced calcined kaolin-fly ash based geopolymer,” *J. Cent. South Univ. Technol.*, pp. 1–4, 2009.

[177] P. A. Zapata, H. Palza, L. S. Cruz, I. Lieberwirth, F. Catalina, T. Corrales, and F. M. Rabagliati, “Polyethylene and poly (ethylene-co-1-octadecene) composites with TiO_2 based nanoparticles by metallocenic ‘ in situ ’ polymerization,” *Polymer (Guildf).*, vol. 54, no. 11, pp. 2690–2698, 2013.

[178] K. Kumar, P. K. Ghosh, and A. Kumar, “Improving mechanical and thermal properties of TiO_2 -epoxy nanocomposite,” *Compos. Part B*, vol. 97, pp. 353–360, 2016.

[179] C. C. Torres, C. H. Campos, C. Diáz, V. A. Jiménez, F. Vidal, L. Guzmán, and J. B. Alderete, “PAMAM-grafted TiO_2 nanotubes as novel versatile materials for drug delivery applications,” *Mater. Sci. Eng. C*, vol. 65, pp. 164–171, 2016.

[180] H. Y. Mirigul Altan, “Mechanical and Morphological Properties of Polypropylene and High Density Polyethylene Matrix Composites Reinforced with Surface Modified Nano Sized TiO_2 Particles,” *World Acad. Sci. Eng. Technol. Int.*, vol. 4, no. 10, pp. 231–237, 2010.

[181] K. Ahmed, S. S. Nizami, N. Z. Raza, and F. Habib, “The effect of silica on the properties of marble sludge filled hybrid natural rubber composites,” *J. King Saud Univ. - Sci.*, vol. 25, no. 4, pp. 331–339, 2013.

[182] K. Ahmed, S. S. Nizami, and N. Z. Riza, “Reinforcement of natural rubber hybrid composites based on marble sludge/Silica and marble sludge/rice husk derived silica,” *J. Adv. Res.*, vol. 5, no. 2, pp. 165–173, 2014.

[183] C. L. Yen, D. H. Tseng, and T. T. Lin, “Characterization of eco-cement paste produced from waste sludges,” *Chemosphere*, vol. 84, no. 2, pp. 220–226, 2011.

[184] A. Rasheed, H. G. Chae, S. Kumar, and M. D. Dadmun, “Polymer nanotube nanocomposites: Correlating intermolecular interaction to ultimate properties,” *Polymer (Guildf).*, vol. 47, no. 13, pp. 4734–4741, 2006.

[185] P. Pötschke, P. J. Halley, P. Lemoine, P. Halley, M. Murphy, D. Martin, S. E. J. Bell, G. P. Brennan, D. Bein, P. Lemoine, and J. Paul, "Polyethylene multiwalled carbon nanotube composites . Polymer Polyethylene multiwalled carbon nanotube composites," *Polymer (Guildf).*, vol. 46, no. September, pp. 8222–8232, 2005.

[186] A. Qureshi, D. Singh, N. L. Singh, S. Ataoglu, A. N. Gulluoglu, A. Tripathi, and D. K. Avasthi, "Nuclear Instruments and Methods in Physics Research B Effect of irradiation by 140 Mev Ag 11 + ions on the optical and electrical properties of polypropylene / TiO_2 composite," *Nucl. Inst. Methods Phys. Res. B*, vol. 267, no. 20, pp. 3456–3460, 2009.

[187] J. Zuo, X. Wei, J. Pei, and X. Zhao, "Investigation of meso-failure behaviors of Jinping marble using SEM with bending loading system," *J. Rock Mech. Geotech. Eng.*, vol. 7, no. 5, pp. 593–599, 2015.

[188] B. Ozcelik and I. Sonat, "Warpage and structural analysis of thin shell plastic in the plastic injection molding," *Mater. Des.*, vol. 30, pp. 367–375, 2009.

[189] B. Ozcelik, A. Ozbay, and E. Demirbas, "Influence of injection parameters and mold materials on mechanical properties of ABS in plastic injection molding," *Int. Commun. Heat Mass Transf.*, vol. 37, no. 9, pp. 1359–1365, Nov. 2010.

******

List of publications out of this research work

Publications in Journal

1. Deepak Kumar, G. S. Dangayach and P.N. Rao, "Experimental Investigation on Mechanical and Thermo Mechanical Properties of Alumina Filled Polypropylene Composites Using Injection Molding Process" accepted & article in press in **International Polymer Processing** (**2016**) (**Sci Indexed**, Hanser Publishers).

2. Deepak Kumar, G. S. Dangayach and P.N. Rao, "An Experimental Investigation to Optimize Injection Moulding Process Parameters for Plastic Parts by Using Taguchi Method and Multi-Objective Genetic Algorithm" **International Journal of Process Management and Benchmarking** (accepted and article in press), **2016.**

3. G. S. Dangayach and Deepak kumar, "Reduction in defect Rate by Taguchi method in plastic injection molded components" paper published in **Advanced Materials Research** Vols. 488-489, **2012**, pp 269-273.Trans Tech publications, **Switzerland**. (www.scientific.net/AMR 488-489 269).

National and International Conferences

1. **Deepak Kumar** and G. S. Dangayach, "Optimization of Parameters for Volumetric Shrinkage of Plastic Parts by Genetic Algorithm" proceedings of **National Conference** on Sustainable Manufacturing for Brighter a future, MNIT, Jaipur, 2-3 January, 2015.
2. **Deepak Kumar**, G. S. Dangayach and P.N. Rao, "An Investigation on Optimization of Parameters for Injection Molded Polypropylene–Marble Composites with Multi Objective Genetic Algorithm" presented in **IEEE International Conference** on Recent Advances and Innovations in Engineering (ICRAIE-2016), December 23-25, 2016, Jaipur, India.

*****

Brief Bio-Data of the Author

The author Deepak Kumar, graduated in Mechanical Engineering from Government Engineering College, University of Rajasthan in the year 2001. He did his post graduation in the Mechanical engineering with the specialization of Manufacturing System Engineering, Malaviya National Institute of Technology (MNIT), Jaipur., in the year 2011. Before joining for the Ph.D. programme at Malaviya National Institute of Technology, Jaipur, he had served as a faculty in the Department of Mechanical Engineering at various institutions such as Government Engineering College, Ajmer, Yagyvalkya Institute of Technology, Jaipur and Poornima Group of Colleges, Jaipur, Rajasthan. He has 15 years of teaching and industrial experience and delivered invited lectures at various forums.

He has published six research papers in National and International Journals and presented four research papers in International and National Conferences to his credit. Since 2012, he has been engaged in his Doctoral Research in the area of Development and characterization of polymeric materials at MNIT, Jaipur. His areas of interests are polymer composites, plastic injection moulding, optimization, simulation and artificial intelligence. He has guided 13 M. Tech. Dissertations.